MASTER THESIS

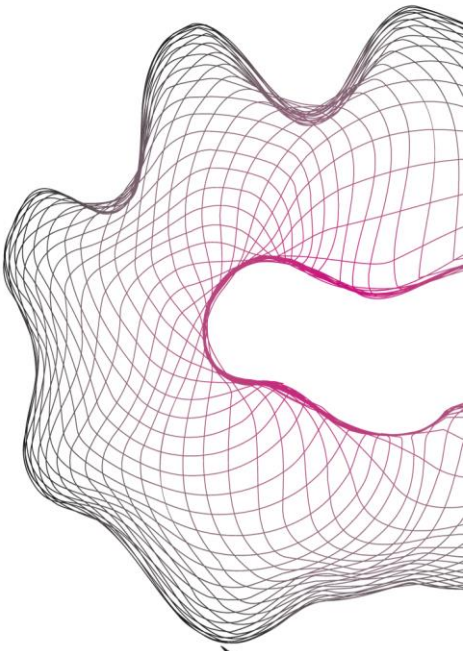

EXPLORING SUSTAINABLE MATERIALS FOR 3D PRINTED SPLINTS IN MEDICAL APPLICATIONS

M.C.I. Meijer

FACULTY OF ENGINEERING TECHNOLOGY
DEPARTMENT OF BIOMECHANICAL ENGINEERING

EXAMINATION COMMITTEE
Prof. dr. ir. Gabriëlle Tuijthof
Dr. ir. Maartje Leemans.
Dr. Sara Roldan Velasquez
Dr. Vincent Stirler

UNIVERSITY OF TWENTE.

27-11-24

ABSTRACT

This thesis examines sustainable materials for 3D printed patient-specific splints for wrist fractures. The currently used print material, ST45, is neither recyclable nor biodegradable, contributing to the ever-growing hospital waste pile, highlighting the urgent need for sustainable, recyclable material alternatives that align with the principles of circular economy. First, a systematic literature analysis was conducted to identify suitable materials, which were evaluated with a multi-criteria decision analysis (MCDA) on their sustainability (i.e., recyclability), material properties (i.e., fracture immobilization), patient safety and logistical practicality (i.e., compatible with in-house 3D printers). Recycled polylactic acid (rPLA) and recycled polyethylene terephthalate glycol (rPETg) were identified as the two most ideal candidates.
Second, the feasibility and sustainability of the production process for rPLA and rPETg were investigated based on production, energy, and quality metrics. The results showed that the rPETg recycling process, in collaboration with NHL Stenden, was more feasible compared to the CHILL recycling production process based on production efficiency, filament quality, and scalability.
Third, the mechanical properties of the virgin and recycled PLA and PETg 3D printed specimens were evaluated and the recycled materials were compared to the ST45 benchmark. The results show that rPLA and rPETg did not show statistically significant differences in terms of impact energy, E-modulus, and tensile strength compared to ST45. However, rPETg showed a statistically significant deviation in tensile strength. The recycling of PLA and PETg did not show statistically significant differences in the E-modulus, but there was a significant increase in tensile strength between the virgin and recycled samples. For rPLA, the impact energy remained consistent with that of the virgin material, showing no significant differences between cycles. For rPETg, the impact energy increased significantly after the first recycling cycle, indicating a temporary improvement. However, after two recycling cycles, the impact energy decreased significantly and performed worse than the virgin material.
The findings suggest that, taken into consideration, the recycling production of rPETg shows potential as a viable material for 3D printed wrist splints. However, design modifications should be explored to enhance its mechanical performance. Further research should focus on optimizing recycling processes in filament consistency and evaluating long-term material performance, over multiple recycling cycles, and during use. Furthermore, design modifications and optimizations of the wrist splint should be explored to enhance its performance.

PREFACE

Before you lies the master thesis 'Exploring sustainable materials for 3D printing splints in medical applications'. It was established by the criteria for graduating from the University of Twente's Biomedical Engineering degree.

I would like to express my gratitude to my daily supervisor, prof. dr. ir. Gabriëlle Tuijthof, for her invaluable guidance in helping me develop key research skills, responsibility, and effective time management throughout this process. I am also thankful to dr. ir. Maartje Leemans, who joined as my second supervisor in June and provided thoughtful insights and support. My sincere thanks go to my external supervisor, dr. Sara Roldan Velasquez, for her valuable lessons on materials and sustainability. Lastly, I am grateful to my supervisor from MAINIAC and RadboudUMC, dr. Vincent Stirler, whose teachings on communication and trust have been instrumental in shaping my experience.

I also would like to thank CHILL, MAINIAC partner, for providing me with the opportunity to perform tests, tackle challenges, and gain valuable experience in material recycling and 3D printing. A special thanks to PhD student Mariska van Cronenberg from NHL Stenden for sharing her expertise in the recycling process and filament production. Additionally, I am grateful to NHL Stenden and HartPlastic for allowing me to use their equipment, which enabled me to explore the potential of hospital waste for new applications.

I would like to thank my friends and fellow students for their support throughout this journey. Eliane, a fellow Biomedical student, was always there to discuss challenges and offer her advice whenever I faced difficulties. I also thank Laura, who provided valuable guidance and lessons on how to work effectively on this project. I extend my thanks to the students of the BE-BDDP group, with whom I collaborated during the first few months before moving to Utrecht. Lastly, I appreciate the students at RadboudUMC, who not only shared project-related discussions with me, but also made our lunch walks a much-needed break.

Finally, I would like to express my deepest gratitude to my family for their constant support, encouragement, and patience throughout this journey. To my partner, Hille, I am especially thankful for his unwavering love, understanding, and support not only during the writing of my master's thesis but throughout all my academic years. He has been my source of motivation, providing thoughtful feedback, helping me navigate obstacles, and always offering practical solutions to the challenges I faced.

Muriël Meijer
November 20, 2024

NOMENCLATURE

Term	Definition	SI Unit
AM	Additive Manufacturing	
ASTM	American Society for Testing and Materials	
CE	Circular Economy	
CFF-PLA	Continuous Fiber Reinforced Polylactic Acid	
DLP	Digital Light Processing	
E-modulus	Young's Modulus	Pa
F	Force applied during a tensile or impact test	N
FM	Flexural Modulus	Pa
FDM	Fused Deposition Modeling	
FFF	Fused Filament Fabrication	
H	Hardness	
ISO	International Standardization Organization	
LCA	Life cycle assessment	
MCDA	Multi-Criteria Decision Analysis	
PA	Polyamide	
PEEK	Polyether Ether Ketone	
PET	Polyethylene Terephthalate	
PETg	Polyethylene Terephthalate glycol	
PLA	Polylactic Acid	
PLLA	Poly-L-Lactic Acid	
PLA/Wood	Polylactic Acid with Wood components	
PP	Polypropylene	
PRISMA	Preferred Reporting Items for Systematic Reviews and Meta-Analyses	
ρ	Density	kg/m^3
SDS	Safety Data Sheet	
SLA	Stereolithography	
SLS	Selective Laser Sintering	
ST45	reactive urethane photopolymer	
σ	Stress	Pa
T	Temperature	°C
TD	Thermal Decomposition	°C
TDS	Technical Data Sheet	
UTS	Ultimate Tensile Strength	Pa
V	Volume of the printed object	m^3
YS	Yield Strength	Pa
ε	Strain	

Contents

1 INTRODUCTION

The modern healthcare system is highly dependent on single-use materials and disposable items to maintain sterility and safety, resulting in significant waste, which averages 3.23 kg per hospital bed per day [1]. Conventional splints or casts are made of plaster or gypsum, although effective for immobilizing these fractures, contributing to this medical waste. Although effective in immobilization, they often cause discomfort in patients, being bulky, itchy, difficult to keep clean, and not water resistant [2, 3]. These challenges underscore the urgent need for more sustainable and patient-friendly solutions in healthcare [4, 5].

In response to these challenges, Radboudumc, a leading trauma and university medical center in Nijmegen, has collaborated with the MAINIAC (Military AI and Innovations in Acute Care) initiative to develop an alternative for these conventional casts. The mission of MAINIAC is to provide patient-specific solutions that enhance the resilience of military personnel. Their approach integrates smart logistics to optimize patient flows, enabling the efficient management of large-scale casualties while fostering greater autonomy in operational healthcare. Furthermore, MAINIAC emphasizes sustainability with the goal of reducing environmental impact. This aligns closely with Radboudumc's commitment to sustainable healthcare practices, including promoting a circular economy in hospital settings [6].

The alternative that Radboudumc and MAINIAC are developing is the 3DxSplint. This patient-specific 3D printed splint is designed to be more sustainable and offer greater patient comfort than traditional casts [7]. It is printed with a reactive urethane photopolymer (ST45) UV resin material [8] using digital light processing (DLP) technology. This technology uses a digital light projector to cure liquid resin layer by layer [9]. Figure 1.1 illustrates a fracture in the lower arm, the traditional fiberglass cast, and the 3DxSplint made of ST45 resin material, visually highlighting the key differences between conventional and innovative treatment approaches.

Figure 1.1: Illustration of a fracture in lower arm. A: Schematic representation highlighting the anatomy involved in the fracture [10]. B: Image of a conventional fiberglass forearm cast used for immobilization [11]. C: Image of a 3DxSplint design applied to the wrist, made from ST45 resin material.

DLP is currently preferred for the Radboudumc and MAINIAC splint applications because of its precision and efficiency. In terms of sustainability, Verschoor et al. [12] concluded that the 3DxSplint, created with DLP technology, generates less waste and has a smaller environmental

impact compared to conventional splints and casts. Figure 1.2 outlines the workflow for the production and implementation of the 3DxSplint, demonstrating the potential for more sustainable processes throughout the treatment lifecycle. However, there is room to further improve the

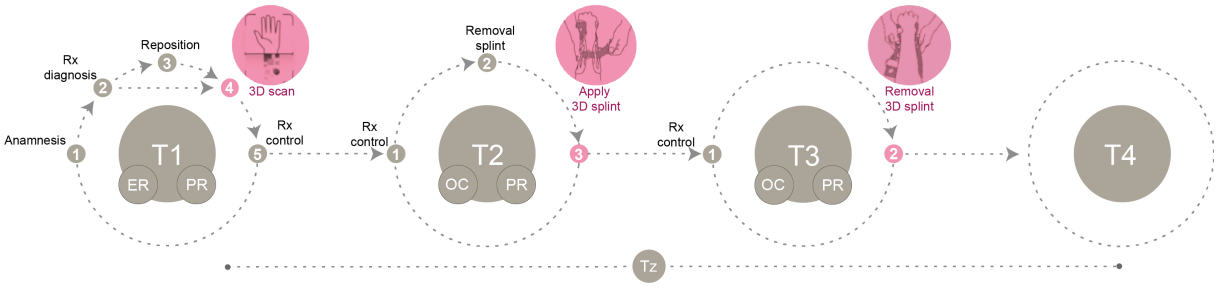

Figure 1.2: The schematic representation of the proposed workflow for the 3DxSplint. The timelines T1-T3 denote standard hospital visits for patients. T4 indicates additional hospital visits suggested by healthcare professionals for extended follow-up care. Tz represents any patient-initiated hospital visits, which may be influenced by factors such as pain or other relevant concerns [Adapted from [7]].

sustainability of the splint, by exploring recyclable or biodegradable alternatives to the current ST45 print material. Since ST45 cannot be remelted or reshaped after curing, which limits the options for recycling and biodegradability. Besides DLP, Radboudumc has also access to other 3D printing technologies. These technologies include fused deposition modeling (FDM) and stereolithography (SLA). FDM operates by extruding thermoplastic filaments through a heated nozzle, while SLA, similar to DLP, uses a laser to cure liquid resin into solid plastic but typically at a slower rate [13].
These alternative 3D printing technologies, particularly FDM with its use of thermoplastics, offer promising avenues for incorporating recyclable or biodegradable materials into the production process. Such advancements would reduce the environmental footprint of the 3DxSplint while maintaining its customizable and effective design [14], [15], [16].

Problem statement

Conventional splints or casts are made of plaster or gypsum, though effective in immobilizing lower arm fractures, contributing to medical waste and patient discomfort. Although 3D printed splints offer advantages, their sustainability could be further improved by finding an alternative printing material. The currently used ST45 UV resin is not recyclable nor biodegradable and still contributes to the increase in medical waste. There is an urgent need to explore and implement an alternative sustainable, recyclable, or biodegradable material to minimize waste, streamline logistics, and support the principles of circular economy (CE). The 6R framework of reduce, reuse, recycle, recover, redesign, and remanufacture, as explored by Nazir and Capocchi [17], offers a comprehensive approach to integrating sustainability into production processes. In addition, adopting local and on-demand production methods can further enhance resource efficiency, reduce transportation costs, and facilitate a more sustainable approach to healthcare.

Objectives

The overall goal of this whole study is to advance the development of sustainable 3D printed splints for lower arm fractures. To achieve this, the study will focus on three main areas:

1. Sustainable materials analysis through systematic literature study. This involves a thorough review of the existing literature to identify potential sustainable materials for 3D printing medical devices. The focus will be on materials that are biobased, biodegradable, or recyclable, while also meeting the requirements necessary for the 3DxSplint.

2. Identification of the recycling process. This objective investigates the sustainability and feasibility of producing the identified sustainable materials for the 3DxSplint, focusing on the production, energy, and quality metrics. The goal is to contribute to a circular economy in medical 3D printing, reducing waste and promoting resource efficiency.

3. Mechanical testing of identified materials. This includes the mechanical testing of the recycled materials identified in the literature review to assess their suitability for use in 3DxSplint. The tests will focus on tensile strength and impact resistance to ensure that the materials can provide adequate support during use.

2 EVALUATING SUSTAINABLE ALTERNATIVE MATERIALS TO ST45 FOR 3D PRINTED MEDICAL SPLINTS: A SYSTEMATIC LITERATURE REVIEW

Introduction

The literature review aims to assess the current state of publicly available information to answer the research question. What materials exhibit sustainable properties for 3D printing in the context of medical splints? Currently, the 3D printed splint is made from ST45 resin, which, while effective in producing strong and customizable splints, is non-recyclable and non-biodegradable. This presents a need for exploring alternative materials that meet sustainability requirements without compromising the functionality of the splint.
ST45 has been the ”golden standard” for the 3DxSplint due to its reliable mechanical, thermal, and print properties [18]. However, its environmental limitations are clear and finding sustainable alternatives is crucial in the context of increasing demand for sustainable solutions in healthcare. Alternative materials must meet key criteria: sustainability, mechanical suitability for immobilization, patient safety, and logistic practicality. This balance will ensure that future materials are environmentally friendly while maintaining the high performance of the splint and patient safety standards.
To identify suitable alternatives, this systematic literature review will employ a systematic approach to collect, analyze, and compare relevant articles and studies. The study will focus on biodegradable and recyclable materials that align with the sustainability goals of the 3DxSplint, without compromising its performance. By exploring these alternatives, the review aims to provide guidelines for material selection, production processes, and testing plans. Ultimately, this will help initiate a more sustainable production process for the 3DxSplint while retaining its effectiveness in medical applications.

Methodology

For this systematic review of the literature, PubMed and Scopus databases were used to identify relevant studies, the search being carried out in March 2024. The search strategy employed a combination of relevant search terms and synonyms, yielding the following query for the Scopus database: *(recycl* OR reus* OR reproces* OR upcycl* OR refurbish* OR repurpos* OR redeem*) AND (”3D print*” OR ”Additive manufactur*” OR ”Three-dimensional print*” OR ”Fused deposition model*” OR ”Rapid prototyp*” OR ”Layered manufactur*” OR ”Stereolithography” OR ”Digital light processing”) AND (sustain* OR eco-friendly OR ”Circular economy” OR ”Environmentally friendly” OR nature-based OR renewable) AND (material* OR filament* OR polymer* OR plastic* OR compound*) AND (”Trauma care” OR splint* OR ”Fracture management” OR brace OR ”Orthopedic treatment” OR immobiliz*)*. This search was limited to specific fields by excluding keywords such as ”Tissue” and ”Hydrogels” that were deemed irrelevant to the study focus (the whole search string is shown in Appendix A).

Table 2.1: Inclusion and exclusion criteria for selecting studies on sustainable materials for 3D Printed medical splints.

Inclusion criteria	Exclusion criteria
• Investigated materials that are suitable for 3D printing, specifically for use in external medical devices (CLASS I) and biocompatible. • Provided information on life cycle assessments, material reusability, or biodegradability of the materials. • Reported on material properties (e.g., strength, flexibility, durability) relevant to the mechanical requirements of trauma care applications. • Focused on materials only compatible with FDM, SLA, or DLP additive manufacturing techniques.	• Focused primarily on materials intended for non-medical applications, such as food packaging, consumer electronics, or general manufacturing, without direct relevance to healthcare or trauma care. • Reported on non-recyclable or non-sustainable materials, such as those made entirely of metals or non-biodegradable polymers. • Addressed internal medical applications, including tissue engineering, bone regeneration, or drug delivery systems, which do not apply to the external mechanical support of splints. • Theoretical studies or simulations without experimental data on material performance. • Not available in English or did not provide full-text access.

The results were sorted by relevance, yielding a total of 118 relevant publications. For the PubMed database, a similar search query was executed, resulting in 180 relevant publications. Following the search, duplicate records were removed and the titles and abstracts of the remaining articles were evaluated. Studies that met the inclusion criteria (Table 2.1) were further evaluated based on full text analysis. In total, 298 articles were identified, of which 41 met the inclusion criteria. Subsequently, these articles were analyzed with respect to the investigated materials, methodologies, and reporting of the properties of sustainable materials. The literature selection and evaluation process is visually represented in a PRISMA flow diagram (Figure 2.1), illustrating the steps from the initial search to the final selection of studies for analysis. Data were systematically compiled into an Excel spreadsheet, documenting key information such as authors, publication dates, materials used, and findings related to sustainability and material properties (shown in Appendix A).

Key criteria for material selection, developed in collaboration with medical experts and researchers (Figure 2.2) from the 3DxSplint project. Encompass four main areas: sustainability, fracture immobilization, patient safety, and logistical practicality.
For sustainability, the material must be biodegradable or recyclable to reduce the environmental impact. Furthermore, sourcing materials that are commercially available within the EU is preferred, as this minimizes transportation emissions and ensures compliance with local regulatory standards. In terms of immobilization of the fracture, the material must provide mechan-

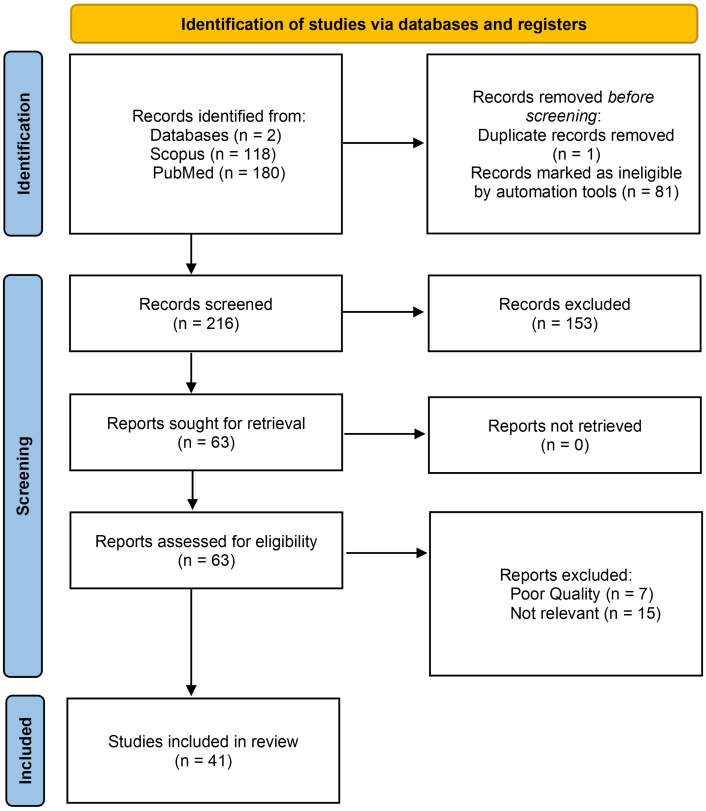

Figure 2.1: PRISMA flow diagram for the systematic literature review.

ical properties comparable to ST45 resin, offering sufficient strength and rigidity for effective immobilization of the fracture of the lower arm. Regarding patient safety, the material must be flame resistant, water resistant, non-explosive, and non-flammable to ensure safe, prolonged use under various conditions. These safety standards are consistent with those of the ST45 resin currently used. Lastly, logistical practicality requires compatibility with existing 3D printing technologies (FDM, DLP, SLA) employed at Radboudumc. This ensures seamless integration into current production workflows without adjustments. These criteria not only address the functional demands of the 3DxSplint but also align with broader sustainability and regulatory goals.

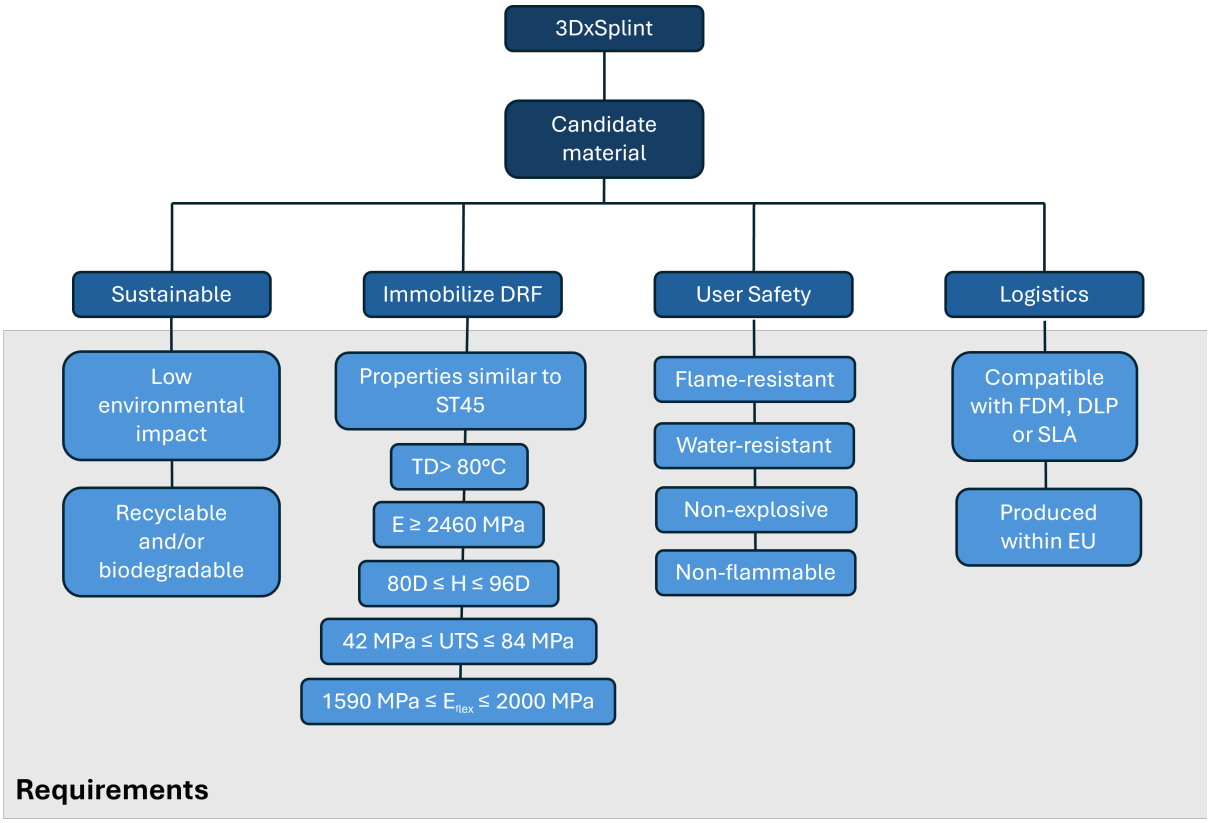

Figure 2.2: Material requirements for the 3DxSplint

Table 2.2: Materials from literature review, with green indicating that the materials have similar mechanical properties to the reference material ST45, and orange indicating sufficient mechanical strength to provide proper functionality of the 3DxSplint.

Material	Print method	Tensile strength (MPa)	E-modulus (MPa)	Available by	Ref.
rPET	FDM	30-68	650-3670	Formfutura	[19] [20] [21] [22] [23] [24] [25] [26] [27]
PLA/Wood**	FDM	15-57	1500-4000	3DJake	[28] [29] [30] [31]
rPETg	FDM	27-53	183-2700	Formfutura	[32] [33] [34] [35]
rPLA	FDM	21-60	350-3500	Formfutura	[36] [37] [35] [31] [38] [39] [26]
rPP	FDM	4-40.00	740-1340	Formfutura	[40] [41] [27] [42]
CFF-PLA*	FDM	9-254	217-23300	Nanovia	[43] [44] [45] [46]
PLLA	FDM	150.00	2700	3D4Makers	[36]

* 26% flax fibers in PLA

** wood in PLA (wood flour 10-50 wt.% and wood fibers 15-25 wt.%)

Table 2.3: The materials found through a web-based search of properties of materials from the literature review. Green indicates that the materials have similar mechanical properties to the reference material ST45, and orange means it has sufficient mechanical strength to provide proper functionality of the 3DxSplint.

Material	AM	Tensile strength (MPa)	E-modulus (MPa)	Available by	Ref.
GreenTEC	FDM	46	3300	Extrudr	[47]
GreenTEC Pro	FDM	58	4300	Extrudr	[48]
niceBIO filaments	FDM	55	5100	3DJake	[49]
PolyHydroxy Alkanoates	FDM	26	2500	ColorFabb	[50]
Recycled PEEK	FDM	90	3400	3D4Makers	[51]
Plant-based UV resin	DLP	52	1200-1600	Anycubic	[52]
Multicomp Pro MP004398	LCD	50	307	Multicomppro	[53]
Biofusion	FDM	41	3200	Extrudr	[54]
Hard resin with 85% Bio content	DLP/SLA	<10	1000-1300	3Dresyn	[55]
Elastic resin with 85% Bio content	DLP/SLA	<1	5	3Dresyn	[56]
Flexible resin with 85% Bio content	DLP/SLA	<5	800	3Dresyn	[57]

Material selection

In the material selection process for the 3DxSplint, priority was given to materials that were recyclable or biodegradable to meet sustainability goals. Compatibility with FDM, DLP, and SLA 3D printing technologies was evaluated to ensure smooth integration into existing production methods, with a preference for materials sourced and commercially available within the EU to reduce logistical complexity and transportation-related emissions.

Mechanical properties, specifically tensile strength and E-modulus, were analyzed as key indicators of the material's ability to immobilize fractures effectively. Comparisons were drawn with conventional materials used in plaster and fiberglass casts, which have proven effective in lower arm fractures [58, 59]. Plaster casts have a tensile strength of 6.04 MPa ± 0.53 MPa and an E-modulus of 443 MPa ± 75.0 MPa, while fiberglass casts offer higher values, with a tensile strength of 33.8 MPa ± 3.6 MPa and an E-modulus of 3498 MPa ± 192 MPa [60]. The candidate materials for the 3DxSplint must have tensile strengths greater than 20 MPa to provide sufficient stability during weight-bearing activities and minimize complications during healing [61].

The materials selected in this step are summarized in Table 2.2, where the color code indicates their mechanical properties relative to ST45: The materials highlighted in green exhibit similar properties, while those marked in orange meet the minimum requirements for fracture immo-

bilization, comparable to plaster and fiberglass casts. Materials indicated in red are deemed unsuitable for the 3DxSplint due to inadequate mechanical performance. Furthermore, during the literature review, other suitable materials were identified through technical data sheets available on various websites, which are presented in a separate table 2.3.

Scoring system

The scoring process followed a multi-criteria decision analysis (MCDA) framework to ensure that candidate materials identified in the literature were consistently evaluated in all criteria. MCDA is widely recognized as an effective tool for objective material selection [62, 63, 64]. This framework, detailed in Appendix A, systematically evaluates the four key criteria for the 3DxSplint: sustainability, mechanical properties, safety, and logistics (Figure 2.2). Sustainability was assessed based on environmental impact and recyclability. A high score of 5 was awarded to materials with low environmental impact that are recyclable and/or biodegradable. The immobilization properties were measured against the specific mechanical requirements essential for the support of the fractured lower arm: thermal decomposition temperature (> 80°C), ultimate tensile strength (42-84 MPa), flexural modulus (1590-2000 MPa), hardness (80-90D) and E modulus (2460 MPa). A score of 5 was given if a material met the required specifications, with lower scores as the performance deviated from these thresholds. The safety of the user was focused on solubility, flammability, and reactivity. The materials had to be insoluble, nonflammable, nonexplosive, and not prone to self-ignition to achieve a high score of 5. Logistics considered the location of production and the compatibility with the RadboudUMC 3D lab printing methods. Materials produced outside the EU or unsuitable for reliable printing scored 1, while locally produced compatible materials scored 5, reflecting logistical convenience and minimal environmental impact. Each criterion was weighted equally in the final evaluation. The scoring relied primarily on technical and safety specifications from manufacturers. If data were unavailable, they were supplemented from the existing literature, and where information could not be found, a default score of 1 was assigned to indicate potential limitations. The overall score for each material was the average of all requirements, with detailed scoring provided in the appendix A.

Results

Table 2.4 presents the materials and their scores assigned according to the MCDA criteria. The sustainability assessment identified rPLA as the highest scoring material, achieving maximum scores for low environmental impact and strong recyclability or biodegradability. rPLA is classified as a recycled and biobased material, which is compliant with the REACH and RoHS regulations. Its recyclability and biodegradability contribute to its score of 5. Several materials scored 4.5 in the sustainability assessment, including rPETg, CFF-PLA, PLLA, PLA/Wood, GreenTEC, and GreenTEC Pro. Although these materials exhibit favorable sustainability attributes, they differ from rPLA primarily in their recyclability and biodegradability ratings. By comparison, Polyamide 12 received a low score due to its petroleum-based composition and limited recycling options, indicating a higher environmental footprint. Likewise, Multicomp Pro MP004398 and plant-based UV resin were assigned similar scores because they are neither biodegradable nor recyclable. The variation in scores reflects differences in material composition, established recycling processes, and biodegradability.

rPETg, CFF-PLA, and PLLA achieved the highest scores in the immobilization criteria, with overall ratings of 4.2, 4.4, and 4.2, respectively. rPETg satisfies three out of five criteria, with only slightly lower hardness (69D) and a reduced Young's modulus (1640 MPa) compared to the ST45 benchmark. CFF-PLA meets two out of five requirements, showing marginally lower

ultimate tensile strength (41 MPa) and Shore hardness (77D) than the required standards, while its flexural modulus is somewhat higher (2300 MPa). PLLA, which meets four out of five criteria, has a high flexural modulus (3350 MPa), which contributes to a slight reduction in its overall score. In contrast, the elastic and flexible resins with 85% bio content scored lower. Their tensile strengths (<1 MPa and <5 MPa, respectively), hardness and Young's modulus fall considerably below the necessary levels for effective immobilization. Additionally, a lack of available data on thermal decomposition and flexural modulus further limits their suitability in applications requiring robust immobilization.

The user safety assessment showed that rApolloX (ASA-based filament), BioFusion, GreenTEC, and GreenTEC Pro (PLA-based filament) scored highly because they met all necessary safety requirements. However, other materials from different manufacturers, such as plant-based UV resin, PLLA, and niceBIO filament, received lower scores due to the missing critical safety data, particularly regarding their flammability and potential hazards.

The logistics assessment demonstrated that rPLA, PLLA, rPET, rApolloX, and rPETg achieved high scores due to their availability within the EU and compatibility with various printing methods. This, in turn, enhances their availability and ease of integration into manufacturing process of the 3DxSplint at Radboudumc. In contrast, plant-based UV resin scored lower due to production outside the EU and limited compatibility with specific printing methods, potentially complicating supply chain logistics and increasing associated costs.

Table 2.4: Scoring of candidate Materials for 3DxSplint using Multi-Criteria Decision Analysis (MCDA) framework based on Sustainability, Immobilization Performance, User Safety, and Logistics. The materials are ordered from the highest total score at the top to the lowest at the bottom. The reference is added where the values are obtained from.

Material	**Sustainability** (1-5)	**Immobilization** (1-5)	**User Safety** (1-5)	**Logistics** (1-5)	**Total Score**
rPLA	5	3.8	4.75	5	18.55
rPETg	4.5	4.2	4.75	5	18.45
PLLA	4.5	4.2	4.5	5	18.2
rApolloX	4.5	3	5	5	17.5
rPET	4	4	4.5	5	17.5
GreenTEC	4.5	3.4	5	4	16.9
GreenTEC Pro	4.5	3.4	5	4	16.9
CFF-PLA	4.5	4.4	4.25	3.5	16.65
PLA/Wood	4.5	3.8	4.75	3.5	16.55
Biofusion	3.5	4	5	4	16.5
PolyHydroxy Alkanoates	4.5	3	4	4.5	16
Recycled PEEK	3.5	3.2	3.25	4	13.95
rPP	4	2.6	4.25	3	13.85
Hard resin with 85% Bio content	4	1.8	4.5	3	13.3
Polyamide 12	2	3.6	4	3.5	13.1
Elastic resin with 85% Bio content	4	1	4.5	3	12.5
Flexible resin with 85% Bio content	4	1	4.5	3	12.5
niceBIO filaments	4	2.6	1	3.5	11.1
Multicomp Pro MP004398	2	2.4	2.5	3	9.9
Plant-based UV resin	2	2.4	1	2.5	7.9

In this MCDA, rPLA and rPETg were identified as the highest-scoring materials of the literature review and the Web-based search. Both materials demonstrated strong performance on all the criteria evaluated. These results indicate that they are the most viable alternatives for replacing ST45 in the production of medical splints.

Discussion

The scoring system used in the MCDA framework to evaluate materials for the 3DxSplint project relied heavily on manufacturers' technical and safety data. In cases where there was no additional literature source available, as with several web-based materials, only the technical and safety data sheets from the manufacturers could be referenced. Missing data for some materials resulted in a default score of 1, which may not fully capture their potential. In the initial MCDA, this conservative approach led to lower scores for several materials, which were later refined with literature findings where available. For example, additional data for rPETg revealed a decomposition temperature above 300°C, a Shore hardness of 69D, and an E-modulus of 1640 MPa, suggesting improved safety and rigidity that meet the immobilization criteria better than initially assessed [65]. Similarly, the absence of flexural modulus and hardness data ini-

tially lowered the PLA/Wood score, while the literature shows these values at 3940 MPa and 73.6D, fully meeting the immobilization requirements [66, 67]. The cautious scoring of PLLA due to the lack of safety data was revised based on the findings that showed a decomposition temperature above 200 ° C, non-flammability and resistance to water [68]. In other cases, the literature helped refine the initial conservative scores. For example, the CFF-PLA E-modulus of 2300 MPa, although slightly below ideal, still supports adequate splint rigidity [69]. rPP and rPLA initially lacked hardness data, which was later confirmed as 67A and 65D Shore hardness, respectively. Although potentially insufficient for immobilization, rPP's non-flammable characteristics remain beneficial [70]. rPLA also resists fire propagation [71]. This re-evaluation thus provides a more reliable and accurate representation of each material's potential for 3D printed splint applications.

Limitations

One limitation of this MCDA evaluation framework is that manufacturers use different testing methods. Importantly, there is no unified testing standard for 3D printed materials; existing standards apply primarily to specimens produced through injection molding. This lack of specific standards for additive manufacturing complicates the direct comparison of material properties between different studies and manufacturers [72].

A further limitation lies in the equal weighting of all criteria (sustainability, mechanical properties, user safety, and logistics). Sustainability and mechanical properties are likely more critical to the functionality of the splint and therefore should carry greater influence in the overall assessment. Future analyzes could improve accuracy by assigning different weightings to these parameters and calculating a weighted average total score to better reflect the relative importance of each criterion.

Lastly, even though efforts have been made to remain objective, assessing factors such as user safety and environmental impact can still involve some subjectivity. These factors are harder to measure and are largely dependent on existing literature and safety data. Involving experts with specialized knowledge could offer a clearer understanding of safety, environmental, and usability issues, making the evaluation more thorough, especially for criteria that are difficult to measure.

Future research

To address the limitations identified within the MCDA framework and assess the feasibility of using sustainable materials in the 3DxSplint project, more research is needed in several key areas.

The first area of research should focus on the practical implementation of rPETg and rPLA in hospital settings, particularly in terms of their recyclability at RadboudUMC and 3DLAB. This study should investigate whether the recycling process for these materials is sustainable, cost-effective and scalable in the specific context of medical 3D printing. In addition, the quality of the filament produced after recycling should be evaluated to ensure that it maintains the necessary mechanical properties and meets the required standards for clinical use. This research would help determine whether the use of recycled filaments for the 3DxSplint aligns with sustainability goals while maintaining the performance and reliability required for medical applications.

Another area of research should focus on how the 3D printing process influences the mechanical properties of rPETg and rPLA. This involves investigating any deviations between the printed materials and the manufacturer's technical data sheets in terms of tensile strength, flexural

modulus, and other relevant properties. Understanding how printing parameters, such as extrusion temperature, layer height, and print speed, affect the final material properties will provide insight into whether the materials can consistently meet the standards necessary for medical applications. This will also help optimize printing conditions to achieve the best possible material performance.

Finally, research should assess the user safety and comfort of rPETg and rPLA in real-world conditions. Specifically, this study should test the materials under realistic environmental conditions, including exposure to moisture, humidity, dust, and prolonged wear. This will determine whether rPETg and rPLA can withstand the stresses of everyday use, ensuring that they remain safe, durable, and comfortable for end-users. The testing could involve both mechanical durability tests and surveys or interviews with users to assess comfort and safety in practical scenarios, like wearing splints for extended periods in various environmental conditions.

Conclusion

In this literature review, 41 studies were systematically evaluated to identify and analyze potential sustainable materials for replacing ST45 in the 3DxSplint project. A multi-criteria decision analysis (MCDA) framework was applied to rank the materials based on four criteria and their requirement that align with the project's sustainability and performance goals. The analysis identified rPLA as the most promising substitute for ST45, offering both sustainability and logistical advantages. Other candidates, including rPETg and PLLA, demonstrated favourable properties, though trade-offs between mechanical performance, safety, and sustainability were noted.

While this study provides valuable insights into sustainable materials, more research is needed to assess their clinical feasibility. Future studies should focus on the recyclability and their practical implementation in hospital settings, the impact of 3D printing on the properties and striving for consistency in recycled materials. Finally, evaluating the user safety, comfort, and durability of these materials under real-life conditions is essential for their successful integration into the 3DxSplint application.

3 INVESTIGATING THE RECYCLING OF RPLA AND RPETG FOR THE 3DXSPLINT

Introduction

Recycling for 3D printing involves converting used plastic materials into new, printable filaments. Common methods include mechanical recycling shown in figure 3.1. Mechanical recycling involves physically shredding and melting the material to form a new filament. This simple and cost-effective process can degrade the properties of the material over repeated cycles [73, 74]. This degradation occurs due to the physical processes of shredding and melting, which expose the polymer chains to heat and shear forces, leading to chain scission, reduced molecular weight, and ultimately compromised mechanical properties [75]. The increasing emphasis on

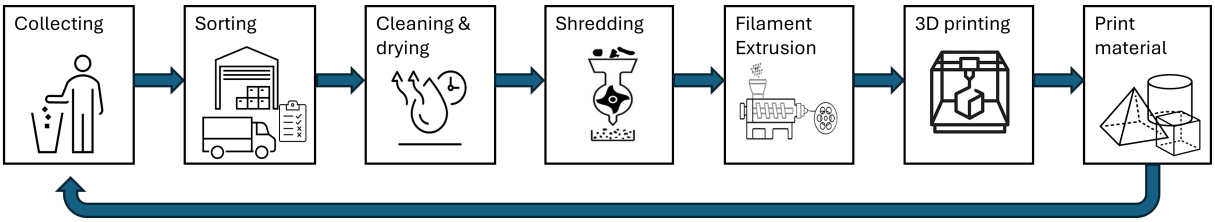

Figure 3.1: Mechanical recycling process for creating new printable filaments.

sustainable materials is also evident in the healthcare sector, where recycled plastics are increasingly applied in the production of medical devices, packaging, and prosthetics [76, 77]. Initiatives like those of SUEZ Recycling and Recovery in the UK and Philips in the Netherlands illustrate the efforts to incorporate recycled plastics into the manufacturing of medical products, improving sustainability without compromising quality [78, 79]. Similarly, Reflow, a Dutch company that specializes in sustainable 3D printing filaments, partners with research institutions to convert medical plastic waste into high-quality filaments for various applications [80]. Despite the presence of large-scale industrial recycling projects, local recycling options remain limited.

In the context of 3DxSplint and similar projects, several academic and industrial collaborations support the goals of this study. The Fraunhofer Innovation Platform for Advanced Manufacturing at the University of Twente focuses on advancing recycling and additive manufacturing processes, with relevant projects such as ”Waste2Print,” which investigates the use of recycled ABS to produce high-quality 3D printing filaments [81]. Furthermore, the Brightlands Chemelot Campus, through its CHILL (Chemelot Innovation and Learning Labs) initiative, is emerging as a hub for circular chemistry, focusing on the sustainable processing of raw materials, including plastics, aligning with the growing global demand for sustainable practices in 3D printing [82]. Furthermore, NHL Stenden University collaborates with Hartplastic to develop innovative solutions to minimize plastic waste in healthcare. This partnership emphasizes efficient resource management while maintaining high standards of patient care, thereby promoting circular economy practices within the medical sector [83, 84].

In light of these collaborations, the review of the literature in Chapter 2 identifies recycled Polylactic Acid (rPLA) and recycled Polyethylene Terephthalate Glycol (rPETg) as promising sustainable materials for the production of the 3DxSplint. Both materials exhibit high sustainability ratings, adequate mechanical properties, and strong safety profiles [34, 33, 40]. rPLA stands out because of its biodegradable nature and versatility. PLA has demonstrated potential as a biomaterial in numerous healthcare applications [36] and PETg is utilized as sterile packaging material for medical devices. The growing demand for PETG in medical applications highlights a high increase in potential plastic waste from medical grade PETG items, such as disposable medical products, packaging, and device components. As the market is projected to expand at a compound annual growth rate of 7% from $174.68 million in 2023 to $262.15 million in 2029, PETG consumption will increase substantially [85]. If PETG waste is not managed sustainably, this increase can contribute to medical plastic waste in hospitals. Its established use in hospitals and identification as a top candidate in the literature review further emphasize recycled PETg's potential for sustainable 3D printing applications. Previous research by NHL Stenden has also explored the recycling potential of rPETg, reinforcing its selection for this study as a viable option for sustainable 3D printing [86].

This study evaluates the feasibility of integrating the rPLA and rPETg recycling processes for the production of 3D printed splints. This objective is supported by collaborations with MAINIAC, RadboudUMC, CHILL, and NHL Stenden, utilizing industry and academic expertise. This investigation will assess material quality, production efficiency, and production scalability. To confirm whether these recycled materials can reliably meet the demands of clinical 3D printing workflows. Recycled materials in one cycle are expected to meet the quality standard for the splint. The recycling process of rPLA and rPETg will show increasing efficiencies as the scale of production increases. rPLA will be more scalable than rPETg, as rPLA is widely used in recycling processes and has established methods for handling larger production volumes.

Method

Partnerships were established with CHILL and NHL Stenden for the 3DxSplint project to assess the available recycling facilities. Communication with representatives of these institutions clarified their operational capabilities and limitations. Based on this information, a recycling setup was designed and implemented at both locations. Figure 3.2 illustrates the established recycling process.

Recycle production process of rPLA

At CHILL, the recycling process focused on post-extrusion PLA regrind sourced from ColorFabb [87]. To establish a baseline for comparison, BASF virgin PLA was evaluated at two filament diameters: 2.85 mm and 1.75 mm. After trials, 1.75mm was determined to offer more consistent extrusion quality. These are detailed in the Appendix B.

Printed material: Regrind PLA was first printed using a Bambulab X1 Carbon 3D printer with standard PLA settings and a 0.4 mm nozzle.
Shredding: The printed PLA was granulated using a ZERMA GSL-180/180 granulator, producing flakes with an average size of 4 mm.
Pelletizing: The granulated flakes were processed through a Coperion ZSK 18 MEGAlab twin-screw extruder. The material flow rate was set at 300 RPM, with the screw motor operating at 120 rpm. The extruder was configured with ten heating zones, ranging from 175 °C in the feed zone to 210 °C near the nozzle, increasing by 5 °C per zone. The nozzle temperature was maintained at 217 °C and the extrusion pressure was 18 bar. After extrusion, the material

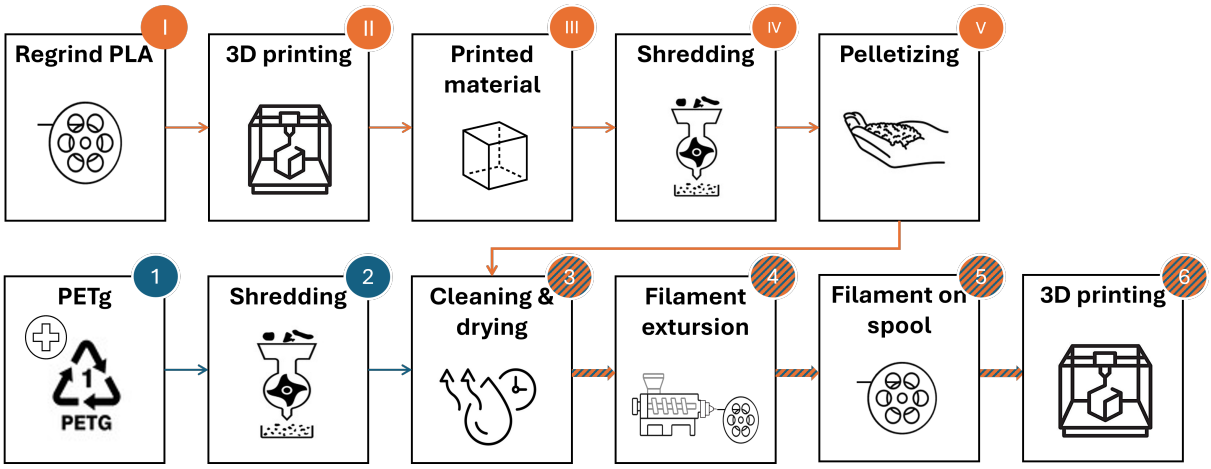

Figure 3.2: Recycling process established at CHILL and NHL Stenden. The workflows of both processes overlap at steps 3-6, where the labels I-V + 3-6 represent the steps taken at CHILL, while steps 1-6 denote those taken at NHL. At CHILL, the materials processed included regrind PLA from ColorFabb that was printed and recycled, whereas at NHL, PETG packaged hospital waste was utilized.

was cooled using a 20 °C water bath to ensure proper solidification and filament formation and followed by the blow drying and pelletization step with a rate of 9 m/min.
Cleaning & drying: The pellets were dried for 1.5 hours at 80 °C using a Binder VD3 vacuum oven to remove residual moisture.
Filament extrusion: The filament extrusion was performed using a 3Devo Precision 450 Filament Maker with the following settings: Heater 1: 180°C, Heater 2: 190°C, Heater 3: 185°C, Heater 4: 160°C, Extrusion speed: 3.7 RPM and fan speed: 60%. The final filament was produced with a diameter of 1.75 mm. The choice of these settings was based on prior experience with PLA recycling at CHILL.
3D printing: The filament was printed using PLA default settings on the Bambulab X1

Recycle production process of rPETg

At NHL Stenden, the recycling process utilized virgin PETg material, sourced from packaging used for sterile hospital instruments (without adhesive borders).

Shredding: The PETg material was granulated using a GP20 Plastic Shredder Hybrid from 3Devo to prepare the material for extrusion.
Cleaning & drying: Material was dried for 4 hours at 60 ° C using a 3Devo AIRID polymer dryer to ensure there was no moisture, which could affect the quality of extrusion.
Filament extrusion: The granulated PETg was extruded using a 3Devo Precision 350 filament maker, with a filament diameter of 2.85 mm, the machine set to 2.82 mm for precision. The extrusion settings were as follows: Heater 4: 210°C, Heater 3: 220°C, Heater 2: 230°C, Heater 1: 220°C, Extrusion speed: 6.5 RPM, Fan speed: 100%. The extrusion settings for rPETg were based on prior research by a PhD student who optimized parameters for this material type.
3D printing: The resulting filament was printed using modified settings of the default PETg setting of an Ultimaker 5S in the RadboudUMC 3D lab. Detailed protocol settings for these trials are provided in Appendix B.

Production Metrics

Effiency Metrics To quantify the production efficiency of the recycling processes, the following production metrics were tracked:

- **Material Loss:** With the material loss, the material efficiency can be determined, as it represents the remaining portion of the material after the process.
- **Production Time:** The time taken to complete each step is important for assessing operational efficiency
- **Production Energy:** The energy consumption of each machine during recycling steps was measured by multiplying the machine's power rating by the time the machine operated. Measurement of energy consumption highlights the environmental and economic impact of the recycling process.

Quality Metrics To ensure that the recycled filament was of high enough quality for applications, the following evaluations were performed:

- **Filament Weight:** The final weight of the filament was measured after the spooling step to assess the material yield.
- **Filament diameter upper and lower limits:** For a filament to be printable, its diameter must consistently fall within a specific range; diameters too small leads can cause underextrusion due to insufficient material flow, while diameters larger can result in blockages or jamming in the extrusion system. The filament diameter was manually measured at multiple points to determine deviations from the target diameter of 1.75 mm +- 0.05 mm (for rPLA) and 2.85 mm +- 0.05 mm (for rPETg).
- **Visual Inspection:** Filaments were visually inspected for inconsistencies, defects, or discolorations that could affect their usability.
- **Printability Assessment:** Filaments were tested on a Bambulab X1 Carbon 3D printer (for rPLA) and an Ultimaker 5S (for rPETg) to assess their printability. The successful printing of a 3DxSplint model was used as a benchmark for this assessment.

Scaling Potential Metrics To evaluate how efficiently a process performs, on a per-unit basis (one splint) or for larger-scale production (multiple splints):

- **Time and energy per unit:** The total time and energy required to produce enough filament material for a 3DxSplint (details provided in Appendix B). They were recalculated by factoring in material losses during recycling and standardizing the output material. This adjustment ensures an accurate scalability assessment, providing normalized comparisons for both time and energy that eliminate bias from differing initial volumes.
- **Upscaling:** Based on the recalculated values for a single 3DxSplint, an extrapolation was performed to predict the performance of the process when scaling to larger quantities (up to n = 50). These numbers were chosen because 53,000 patients with lower arm fractures were treated in emergency care locations. This averages to approximately 54 patients per month per location. However, not every patient is suitable for 3D printed splint treatment, making 50 a reasonable and manageable number to assess feasibility in Radboudumc. The time and energy consumption for the shredding, pelletizing, and filament extrusion steps was directly related to the volume of the material and was scaled proportionally to the number of 3DxSplints being processed. The cleaning & drying step and the spooling before and after the filament extrusion were considered independent of the volume of the material.

Table 3.1: Production metrics of both recycling processes

Production metrics	PLA recycling at CHILL	PETg recycling at PETg
Efficiency		
Material loss	53.5 %	31.4 %
Production energy	19.6 kWh	5.4 kWh
Production time	330 min	345 min
Quality		
Filament diameter range	1.6-1.82 mm	2.6-3.00 mm
Filament weight	202 g. (75m)	212 g. (48m)
Visual inspection:	Diameter fluctuations	Encapsulated flakes
Printability:	Unsuccessful	Successful
Scaling potential		
Time for a 3DxSplint	149 min	283 min
Energy for a 3DxSplint	2.9 kWh	4.2 kWh
Upscaling	factor 10x increase	factor 3-4x increase

Results

The results of the metrics, efficiency, quality, and scaling potential, obtained from the rPLA and rPETg recycling processes, are presented in Table 3.1. Production efficiency is determined by the energy consumption, time consumption, and material loss (ML) measured for each step. Figure 3.3 illustrates the power consumption (P), the total duration (T), and the material loss (ML) for each phase of the process.
The key difference between rPLA and rPETg recycling lies in the filament extrusion phase. rPLA demonstrates a two times higher ML of 49.5%, mainly due to diameter inconsistencies and removal of contaminated material. In contrast, rPETg achieves a lower ML of 25.9%, thanks to the optimized spooling time and the rapid achievement of a consistent filament diameter. This optimization resulted in a one hour shorter extrusion time.

Additional ML for rPLA were observed during pelletization (5.6%) and shredding (2.3%). These phases involved the formation of dust, the escape of flakes, and residual material. The pelletization was an additional step compared to the rPETg process. This required more time (75 min) and energy (14.75 kWh), making it the most energy-intensive step. In contrast, rPETg experienced higher losses in shredding (6.81%) but minimal losses in the cleaning and drying phase (0.65%). However, this final step for rPETg was the most time consuming (4h), requiring an additional 2.5h compared to rPLA, where the duration was reduced due to time constraints.

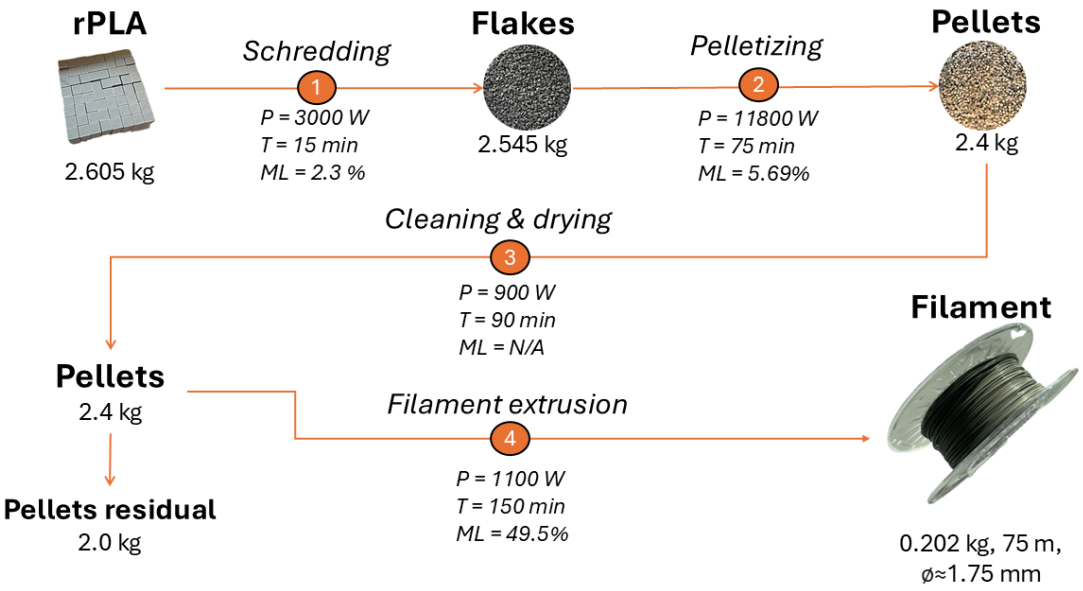

(a) This figure illustrates the recycling process for rPLA at CHILL, showing each recycling step: 1) Shredding, 2) Pelletizing, 3) Cleaning and Drying, and 4) Filament Extrusion. The power consumption (P), total duration (T), and material loss (ML) percentage are provided for each step. The produced filament is depicted at the end of the process.

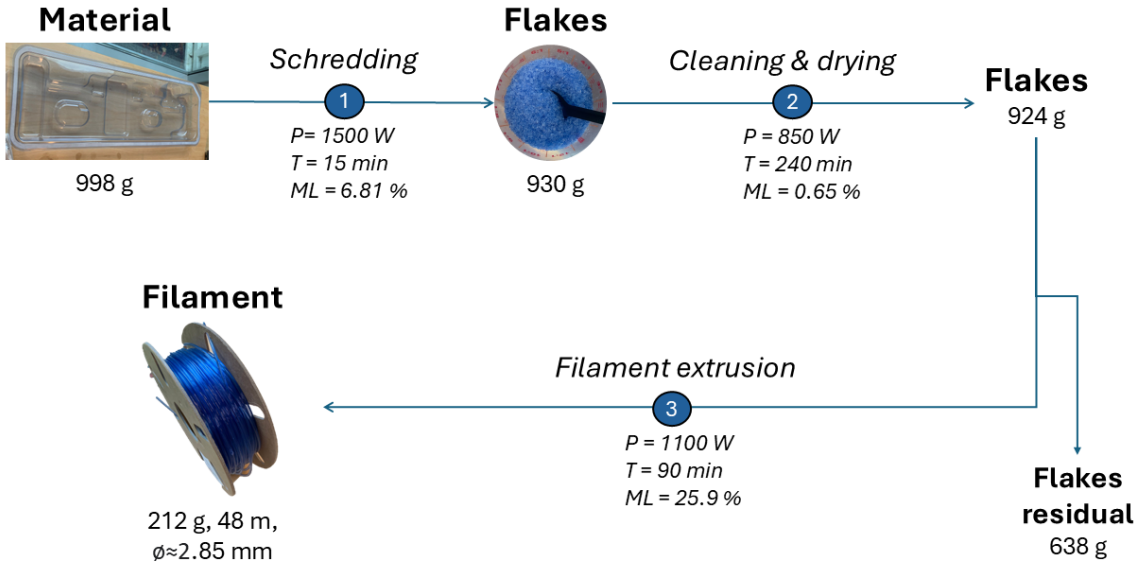

(b) This figure presents the recycling process for rPETg at NHL, with the steps: 1) Shredding, 2) Cleaning and Drying, and 3) Filament Extrusion. For each step, the power consumption (P), total time (T), and material loss (ML) percentage are shown. The produced filament is depicted at the end of the process.

Figure 3.3: Comparison of Recycling Timelines, Duration, and Energy Consumption for rPLA and rPETg recycling processes at NHL and CHILL.

A total of 220 grams (75 meters) of rPLA filament was produced, compared to 212 grams (48 meters) of rPETg filament. The quality of the rPLA filament exhibited a consistent round shape with visible fluctuations in diameter. The filament was tightly packed; no air bubbles, moisture,

or dust were present. The rPETg filament showed a constant diameter and encapsulated flakes were observed. No dust or air bubbles were detected.

For the printability assessment, rPLA was unsuccessful. Issues such as nozzle clogging and filament inconsistencies were encountered, leading to print failures on the Bambu Lab printer when using default PLA settings. For rPETg, the printability assessment was successful; however, there were some extrusion errors caused by encapsulated flakes, which led to nozzle blockages and inconsistent material flow. In Figure 3.4, the successful 3DxSplint printed with rPETg material is displayed.

Figure 3.4: The 3DxSplint printed without support structures using recycled PETg material on an Ultimaker S5, employing generic PETg print settings and a print temperature of 230°C

The 3DxSplint requires 43 grams of material to print the design with Ultimaker S5 (design in figure 3.4). Taking into account material losses in recycling processes, rPLA incurs a total loss of 53.5%, requiring 92.4 grams of material to produce 43 grams of filament. In contrast, rPETg has a total loss of 31.4%, which requires 62.7 grams of material to produce the same filament. Following this, the total processing time and energy consumption for each material were calculated to produce one 3DxSplint (shown in figure 3.5). For rPLA, the total processing time was updated to approximately 148.69 minutes (approximal 2.5 hours), In contrast, the processing time for rPETg was determined to be approximately 283.14 minutes (or 4.7 hours). The total energy consumption of rPLA after reanalysis was 2.9 kWh, with the cleaning and drying step accounting for 46% of this total. In contrast, the rPETg recycling process consumed 4.2 kWh, with 81% of the energy attributed to the cleaning and drying step.

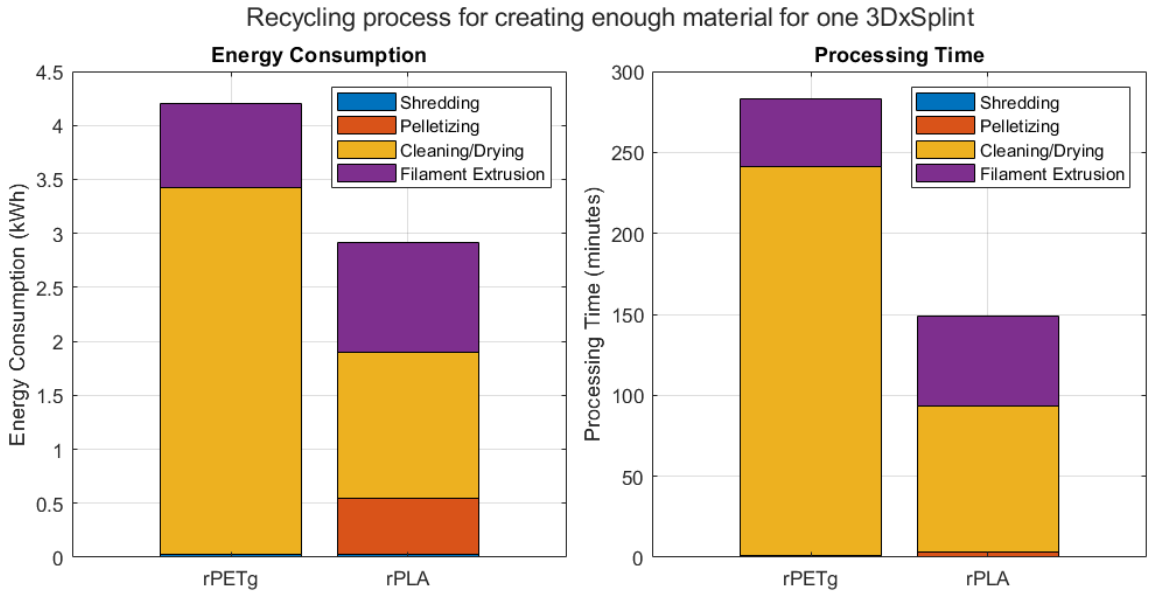

Figure 3.5: Stacked bar plot depicting the energy consumption and processing time associated with each step of the recycling process, calculated for the production of a single 3DxSplint, with distinct data presented for rPLA and rPETg

The stack bar graphs (Figures 3.6, 3.7) illustrate how time and energy consumption evolve as the number of splints increases both rPLA and rPETg. For the rPETg recycling process, producing enough material for 50 splints requires approximately three times the time consumption and four times the energy compared to producing material for a single splint. In contrast, the rPLA recycling process requires ten times more time and energy to generate sufficient material for 50 splints. The filament extrusion step exhibits the greatest increase in both time and energy consumption as the number of splints increases, especially considering the fixed spooling time.

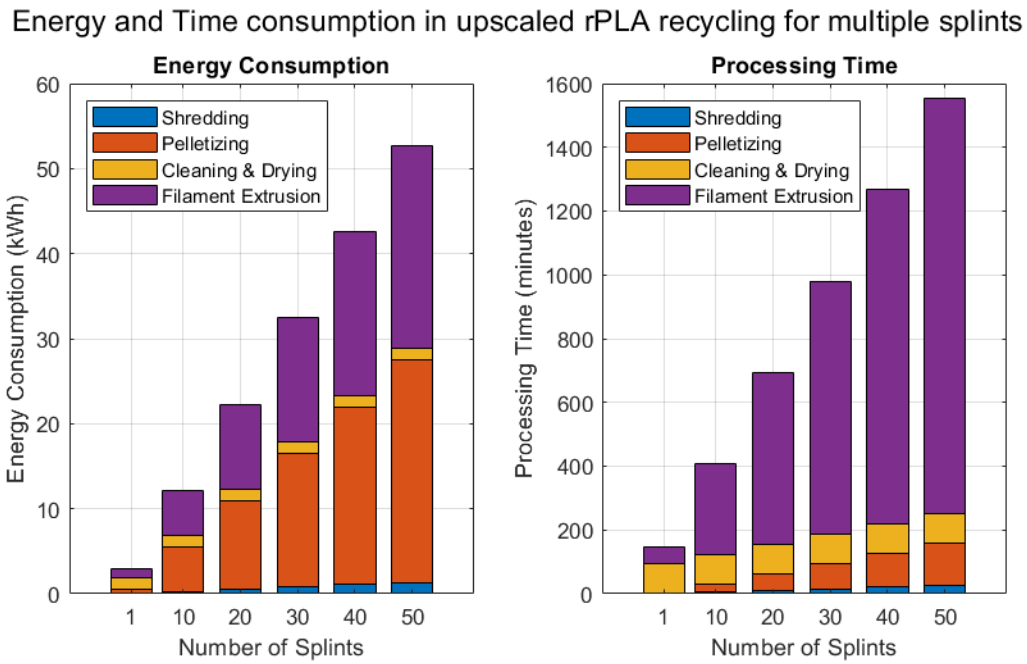

Figure 3.6: Stacked bar plot showing the expected time and energy consumption for each step of the rPLA recycling process when upscaled to produce multiple 3DxSplints. The plot includes the total consumption for varying quantities of splints (n = 1 to 50), highlighting the impact of scaling on time and energy requirements across the shredding, pelletizing, cleaning/drying, and filament extrusion steps.

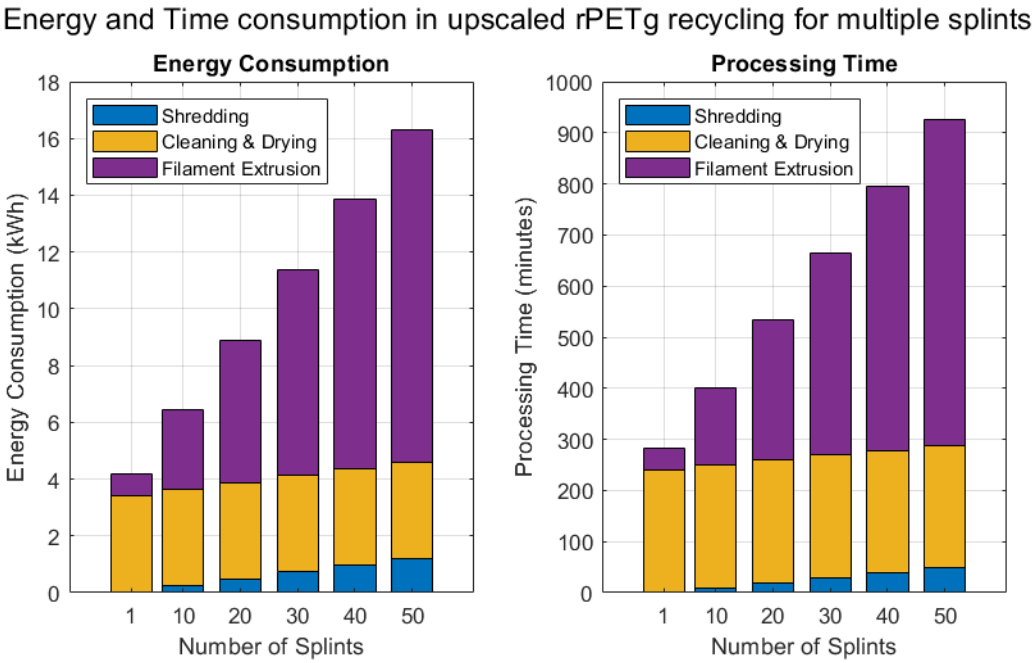

Figure 3.7: Stacked bar plot illustrating the anticipated time and energy usage for each stage of the rPETg recycling process when scaled up for the production of multiple 3DxSplints. The chart displays the total consumption for different quantities of splints (n = 1 to 50), emphasizing how scaling influences the time and energy demands in the shredding, cleaning/drying, and filament extrusion stages.

Discussion

This investigation evaluates material quality, production efficiency, and scalability to determine whether the recycled PLA and PETg process can meet the demands of clinical 3D printing. The findings suggest that, while both materials have potential, the PETg recycling process in NHL shows better efficiency and scalability. Furthermore, the quality of the rPETg filament was sufficient for the 3D printing of a splint, making it a more viable option for clinical applications.

Based on the results obtained from this study, rPLA does not appear to be a feasible option to integrate the recycling process. Both recycling processes were expected to meet the quality demand; however, the primary challenge observed was related to the equipment used. At the CHILL location, numerous issues arose with the 3Devo filament maker, and the absence of a backup system limited the options to address these challenges. This equipment became a significant bottleneck, consuming considerable time and material resources. According to 3Devo, PLA is recyclable but suggests using small shredding pieces using the GP20 shredder & Granulator before the filament extrusion step [88].

The recycling process efficiency was also expected to increase as the volume increased. This was experienced with the process. During the pelletization step, material loss could decrease with increased volumes due to the fixed volume of material required to fill and spool the screw. Similarly, the volume needed and the time for spooling remain constant with each startup for the 3devo filament maker. It would be ideal if every step could run for longer periods. This would minimize material loss, spooling time, and eventually production efficiency.

For rPETg, the production of filament for multiple splints required approximately three times the time and energy of the production of a single splint, whereas rPLA requirements increased tenfold, pointing to greater energy and resource efficiency in rPETg. This is due to the optimized protocol at NHL scaling up production with rPETg, which is likely to result in more energy and resource savings. These advantages highlight the potential of rPETg as a sustainable material choice for high-demand manufacturing environments, where energy efficiency and process consistency are paramount for both economic and environmental reasons. In contrast, rPLA recycling was in earlier phases at CHILL, where filament production equipment was less frequently used, and was shorted in the drying step because of time constraints. This underscores the need for expertise and optimized protocols before it has scalability potential.

The rPLA filament produced at CHILL measures 1.75 mm, which is incompatible with the current 2.85 mm RadboudUMC printers. This diameter was chosen because extrusion and diameter consistency were better than trying to achieve this with a 2.85 mm filament. In addition, this Bambu Lab X1 Carbon printer is better equipped to adjust the extrusion flow from the nozzle. If it detects a slightly larger or smaller filament diameter, the flow rate is automatically adjusted. However, this adjustment only works effectively if the diameter is consistently smaller than or larger than 1.75 mm. It cannot handle fluctuations that alternate between being larger and smaller. The Bambu Lab, already tested in this process, is a promising option. It can print a splint in approximately 1 hour and 19 minutes, faster than the 6 hours and 37 minutes required on the current Ultimaker S5 from RadboudUMC [89]. Equipped with advanced features, including active vibration compensation for high accuracy and smooth prints, the Bambu Lab printer offers improved efficiency, allowing faster delivery of custom splints and improving patient care, making it a valuable investment for RadboudUMC.

Limitations

A limitation of this study is the difference in the locations and equipment used for recycling processes, making a direct comparison difficult. At CHILL, the 3Devo filament maker was underutilized and lacked optimization due to inexperience, while at NHL, the process was refined and optimized by an experienced PhD researcher. These variations in equipment use and expertise may have influenced the results and should be considered when comparing the two recycling methods.

The extrapolation for the scalability assessment of multiple splints for rPETg and rPLA were based on data from a single recycling process. This limitation may influence the accuracy of the calculations as it assumes that the conditions and efficiencies observed in the production of one splint will remain consistent when scaling up. Variations in material quality, machine performance, or process optimization on larger scales could lead to deviations from the extrapolated results, affecting the reliability of the scalability assessment.

Another limitation of current recycling processes is the need for close monitoring during the filament extrusion step. This step requires continuous oversight to ensure that the material flow rate is consistent, that there are no issues with the filament spooling process around the spool, and that there is an adequate supply of material in the feeder. These factors must be carefully checked to avoid interruptions or inconsistencies in filament production. However, if the production process was to be scaled up, the need for prolonged monitoring would become a major challenge, as it would require more time and attention. This level of oversight is not the most practical solution for large-scale or continuous production, as it adds logistical complexity and increases labor demands.

The rPETg filament production process reveals limitations that impact the suitability of recycled filaments for 3D printing splints. When comparing printability with earlier batches of recycled PETg made at NHL, adjusting the settings for each new batch was necessary, highlighting inconsistencies in filament quality. Although 3D printed splints can be made with recycled PETg material, the current production process makes it difficult to produce high-quality and reliable filaments in every recycling phase.

Future research

To enhance the effectiveness and sustainability of the recycling process for rPLA and rPETg, optimizing filament production is essential. This involves determining the optimal volume of material that should be recycled in a single batch to minimize material loss during the extrusion process. Specifically, it is crucial to identify a threshold volume that allows material loss reduction to its lowest possible level while avoiding the inefficiencies associated with recycling over multiple days.

To enhance the production of printable filament from rPLA in future iterations, some recommendations should be considered. First, extend the drying step, since a longer drying duration will effectively remove moisture, which is important for improving filament quality and ensuring successful printing. Second, incorporating 3DevoVision software for real-time monitoring of filament diameter would enable immediate adjustments, fostering greater consistency in filament quality, which is necessary for reliable 3D printing.

Furthermore, future research should compare the energy consumption and production time of 1.75 mm and 2.85 mm FDM 3D printers for printing splints, while also determining the quality

of the prints. This study would help identify the most efficient filament size for producing high-quality medical splints quickly, balancing sustainability with the need for timely patient care. Additionally, it would assess whether a 1.75 mm printer would be a good investment for the 3D lab at Radboudumc to print 3DxSplints in the future.

Additionally, it is imperative to investigate whether recycled rPETg and recycled PLA meet the immobilization requirements for 3D printed splints. Mechanical testing is recommended to evaluate its suitability. By addressing these considerations, the overall efficiency and applicability of the recycling process can be improved, ensuring that the materials produced meet the necessary performance standards, while also being economically viable.

Conclusion

This study evaluated the feasibility of integrating rPLA and rPETg for the production of 3DxSplints. The comparison between the recycling processes of rPLA at CHILL and rPETg at NHL highlighted notable differences in efficiency, quality, and scalability. PLA recycling struggled with significant material losses and high energy consumption, though it was slightly faster in production. PETg was shown to be more efficient with lower material losses and energy requirements despite taking slightly longer to process. In terms of quality, PLA filament exhibited inconsistent diameters, leading to unsuccessful printing, while PETg maintained better diameter stability, resulting in successful printability despite some visual imperfections. Scalability analysis showed that, when normalized for a single 3DxSplint, PLA consumes less time and energy than PETg. This makes PLA seem more efficient for producing individual units. However, when the production process is scaled to support multiple splints, the inefficiencies of PLA become apparent. Due to its time and energy demand, PLA recycling increases significantly more than PETg recycling, which remains more stable and reliable under higher production volumes. This disparity highlights PETg recycling as a more efficient and practical option for upscaling and integration in the production of 3DxSplints. More research is needed to optimize the consistency of the filament and scalability of the processes to explore the potential of a circular economy. In addition, mechanical testing of the recycled filaments is essential to confirm their suitability for 3D printed splints.

4 MATERIAL TESTING

Introduction

The chapter 3 underscores the potential of using rPLA and rPETg in 3DxSplint production. Before adopting a local recycling cycle for materials used in the production of the 3DxSplint, it is crucial to assess the mechanical properties of the recycled materials. For these recycled materials to be suitable, they must exhibit mechanical properties similar to ST45 or at least show predictable changes in mechanical properties, ensuring that they provide support, protection, and durability (immobilization of the lower arm fracture) for the 3DxSplint as stated in Figure 2.2. Mechanical tests like tensile and impact tests are important because they evaluate the influence of recycling on material properties and assess whether recycled materials can be suitable alternatives to the ST45 material currently used in the 3DxSplint.

To date, most technical data sheets (TDS) for 3D printing materials present mechanical properties based primarily on injection-molded specimens, as required by standardized testing protocols such as ISO and ASTM [90, 91]. These standards specify that mechanical properties should be measured using injection-molded samples to ensure consistency and comparability between materials and testing methods. However, for 3D printing applications, it is more relevant to assess material properties based on printed specimens rather than molded samples, as the specific characteristics of the printing process, including layer adhesion, anisotropy, and surface finish, significantly influence the final mechanical properties. Gardan (2016) underscores that additive manufacturing introduces unique variables not present in traditional manufacturing, highlighting how parameters such as print orientation, layer thickness, and infill density affect part performance and durability in ways that standardized molding processes do not account for [92]. A review of the literature suggests that these materials may perform better in specific categories than initially scored based on technical data sheets of only one available material [72].

Manufacturers are adapting their testing approaches to better align with the unique properties of 3D printing. For example, companies such as Ultimaker provide mechanical property data for specific print orientations, allowing users to understand how strength and durability vary according to the orientation of parts during printing [93]. ColorFAbb offers comprehensive data that include injection-molded and 3D printed specimens, providing a broader perspective on material performance under different manufacturing conditions [87].

The primary objective of this study is to evaluate the mechanical properties of virgin and recycled PLA and PETg compared to ST45, the resin material currently used in 3D printed splints. Furthermore, the study seeks to assess how the recycling process impacts the mechanical properties of these materials. This is framed by the following research question.

Research Question:
How do the mechanical properties of virgin and recycled PLA and PETg compare with the mechanical properties of ST45 resin, and what is the influence of recycling on the performance of

PLA and PETg?

Hypothesis:
Recycled PLA and PETg will exhibit lower mechanical performance compared to their virgin counterparts due to material degradation during the recycling process. However, rPLA is expected to demonstrate mechanical properties more comparable to those of ST45 resin than those of rPETg, positioning it as a closer sustainable alternative for applications in the 3DxSplint. Both recycled materials, despite their reduced performance, will show sufficient potential to serve as sustainable options.

Method

The materials used include the current material in the splint, the virgin options of PLA and PETg, and the recycled material. The rPETg is made from the recycling process analyzed in the previous study at NHL Stenden. The choice of virgin materials manufacturers was determined by the availability of filaments in the 3D lab at Radboudumc, rather than any other specific reason.

- **Ultracure3D® ST45 B**: Available by BASF, ST 45 produced by Forward AM, is a reactive urethane photopolymer developed for tough applications that require an exceptional combination of mechanical strength, long-term toughness, and impact resistance [8]. This material can be printed using stereolithography, digital light processing, or liquid crystal display machines. This material is the reference material in this study, as it is currently used in the 3DxSplint at RadboudUMC [7],[12].
- **Ultrafuse® PLA**: For a virgin material, we can compare the recycled data with the PLA produced by forward AM and available by BASF. PLA is the most used print material, since its plant-based origin and has a high printing speed, combined with low warping and sharp corners [94].
- **ColorFabb PLA Regrind**: PLA Regrind is manufactured entirely from postproduction waste generated during the extrusion of colorFabb's high-quality printing filaments. The production team carefully collects and segregates PLA filament that does not meet the specifications, which is then processed internally to produce the recycled PLA regrind [87].
- **Ultimaker® PETg**: This is the virgin material with which we compare the mechanical properties of the recycled PETg material. PETg is a good all around material and is more heat resistant and chemical resistant than PLA and easy to use [93].
- **Hartplastic rPETg**: The recycled PETg material comes from clean PETg waste collected from Leeuwarden Hospital, then recycled once and manufactured at NHL Stenden Hoggeschool in collaboration with Hartplastic [95], a start-up company based in The Netherlands.
- **Hartplastic rPETg 2th cycle**: The recycled PETg material comes from earlier recycled PETg collected, then recycled a 2nd time and manufactured at NHL Stenden hogeschool in collaboration with Hartplastic [95], a start-up company based in the Netherlands.

Tensile testing

The tensile test aims to quantify the mechanical properties of materials by measuring key parameters, including the following:

- Ultimate Tensile Strength (UTS): This is the maximum stress a material can withstand while being stretched before it fractures. Provides information on the load bearing capacity of the material.
- Young's modulus (E-modulus): This parameter measures the stiffness of a material, indicating its ability to resist deformation when subjected to stress. A higher Young's modulus means a stiffer material.

These parameters help to evaluate the mechanical performance of materials intended for use in the 3DxSplint. Tensile testing was performed according to ISO 527-1, which provides the framework for measuring these parameters of plastics [90].

According to this standard, specimens should be prepared by injection molding to achieve uniformity and reproducibility in mechanical testing. However, this study deviated from the ISO 527-1 standard, as the specimens were printed (shown in Figure 4.1). This choice was made to align with the print materials and processes specific to the 3D printing of the 3DxSplint, though it may introduce variability in the results compared to those from some manufacturing TDS. The tensile properties of the ST45 TDS of the manufacturer BAS-F uses ASTM D638, but the TDS of PLA BAS-F uses ISO 527. Whereas Ultimaker uses ASTM D3039 for PETg, colorFabb uses ISO 527-1A. Compared to ISO 527, ASTM D638 is comparable as both use similar dumbbell-shaped specimens and assess plastics under tension. Differences arise in the dimensions and preparation of the specimen, which might slightly affect the results. The ASTM D3039 is not directly comparable due to the different shapes of the specimen and its focus on composites rather than thermoplastics.

Type 1A specimens were printed with the following dimensions, as illustrated in Figure 4.1b and detailed in Table 4.1.

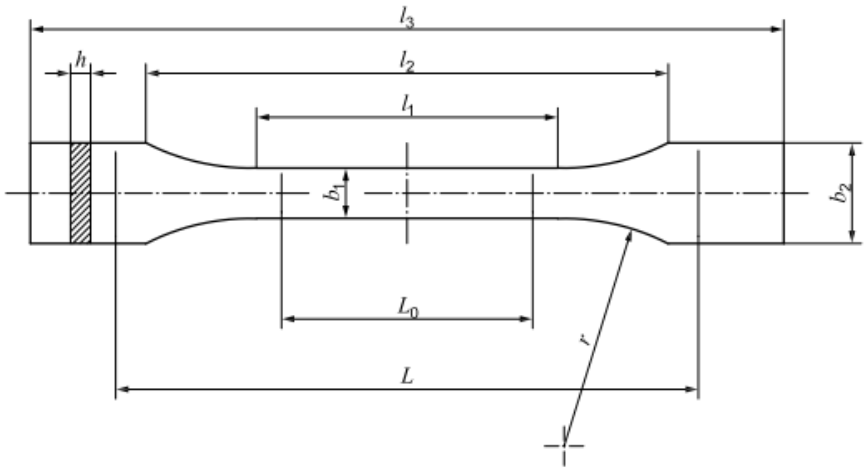

(a) Type 1A tensile test specimen according to ISO 527-1.

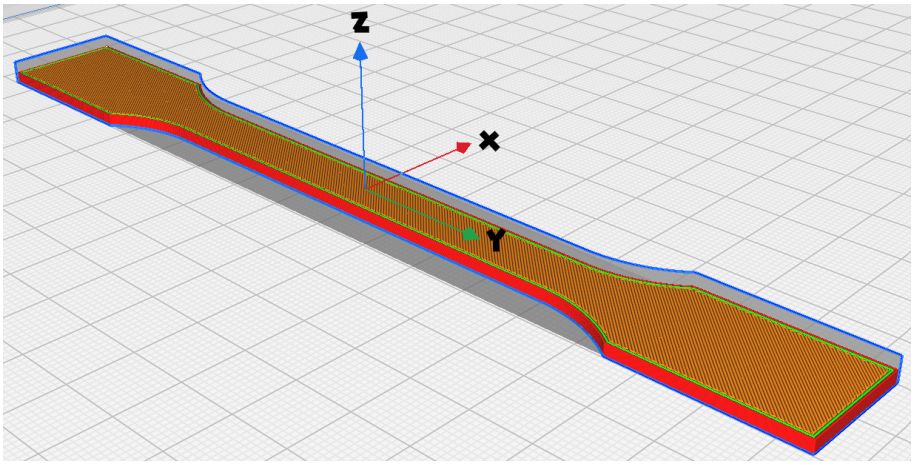

(b) Printed version of the tensile test specimen, with zig-zag pattern and 100% infill, 5 were printed next to each other for the test.

Figure 4.1: Tensile test specimens: dimensions and printed version.

Table 4.1: Dimensions of Specimen Type 1A according to ISO 527-1 and printing parameters

Dimension	**Specimen Type 1A**
Overall length (l_3)	170 mm
Length of narrow parallel-sided portion (l_1)	80 ± 2 mm
Radius (r)	24 ± 1 mm
Distance between broad parallel-sided portions (l_2)	109.3 ± 3.2 mm
Width at ends (b_2)	20.0 ± 0.2 mm
Width at narrow portion (b_1)	10.0 ± 0.2 mm
Preferred thickness (h)	4.0 ± 0.2 mm
Gauge length (L_0, preferred)	75.0 ± 0.5 mm
Gauge length (acceptable if required for quality control or when specified)	50.0 ± 0.5 mm
Initial distance between grips (L)	115 ± 1 mm
Printing Parameters	**Value**
Infill Density	100%
Layer Height	0.15 mm
Nozzle Diameter	0.4 mm

The printing process involved fabricating a minimum of five specimens concurrently for each material category, including virgin PLA, ST45, and virgin PETg. All specimens were printed witch the dimensions and settings as described in table 4.1. Detailed printing settings are available in Appendix C, the printers utilized were Ultimaker S5 and Bambu Carbon X1. The printing parameters were meticulously optimized for each material to ensure consistency and quality across the resultant test specimens.

Tensile testing was performed using the Zwick/Roell Z020 tensile testing machine. The testing protocol involved a crosshead speed of 50 mm/min, with data acquisition occurring at a frequency of 10 Hz via the Zwick TestXpert II V3.71 software according to ISO 527-1. The samples were tested without prior conditioning and all experiments were performed in a controlled laboratory environment to mitigate the influence of external variables. The calibration of the test machine was performed before each session to ensure the precision of the measurement and of each specimen, the thickness (h) and width (b1) were measured. The software calculated the following mechanical properties:

Young's modulus is calculated from the slope of the stress-strain curve in the elastic region:

$$E = \frac{\Delta\sigma}{\Delta\epsilon} \tag{3}$$

Where:

- E is Young's modulus in megapascals (MPa);
- $\Delta\sigma$ is the change in stress (in MPa);
- $\Delta\epsilon$ is the change in strain (dimensionless), calculated as:

$$\Delta\epsilon = \frac{\Delta L}{L_0} \tag{4}$$

  with ΔL being the change in length (in millimetres) and L_0 being the original gauge length (in millimetres).

The ultimate tensile strength is calculated as:

$$\sigma_{UTS} = \frac{F_{max}}{A_0} \tag{1}$$

Where:

- σ_{UTS} is the ultimate tensile strength in megapascals (MPa);
- F_{max} is the maximum force (in newtons) applied to the specimen at the point of fracture;
- A_0 is the original cross-sectional area (in square millimetres) of the specimen, calculated as:

$$A_0 = b_1 \times h \tag{2}$$

Impact test

The impact test is essential for assessing the resistance of the material to sudden and forceful impacts, which is crucial for applications such as 3D printed splints. The primary parameter measured during this test is the following.

- Impact Strength: This is defined as the energy absorbed per unit cross-sectional area of the specimen, indicating the material's toughness and its ability to withstand abrupt forces without fracturing.

For 3D printed splints, high impact resistance is vital to ensure the splint can endure accidental knocks and impacts during daily activities, thus ensuring the reliability and durability of the splint in real-world conditions and providing continuous protection and support to the patient. The impact test is conducted according to ISO 179-1 [96], which specifies the procedure for measuring the impact resistance of materials using notched specimens. Type 1A test specimens were printed for the impact test, as illustrated in Figure 4.2a without notch and detailed in Table 4.2. The specimens were notched using the Zwick/Roell ZNO notch machine with type A notches (available at the testing facility). The printing parameters for each material were optimized to ensure uniformity and quality in all samples. A minimum of 10 samples per material were prepared without conditioning before testing.

The impact energy values from the manufacturer's TDS for the materials show varying degrees of comparability to the ISO 179-1 Type 1A test. For ST45, which uses ISO 179-1, the TDS value is directly comparable, provided the same Type 1A notch is used. However, Ultimaker PETg uses ISO 179-1 with a Type B notch (radius of 1.00mm compared to 0.25mm for Type 1A), which could significantly affect test results, making any comparison more qualitative than quantitative. On the other hand, BASF's PLA, tested under ISO 179-2, is not comparable since ISO 179-2 involves instrumented testing that measures dynamic properties during impact, which differs fundamentally from the non-instrumented ISO 179-1. Lastly, for Colorfabb regrindPLA, the specific ISO 179 substandard and notch type are not mentioned; therefore, it is difficult to compare them.

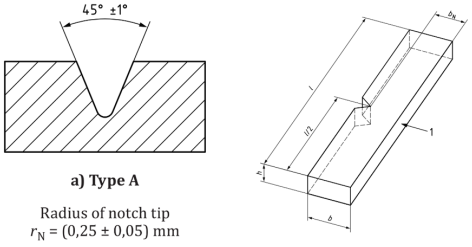

(a) Charpy Impact Test Specimen 1A according to ISO 179-1, where 1 is the angle of the impact load.

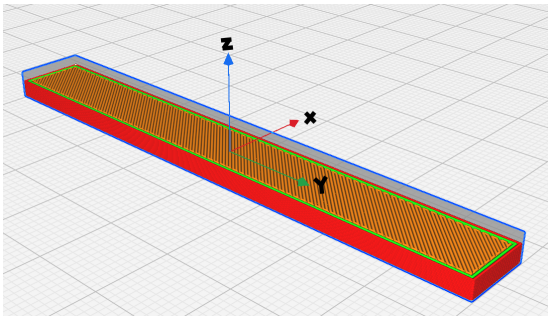

(b) Charpy Impact printed specimen, without notch. Printed with 100% infill and zigzag pattern. The specimens were printed next to each other for the test.

Figure 4.2: Difference between the ISO standard specimen and the 3D printed specimen without a notch.

Table 4.2: Dimensions and Specifications of Charpy Specimen Type 1A according to ISO 179-1 and printing parameters

Dimension	**Specimen Type 1A**
Length (l)	80 ± 2 mm
Width (b)	10.0 ± 0.2 mm
Thickness (h)	4.0 ± 0.2 mm
Span (L)	62 mm
Notch Tip Radius (r_N)	0.25 ± 0.05 mm
Remaining Width (b_N) at Notch Tip	8.0 ± 0.2 mm
Printing Parameters	**Value**
Infill Density	100%
Layer Height	0.15 mm
Nozzle Diameter	0.4 mm

The Charpy impact test was performed using the Zwick/Roell HIT5.5P impact machine according to ISO 179-1/1eA standards. A 1 J pendulum was used to measure the impact strength, which was calculated from the absorbed energy. The Charpy impact strength of the notched specimens, a_{cN}, is calculated with the Zwick testXpert III software using the equation:

$$a_{cN} = \left(\frac{W_c}{h \times b_N} \right) \times 10^3 \tag{2}$$

Where:

- a_{cN} is the Charpy impact strength, in kilojoules per square metre (kJ/m²);
- W_c is the corrected energy, in joules, absorbed by breaking the test specimen;
- h is the thickness, in millimetres, of the test specimen;
- b_N is the remaining width, in millimetres, of the test specimen;

Data processing

Given the small sample size and the assumption of nonnormal distribution in the data, nonparametric tests were selected to ensure robust comparison between groups. To verify the data tested with the properties indicated in the TDS, the properties of the tested material were compared with the manufacturer's TDS values (only comparable ones) using the Wilcoxon signed rank test with a significant level of α = 0.05. The observed differences and similarities provide important information on the accuracy and applicability of the TDS data in real world scenarios. To compare the ST45 values tested with recycled materials, the Kruskal-Wallis test was used to assess differences, while the Mann-Whitney U test was applied for pairwise comparisons between ST45 and rPLA or rPETg. For recycling comparisons, the Kruskal-Wallis test was also used to assess differences in material properties across multiple recycling cycles, while the Mann-Whitney U test was applied for pairwise comparisons between virgin and single-cycle recycled materials. Statistical analysis was used with the R version 4.4.1 software.

Results

Table 4.3 presents the test results from the tensile and Charpy impact tests along with the manufacturer's TDS values and the p-values of the Wilcoxon signed rank tests of comparable

values. In Figure 4.3 the tested values are presented in boxplots and a stress strain graph of the average curve per material.

Table 4.3: Mechanical properties of materials with test and TDS values and p-values from Wilcoxon signed-rank tests ($\alpha = 0.05$) from the manufacturers TDS which used ISO 527 and ISO 179-1/1eA.**No TDS available of 3D print material.

Material	Test Parameter	Test Result	TDS	P-value*
BAS-F® ST45 B	Impact energy [kJ/m^2]	3.06 ± 0.11	2.6	0.006
	Young's modulus [MPa]	2050 ± 47	2000	0.12
	Tensile strength [MPa]	58.7 ± 1.2	53	0.06
BAS-F® PLA	Impact energy [kJ/m^2]	2.82 ± 0.43	2.5	-
	Young's modulus [MPa]	3006 ± 33	2308	0.06
	Tensile strength [MPa]	51.4 ± 1.1	34.7	0.06
ColorFabb PLA Regrind	Impact energy [kJ/m^2]	3.08 ± 0.26	2.9	0.037
	Young's modulus [MPa]	3050 ± 48	3150	0.008
	Tensile strength [MPa]	54.4 ± 0.5	53	0.008
Ultimaker® PETg	Impact energy [kJ/m^2]	2.17 ± 0.6	7.9	-
	Young's modulus [MPa]	1289 ± 41	1939	-
	Tensile strength [MPa]	28.6 ± 0.7	38.5	-
Hartplastic rPETg (1st Cycle)**	Impact energy [kJ/m^2]	3.00 ± 0.91	-	-
	Young's modulus [MPa]	1293 ± 22	-	-
	Tensile strength [MPa]	27.9 ± 0.7	-	-
Hartplastic rPETg (2nd Cycle)**	Impact energy [kJ/m^2]	1.75 ± 0.54	-	-
	Young's modulus [MPa]	-	-	-
	Tensile strength [MPa]	-	-	-

E-modulus

In Figure 4.3a, we observe similar E-modulus values between virgin and recycled materials for both PETg and PLA. The comparison between PETg and rPETg yields a $p = 1$, indicating that there are no statistically significant differences between the two materials in the E-modulus. Furthermore, the comparison between PLA and rPLA shows also no significant difference $p = 0.07$ for the E-modulus. This is also visible in the stress-strain curve in Figure 4.3d, where the slopes of recycled and virgin material follow the same pattern.
The difference for the E-modulus between rPLA and ST45 was significant before adjustment, but after Bonferroni correction, the result is not significant (adjusted $p = 0.08$. Similarly, the difference between rPETg and ST45 was significant before adjustment, but after Bonferroni correction, it was not significant (adjusted $p = 0.12$).

Tensile strength

Figure 4.3b shows similar box plots of PETg and rPETg, however, a p-value of 0.04, suggests a small statistically significant difference between rPETg and PETg. This indicates that the tensile strength of rPETg is significantly higher than that of virgin PETg.
Both virgin and recycled PLA exhibited high initial stiffness, reflected in the values of the E modules, with rPLA closely resembling the mechanical behavior of vPLA, although with a significant difference in the tensile strength $p < 0.05$ (shown in figure 4.3d). Virgin PLA showed a significantly lower tensile strength, reaching the fracture point shortly after giving compared to rPLA. In contrast, vPETg displays a notably lower Young's modulus compared to PLA types, indicating less stiffness. Like PLA, vPETg and rPETg reached their fracture point soon after yielding.
The difference in tensile strength between Regrind PLA and ST45 was significant before ad-

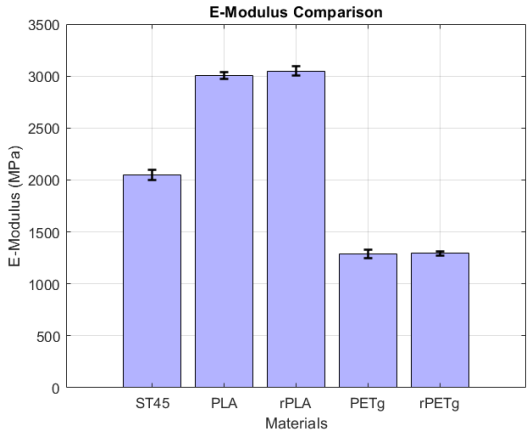

(a) E-modulus values with standard deviation

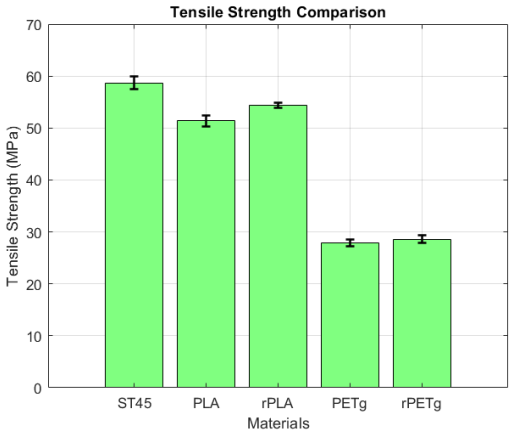

(b) Tensile strength values with standard deviations

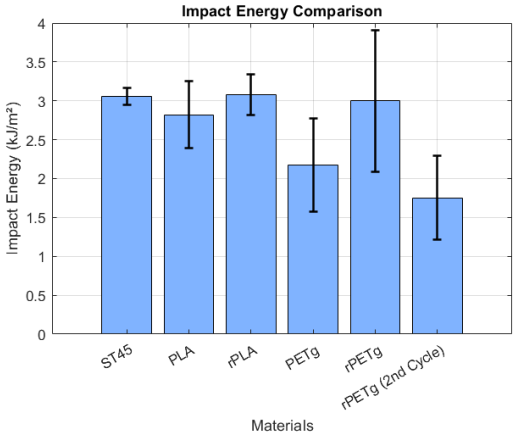

(c) Impact energy with standard deviations

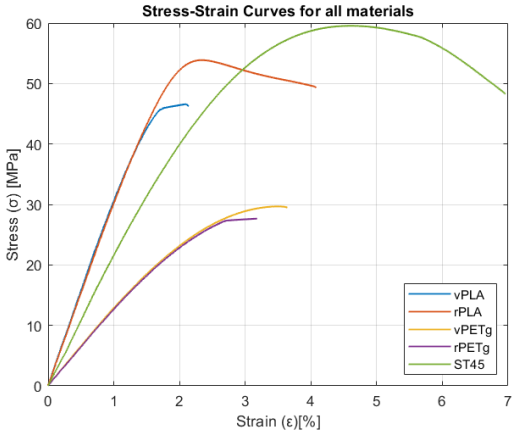

(d) Average stress-strain curves of all materials.

Figure 4.3: Comparative analysis of E-modulus, tensile strength, impact energy, and stress-strain behaviour for ST45, PLA, rPLA, PETg, and rPETg materials.

justment, but after Bonferroni correction, the result is not significant (adjusted $p = 0.08$). The difference between rPETg and ST45 was highly significant both before and after Bonferroni correction $p < 0.001$, indicating a strong difference in tensile strength between these two materials.

Impact Energy

Figure 4.3c illustrates the high standard deviation in impact energy, indicating that the measured values varied significantly between different samples of the same material, suggesting inconsistencies in performance. In particular, there is a significant difference in impact energy between PETg recycling cycles ($p < 0.05$). The results of Dunn's test indicate that rPETg from the first cycle has significantly higher impact energy compared to rPETg from the second cycle ($p = 0.01$). vPETg shows significantly lower impact energy than rPETg from the first cycle ($p = 0.03$), however vPETg in comparison with rPETg from the second cycle there is no statistically significant ($p = 0.32$) difference. That suggests that the first cycle of PETg recycling has an increase in performance, but after that first cycle it decreases significant.
Furthermore, the comparison between virgin PLA and rPLA shows a p-value of $p = 0.09$, suggesting that while there is a trend towards a difference, it is not statistically significant.
The Kruskal-Wallis test for impact energy showed no significant differences between ST45, rPLA, and rPETg (1st cycle), with a p-value of 0.36.

Discussion

This study evaluated the mechanical properties of PLA and PETg recycling compared to ST45 and also the influence of recycling on the performance of these materials. The results indicate that recycled PETg and PLA exhibit mechanical properties similar to those of virgin counterparts. This contrasts with the initial hypothesis that recycled materials would show lower mechanical performance due to degradation during the recycling process. Specifically, there were no significant differences in the E-modulus between virgin and recycled materials, suggesting that recycling does not affect the stiffness of these materials as expected. Tensile strength was expected to be lower in recycled PETg, and indeed, recycled PETg shows a slight decrease in tensile strength compared to virgin PETg. However, recycled PLA demonstrates tensile strength comparable to that of virgin PLA, with only minor variations observed, which was somewhat expected. In terms of impact energy, recycled PETg and PLA perform similarly to their virgin versions, with some variations observed across different cycles of recycled PETg.

Regarding the comparison between recycled materials and ST45, the values of the E module are similar to ST45, with no significant differences found. This aligns with the expectation that recycled PLA could perform similarly to ST45 in terms of stiffness. However, the tensile strength results were less aligned with the hypothesis. rPETg showed a significantly different strength than ST45, while the tensile strength of recycled PLA was similar to that of ST45 after adjustment. This suggests that rPLA may be a more promising alternative to ST45 than rPETg, aligning with the initial expectation of material selection in chapter 2. Finally, in terms of impact energy, there were no significant differences between ST45 and recycled materials, suggesting that recycled PETg and PLA have sufficient potential to serve as sustainable options, as initially predicted, despite some performance variations.

Overall, while the recycled materials did not show the expected degradation in mechanical performance, the differences in tensile strength and impact energy suggest that recycled PLA may be a more viable sustainable alternative to ST45 compared to recycled PETg, although both recycled materials demonstrate sufficient potential for use in sustainable applications such as the 3DxSplint.

Statistical tests revealed significant differences between the impact energy data from the TDS and the actual values tested for ST45 and regrindPLA. This discrepancy indicates that the TDS values may not fully capture the variability introduced by factors such as processing conditions, material history, and environmental factors. Specifically, for impact energy data, the observed differences highlight how real-world applications may present challenges not taken into account in controlled TDS tests.

In contrast, the tensile test results for BASF materials, ST45 and PLA, did not show significant differences compared to the TDS values. This suggests that the tensile properties of BASF's virgin materials can be reliably predicted using the TDS values. However, for regrindPLA, a significant difference was observed. This finding underscores that recycled materials may not perform as expected based solely on TDS data, highlighting that TDS values may not fully account for the variability inherent in recycled materials.

Design modifications can enhance the tensile properties of rPETg, making it more suitable for 3D printed splints. Increasing the thickness of critical sections can improve the ability of the material to withstand tensile forces, reducing the likelihood of failure. In addition, minimizing the size and number of holes in the design or strategically reinforcing areas around these holes can prevent stress concentrations that weaken the structure. Adjusting the infill pattern and density, such as using grid or triangular designs, further enhances stiffness and stress distribution. Aligning the layer orientation with the applied stress and using smaller layer heights can also improve interlayer bonding. These strategies allow for the optimization of the mechanical performance of rPETg while retaining the benefits of using a sustainable material.

The difference in performance of virgin PLA and rPLA may have been affected by differences in printer technology and material composition. Virgin PLA samples were printed using a Bambu Lab printer, while regrind PLA was printed on an Ultimaker. Variations in printing speed, nozzle design, and cooling systems between these printers could affect the mechanical properties of printed materials. Additionally, the virgin PLA used was a blend of different premium filaments from a different supplier than BAS-F where the virgin PLA was from. These differences in printer and raw materials likely influenced the results, beyond the recycled or virgin nature of the PLA.

Limitations

A limitation of this study is that the aim was to include data from the second cycle rPETg; however, due to a printer error and limited available filament, the tensile bars did not meet the ISO-standard dimensions of 4 mm thick and were thus excluded from the results. Notably, while the impact specimens for this batch were successfully printed with the same settings, the tensile bar geometry proved less forgiving, highlighting that different filament spools and thus batches may require more specific adjustments when using recycled materials.

Another limitation of this study lies in the use of different sources of virgin and recycled materials, which may have influenced the observed differences between their mechanical properties. Specifically, the virgin PETg used as a reference for comparison with recycled PETg was sourced from Ultimaker. Since there was no available 3D print material from the virgin material used in rPETg from NHL. Similarly, for PLA, the virgin material was sourced from BASF and the recycled PLA was obtained from ColorFabb, each manufacturer employing different processing methods and formulations. These manufacturing variations could result in subtle differences in the properties of the material, independent of the recycling process itself. As a result, some

of the observed differences or similarities between virgin and recycled materials may not only reflect the effects of recycling but could also be attributed to inherent variations in material composition or processing methods.

In the process of producing the rPETg filament described in Chapter 3, a printable filament was successfully made from the first cycle. However, differences in print settings between filaments from the first and second cycles were necessary to ensure printability. These variations in the print temperature and speed settings could have influenced the mechanical properties of the printed material. As a result, direct comparisons of different cycles of rPETg are challenging and may reflect not only the material properties but also the influence of different process parameters.

Future research

Future research should focus on investigating the mechanical properties of rPETg and rPLA over multiple recycling cycles, using the same base materials processed throughout. This would provide a more accurate picture of how recycling affects the material and help determine the maximum number of cycles that these materials can undergo before their mechanical properties degrade beyond usability.

Evaluate the impact of design modifications on the 3D printed splint, such as varying thickness, infill patterns, and hole placement, in biomechanical tests. This can provide insights into optimizing 3D printed designs to enhance the mechanical performance of recycled materials.

Establishing precise mechanical performance requirements for materials in medical applications, particularly bone immobilization in fracture treatment, is essential. Although current standards are based on ST45, this material may not be the ideal benchmark for medical splints and similar applications. Research should investigate which specific mechanical properties, such as stiffness, tensile strength, and impact resistance, are crucial to minimizing micro-movements in fractured bones, as such motion can hinder effective healing.

Conclusion

This study evaluated the mechanical properties of recycled PLA and recycled PETg over different recycling cycles and compared to the ST45 reference. The results show that rPLA and rPETg did not show statistically significant differences in terms of impact energy, E-modulus and tensile strength compared to ST45. However, rPETg showed a statistically significant deviation in tensile strength. The findings of the recycling cycles revealed that there were no statistically significant differences in the E-modules between the virgin and recycled samples for both materials. However, the tensile strength showed a notable increase for the recycled materials compared to their virgin counterparts, highlighting potential benefits of the recycling process for this property. For impact energy, rPLA did not show significant differences compared to virgin samples, indicating that its resilience remains consistent throughout the cycles. In contrast, rPETg displayed a significant increase in impact energy after the first recycling cycle but experienced a marked decrease in the second cycle compared to virgin samples. This suggests that while rPETg may initially benefit from recycling in terms of impact performance, subsequent cycles could compromise its mechanical integrity. The results underscore the importance of understanding the impact of recycling on mechanical properties, as these effects follow patterns that can influence material selection and design considerations across multiple recycling cycles.

The findings indicate that recycled PLA, with a performance comparable to ST45, holds promise as a viable material for wrist splints, especially when combined with careful design optimization. For rPETg, design modifications such as increasing thickness or optimizing infill patterns could mitigate its reduced tensile properties and expand its applicability.

Looking beyond this chapter, the study suggests that both materials and their recycling processes could be adapted to produce durable and sustainable medical devices. Future research should explore material performance across additional recycling cycles to confirm long-term suitability and refine recycling techniques for even greater consistency.

5 DISCUSSION

This research focused on identifying and evaluating sustainable alternatives to the non-recyclable and nonbiodegradable ST45 print material, currently used for 3D printed patient-specific splints. Through a systematic review of the literature and an MCDA, PLA and rPETg were selected as the most suitable sustainable candidates. By examining both the manufacturing process of recycled filament and its mechanical properties, this study demonstrated not only the theoretical suitability of rPLA and rPETg but also its practical feasibility. The collaboration with NHL Stenden to produce filament has proven that recycled PETg hospital material can be converted more efficiently into usable products than recycling process of rPLA from CHILL.

This study therefore offers a concrete step toward a circular economy in the medical sector by manufacturing 3D printed splints from recycled PETg hospital waste. The use of recyclable materials can help reduce the increase in hospital waste, as previously suggested by Habiba et al. [97], who highlighted the environmental benefits of recycled polymers in additive manufacturing. The identification of rPLA as a sustainable alternative with performance comparable to ST45 supports the feasibility of this change.

In addition, this research has shown that technical data sheets often do not reflect the actual mechanical performance of 3D printed materials. There is no standardization for testing printed specimens, making it difficult to compare materials from different manufacturers, as each may use different standards.

Applicability

The application of recycled materials in the 3D splint will significantly reduce the environmental impact, as analyzed by Verschoor et al. [12]. Although this study provides a clear pathway toward the practical implementation of sustainable materials in the medical sector, several challenges remain when applying recycled materials in 3D printed splints for medical use.

Firstly, according to the European Medical Device Regulations (MDR, Regulation (EU) 2017/745), the reuse of materials in medical devices is strictly regulated [98]. Article 17 of the MDR allows single-use medical devices to be recycled under specific conditions, depending on national legislation. However, this only applies if the devices can be safely reused and the reprocessor satisfies the same obligations as the original manufacturer. This makes reuse of material challenging in medical applications, such as 3D splints due to current regulations. Therefore, it is important to look more closely at optimizing the production process so that recycled materials retain their original properties.

Secondly, successfully integrating recycled materials into 3D printed splint manufacturing processes requires overcoming critical barriers that currently hinder local recycling. Research by Peeters et al. [99] shows that the main barriers to local recycling include the linear economy and a consumer-oriented society, as well as the high-quality expectations of consumers. In the context of medical applications, patients with wrist fractures are expected to be treated

with a reliable, safe, and splint that immobilizes enough. To promote the transition to a circular economy, RadboudUMC and MAINIAC should overcome these barriers. To overcome these barriers, Radboudumc and MAINIAC should balance sustainability goals with the high standards required for medical devices, ensuring that recycled materials meet the necessary performance, safety and regulatory requirements for patient care.

Third, recycling processes are based on precise extrusion parameters, such as careful filament cooling, and prevention of contamination, as noted by Giacomini et al. [100], while Bremer et al. [101] emphasize that uniformity in shredded materials is equally critical. Our study also demonstrated that scaling up in-house recycling is a labor-intensive process that requires constant monitoring to ensure batch consistency. Consequently, the implementation of in-house recycling would require investments in training, infrastructure, and process optimization.

Lastly, the change in print method for 3D printed splints from DLP to FDM technology introduces a challenge in print speed. FDM, using rPETg filaments (2.85 mm), prints significantly slower than the faster curing UV resin ST45 used in DLP, which could delay production in hospital settings where rapid treatment is preferable. Therefore, the slower printing speed of FDM materials needs careful consideration for medical applications.

Limitations

This study provides insights into the potential of recycled PLA and PETg for 3D printed splints, but several limitations need to be addressed.

To begin with, a limited number of sustainable materials were investigated to determine the feasibility of their recycling process and mechanical performance. Although the MCDA identified several potential materials, it was limited to the top two, rPLA and rPETg. The third material from the MCDA, PLLA, was also considered sustainable and recyclable, but due to time constraints and its limited availability at Radboudumc, NHL, and CHILL, it was excluded from further consideration. In addition to that, biodegradable materials were not explored in this study, which could have provided another sustainable alternative for 3D printing applications in the medical field.

Another limitation is due to the quality of the filament from the recycling production process. While rPETg was successfully printed, the rPLA from the recycling production process could not be tested due to logistical constraints. Research at Lapland University of Applied Sciences has demonstrated that with minor adjustments to extrusion protocols, both rPLA and rPETg can produce printable filament [100].

The last important limitation is the absence of multiple batches and cycles of recycled materials to obtain a more in-depth understanding of the variability between cycles and batches. Conducting further assessments with multiple recycled batches could help optimize the recycling process and facilitate the testing of multiple recycling cycles to evaluate the long-term durability and consistency of materials.

Reliability

The reliability of this study is influenced by several methodological considerations and limitations in the data collection process, though it still provides valuable insight into the potential of recycled materials for 3D printed splints.

The MCDA scoring process was chosen because it allowed the evaluation of multiple criteria points, offering a convenient and structured approach to evaluating the materials. However, some criteria required qualitative data rather than quantitative data, which introduces a degree of subjectivity and potential bias in the results. Despite this, the MCDA method is a valuable tool for decision-making, and future studies could improve the precision by supplementing it with more stakeholder input and incorporating diverse perspectives.

Recycling production processes were established through MAINIAC partners, ensuring access to relevant recycling facilities and expertise, which provided a practical foundation for the study. However, the differences in protocols, machinery, and practices between these locations did affect the reproducibility of the results. This not only highlights the need for standardized recycling processes, but also illustrates how real-world variability can influence outcomes.

The feasibility of the recycling processes of rPLA and rPETg was based on a single recycling cycle conducted under specific conditions, which provided important insights but also limits the generalizability of the findings. Expanding the study to include multiple recycling cycles and varied conditions would allow for a more thorough evaluation of the long-term viability and scalability of the recycling process.

Future recommendations

Future research on sustainable materials for 3D printed medical devices presents a significant opportunity to refine and expand on the findings of this study. The mechanical properties of rPETg and rPLA should be explored over multiple recycling cycles, ensuring that the same base materials are used consistently. This approach will provide critical insights into how recycling impacts the structural integrity and usability of these materials over time. Understanding the maximum viable number of recycling cycles before the materials degrade beyond acceptable limits will help establish their long-term feasibility for medical applications, ensuring performance and safety standards are upheld.

Additionally, exploring the effects of design modifications in 3D printed splints is interesting. Variables such as thickness, fill patterns, and hole placement may significantly influence the mechanical performance of recycled materials. Analyzing how these design parameters affect the strength and flexibility of the splints could lead to optimized designs that compensate for any material weaknesses introduced during recycling.

To enhance comparability and reliability across studies, future research should also emphasize the adoption of standardized testing protocols for manufacturers of 3D printed materials. Employing ISO and ASTM standards for mechanical property evaluations, such as tensile strength and impact resistance, will ensure uniformity in test methods.

Finally, before integrating recycled materials into the production of 3D printed splints at Radboudumc, it is essential to conduct further research addressing the practical challenges and feasibility of this transition. This involves analyzing the entire workflow, from the recycling production processes to the final implementation in clinical settings, to ensure that the materials and methods are in line with the high-quality standards of medical applications.

6 CONCLUSION

The increasing demand for sustainable practices in healthcare has underscored the need for innovative solutions to reduce environmental impact. Despite the growing emphasis on sustainability, hospitals continue to rely heavily on non-durable materials, contributing to significant medical waste. This issue is particularly evident in the treatment of forearm fractures, where conventional gypsum or plastic casts are standard. At Radboudumc, an innovative approach aims to replace these traditional solutions with patient-specific 3D printed splints. However, these splints currently use the non-sustainable ST45 material, which does not address the sustainability challenge. To explore alternatives, this study investigated the potential of reusable and recyclable materials, evaluating their suitability for 3D printed splints.

Through the literature review, recycled PLA and recycled PETg were identified as the most suitable candidates based on sustainability, material properties, patient safety, and logistic compatibility with the existing 3D printing infrastructure. The feasibility of recycling production processes for these materials was examined in terms of efficiency, energy, and filament quality. Results indicated that the rPETg recycling process, conducted in collaboration with NHL Stenden, outperformed the rPLA process at CHILL in scalability and production efficiency. Mechanical testing of virgin and recycled PLA and PETg revealed performance comparable to that of the ST45 benchmark material. While rPLA maintained consistent impact energy throughout recycling cycles, rPETg showed temporary improvements after the first cycle but a significant decline after the second. The tensile strength of rPETg differed significantly from ST45, while rPLA performed comparable. Notably, both materials demonstrated promising recyclability with no significant loss in E-modulus between cycles.

The findings indicate that rPETg has promising potential as a sustainable material for 3D printed splints. However, its mechanical performance could benefit from design modifications. Future studies should aim to refine recycling processes to improve filament consistency and assess the long-term durability of materials across multiple recycling cycles and practical use cases. Additionally, optimizing the splint design could further enhance the material's performance and suitability for medical applications.

Bibliography

[1] L. F. Diaz et al. “Characteristics of healthcare wastes”. In: *Waste Management* 28.7 (2008), pp. 1219–1226. DOI: 10.1016/J.WASMAN.2007.04.010.

[2] E. M. Van Lieshout, M. H. Verhofstad, and L. M. Beens. “Personalized 3D-printed fore833 arm braces as an alternative for a traditional plaster castor splint; A systematic review”. In: *Injury* 53 (2022). URL https://linkinghub.elsevier.com/retrieve/pii/S0020138322004946, S47–S52. DOI: 10.1016/j.injury.2022.07.020.

[3] Angus P Fitzpatrick et al. “Design of a Patient Specific, 3D printed Arm Cast”. In: *KnE Engineering* 2.1 (Feb. 2017), pp. 135–142. DOI: 10.18502/keg.v2i2.607. URL: https://knepublishing.com/index.php/KnE-Engineering/article/view/607.

[4] World Health Organization. *Health care waste*. Retrieved from https://www.who.int/news-room/fact-sheets/detail/health-care-waste. 2019.

[5] C. Rizan et al. “Plastics in healthcare: Time for a re-evaluation”. In: *Journal of the Royal Society of Medicine* (2020). DOI: 10.1177/0141076819890554. URL: https://doi.org/10.1177/0141076819890554.

[6] Radboudumc. *Duurzaamheid*. Retrieved from https://www.radboudumc.nl/over-het-radboudumc/duurzaamheid. Radboudumc.

[7] L. Van Ginkel. *3DxSPLINT: A Clinical Comparison of 3D Printed Splints versus Conventional Splints in the Treatment of Distal Radius Fractures*. Enschede, the Netherlands, 2023.

[8] Forward AM. *Ultracur3D® ST 45: Tough Reactive Urethane Photopolymer for 3D Printing*. https://forward-am.com/material-portfolio/ultracur3d-photopolymers/tough-line/ultracur3d-st-45/. Accessed: 2024-09-05. 2024.

[9] I. Gibson, D. Rosen, and B. Stucker. “Development of Additive Manufacturing Technology”. In: *Additive Manufacturing Technologies*. Springer, New York, NY, 2015. DOI: 10.1007/978-1-4939-2113-3_2.

[10] Dr. Matanky. *ORIF Distal Radius Fracture*. https://www.drmatanky.com/orif-distal-radius-fracture.html. Accessed: 2024-10-06. n.d.

[11] LifeCare. *Casting and Splinting*. https://www.lifecare.com.au/blog/casting-and-splinting/. Accessed: 2024-10-06. n.d.

[12] H. Verschoor et al. “LCA conducted on a case study involving the implementing 3D printed personalized splints for traumatic injuries”. In: *Procedia CIRP* 00 (2024), pp. 000–000. DOI: 10.1016/j.procir.2024.03.001.

[13] I. Gibson, D. Rosen, and B. Stucker. “Vat Photopolymerization Processes”. In: *Additive Manufacturing Technologies*. Springer, New York, NY, 2015. DOI: 10.1007/978-1-4939-2113-3_4.

[14] M. N. Andanje et al. “Biocompatible and Biodegradable 3D Printing from Bioplastics: A Review”. In: *Polymers* 15.10 (2023), p. 2355. DOI: 10.3390/polym15102355.

[15] D. Fico et al. “A Review of Polymer-Based Materials for Fused Filament Fabrication (FFF): Focus on Sustainability and Recycled Materials”. In: *Polymers* 14.3 (2022), p. 465. DOI: 10.3390/polym14030465.

[16] V. S. D. Voet, J. Guit, and K. Loos. “Sustainable Photopolymers in 3D Printing: A Review on Biobased, Biodegradable, and Recyclable Alternatives”. In: *Macromolecular Rapid Communications* 42.3 (2020). DOI: 10.1002/marc.202000475.

[17] Sarfraz Nazir and Alessandro Capocchi. “Circular Economy 6Rs and Reporting Practices: The Role of Institutional Pressures”. In: *Sustainability Reporting Practices and the Circular Economy: Analysis and Integrated Strategies*. Cham: Springer Nature Switzerland, 2024, pp. 185–224. ISBN: 978-3-031-51845-4. DOI: 10.1007/978-3-031-51845-4_5. URL: https://doi.org/10.1007/978-3-031-51845-4_5.

[18] Forward AM. *Ultracur3D ST 45*. Retrieved June 11, 2024, from https://forward-am.com/material-portfolio/ultracur3d-photopolymers/tough-line/ultracur3d-st-45/.

[19] C. O’Driscoll, O. Owodunni, and U. Asghar. “Optimization of 3D printer settings for recycled PET filament using analysis of variance (ANOVA)”. In: *Heliyon* 10.5 (2024), e26777. DOI: 10.1016/j.heliyon.2024.e26777.

[20] O. Rashwan et al. “Extrusion and characterization of recycled polyethylene terephthalate (rPET) filaments compounded with chain extender and impact modifiers for material-extrusion additive manufacturing”. In: *Scientific Reports* 13.1 (2023), p. 16041. DOI: 10.1038/s41598-023-41744-8.

[21] A. Oussai, Z. Bártfai, and L. Kátai. “Development of 3D Printing Raw Materials from Plastic Waste. A Case Study on Recycled Polyethylene Terephthalate”. In: *Applied Sciences* 11.16 (2021), p. 7338. DOI: 10.3390/app11167338.

[22] F. Ferrari et al. “3D Printing of Polymer Waste for Improving People’s Awareness about Marine Litter”. In: *Polymers* 12.8 (2020), p. 1738. DOI: 10.3390/polym12081738.

[23] B. S. Kolitha et al. “Repurposing of waste PET by microbial biotransformation to functionalized materials for additive manufacturing”. In: *Journal of Industrial Microbiology & Biotechnology* 50.1 (2023), kuad010. DOI: 10.1093/jimb/kuad010.

[24] N. R. Madhu et al. “Fused deposition modelling approach using 3D printing and recycled industrial materials for a sustainable environment: a review”. In: *The International Journal of Advanced Manufacturing Technology* 122.5-6 (2022), pp. 2125–2138. DOI: 10.1007/s00170-022-10048-y.

[25] N. E. Zander et al. “Recycled polypropylene blends as novel 3D printing materials”. In: *Additive Manufacturing* 25 (2019), pp. 122–130. DOI: 10.1016/j.addma.2018.11.009.

[26] V. Mishra, S. Negi, and S. Kar. “FDM-based additive manufacturing of recycled thermoplastics and associated composites”. In: *Journal of Material Cycles and Waste Management* 25.2 (2023), pp. 758–784. DOI: 10.1007/s10163-022-01588-2.

[27] M. Pepi, N. Zander, and M. Gillan. “Towards Expeditionary Battlefield Manufacturing Using Recycled, Reclaimed, and Scrap Materials”. In: *JOM* 70.10 (2018), pp. 2359–2364. DOI: 10.1007/s11837-018-3040-8.

[28] M. Kariz et al. “Effect of wood content in FDM filament on properties of 3D printed parts”. In: *Materials Today Communications* 14 (2018), pp. 135–140. DOI: 10.1016/j.mtcomm.2017.12.016.

[29] M. J. Le Guen et al. “Influence of Rice Husk and Wood Biomass Properties on the Manufacture of Filaments for Fused Deposition Modeling”. In: *Frontiers in Chemistry* 7 (2019), p. 735. DOI: 10.3389/fchem.2019.00735.

[30] A. H. Kadhum, S. Al-Zubaidi, and S. S. Abdulkareem. “Effect of the Infill Patterns on the Mechanical and Surface Characteristics of 3D Printing of PLA, PLA+ and PETG Materials”. In: *ChemEngineering* 7.3 (2023), p. 46. DOI: 10.3390/chemengineering7030046.

[31] A. Patti et al. “Recovery of Waste Material from Biobags: 3D Printing Process and Thermo-Mechanical Characteristics in Comparison to Virgin and Composite Matrices”. In: *Polymers* 14.10 (2022), p. 1943. DOI: 10.3390/polym14101943.

[32] M. Garwacki et al. “The Development of Sustainable Polyethylene Terephthalate Glycol-Based (PETG) Blends for Additive Manufacturing Processing-The Use of Multilayered Foil Waste as the Blend Component”. In: *Materials (Basel, Switzerland)* 17.5 (2024), p. 1083. DOI: 10.3390/ma17051083.

[33] R. D. Crapnell et al. “Recycled PETg embedded with graphene, multi-walled carbon nanotubes and carbon black for high-performance conductive additive manufacturing feedstock”. In: *RSC Advances* 14.12 (2024), pp. 8108–8115. DOI: 10.1039/d3ra08524d.

[34] N. Vidakis et al. “Sustainable Additive Manufacturing: Mechanical Response of Polyamide 12 over Multiple Recycling Processes”. In: *Materials (Basel, Switzerland)* 14.2 (2021), p. 466. DOI: 10.3390/ma14020466.

[35] K. Zgodavová et al. “3D Printing Optimization for Environmental Sustainability: Experimenting with Materials of Protective Face Shield Frames”. In: *Materials (Basel, Switzerland)* 14.21 (2021), p. 6595. DOI: 10.3390/ma14216595.

[36] V. DeStefano, S. Khan, and A. Tabada. “Applications of PLA in modern medicine”. In: *Engineered Regeneration* 1 (2020), pp. 76–87. DOI: 10.1016/j.engreg.2020.08.002.

[37] J. D. Kechagias et al. “Multi-parameter optimization of PLA/Coconut wood compound for Fused Filament Fabrication using Robust Design”. In: *The International Journal of Advanced Manufacturing Technology* 119.9-12 (2022), pp. 4317–4328. DOI: 10.1007/s00170-022-08679-2.

[38] F. A. Cruz Sanchez et al. “Plastic recycling in additive manufacturing: a systematic literature review and opportunities for the circular economy”. In: *Journal of Cleaner Production* 264 (2020), p. 121602. DOI: 10.1016/j.jclepro.2020.121602.

[39] A. C. Pinho, A. M. Amaro, and A. P. Piedade. “3D printing goes greener: Study of the properties of post-consumer recycled polymers for the manufacturing of engineering components”. In: *Waste Management (New York, N.Y.)* 118 (2020), pp. 426–434. DOI: 10.1016/j.wasman.2020.09.003.

[40] M. A. Morales et al. “Development and Characterization of a 3D Printed Cocoa Bean Shell Filled Recycled Polypropylene for Sustainable Composites”. In: *Polymers* 13.18 (2021), p. 3162. DOI: 10.3390/polym13183162.

[41] G. Occasi et al. “Recovery material from a new designed surgical face mask: A complementary approach based on mechanical and thermo-chemical recycling”. In: *Journal of Environmental Management* 324 (2022), p. 116341. DOI: 10.1016/j.jenvman.2022.116341.

[42] K. Pickering and D. Stoof. “Sustainable Composite Fused Deposition Modelling Filament Using Post-Consumer Recycled Polypropylene”. In: *Journal of Composites Science* 1.2 (2017), p. 17. DOI: 10.3390/jcs1020017.

[43] H. Zhang et al. “Three-Dimensional Printing of Continuous Flax Fiber-Reinforced Thermoplastic Composites by Five-Axis Machine”. In: *Materials (Basel, Switzerland)* 13.7 (2020), p. 1678. DOI: 10.3390/ma13071678.

[44] A. Le Duigou et al. “3D printing of continuous flax fibre reinforced biocomposites for structural applications”. In: *Materials & Design* 180 (2019), p. 107884. DOI: 10.1016/j.matdes.2019.107884.

[45] C. Badouard et al. “Exploring mechanical properties of fully compostable flax reinforced composite filaments for 3D printing applications”. In: *Industrial Crops and Products* 135 (2019), pp. 246–250. DOI: 10.1016/j.indcrop.2019.04.049.

[46] D. Depuydt et al. “Production and characterization of bamboo and flax fiber reinforced polylactic acid filaments for fused deposition modelling (FDM)”. In: *Polymer Composites*. Vol. 40. Society of Plastics Engineers, Inc, 2018, pp. 1–13. DOI: 10.1002/pc.24971.

[47] Extrudr. *GreenTEC*. 2024. URL: https://www.extrudr.com/shop-eu/products/greentec/.

[48] Extrudr. *GreenTEC Pro*. 2024. URL: https://www.extrudr.com/shop-eu/products/greentec-pro/.

[49] 3DJake. *niceBIO Filaments*. 2024. URL: https://www.3djake.nl/3djake/nicebio-rood?sai=6394.

[50] ColorFabb. *PolyHydroxy Alkanoates*. 2024. URL: https://colorfabb.com/allpha-natural.

[51] 3D4Makers. *Recycled PEEK*. 2024. URL: https://www.3d4makers.com/products/r-peek-filament.

[52] Anycubic. *Plant-Based UV Resin*. 2024. URL: https://store.anycubic.com/products/plant-based-uv-resin?_gl=1*18aqy1u*_up*MQ..&gclid=EAIaIQobChMItr2pkc_dhQMVqLKDBx36ZQ4KEAAYASACEgI-MPD_BwE.

[53] Multicomp Pro. *Mulitcomp Pro MP004398*. 2024. URL: https://nl.farnell.com/en-NL/multicomp-pro/mp004398/lcd-pla-resin-red-500g-50/dp/3583627.

[54] Extrudr. *Biofusion*. 2024. URL: https://www.extrudr.com/shop-eu/products/biofusion/.

[55] 3Dresyn. *Hard Resin with 85% Bio Content*. 2024. URL: https://www.3dresyns.com/products/3dresyn-biodeg-corn-bio-based-and-biofegradable-resin-with-85-bio-content.

[56] 3Dresyn. *Elastic Resin with 85% Bio Content*. 2024. URL: https://www.3dresyns.com/products/3dresyn-biodeg-corn-e-bio-based-biodegradable-compostable-elastic-resin-with-85-bio-content.

[57] 3Dresyn. *Flexible Resin with 85% Bio Content*. 2024. URL: https://www.3dresyns.com/products/3dresyn-biodeg-corn-f-bio-based-and-biodegradable-flexible-resin-with-85-bio-content.

[58] S. Meena et al. “Fractures of distal radius: An overview”. In: *Journal of Family Medicine and Primary Care* 3.4 (2014), p. 325. DOI: 10.4103/2249-4863.148101.

[59] British Orthopaedic Association and British Society for Surgery of the Hand. *Best practice for management of distal radial fractures (DRFs)*. Retrieved from https://www.boa.ac.uk/resources/boast-2017-drf.html. 2018.

[60] Ádám Schlégl et al. “Evaluation and Comparison of Traditional Plaster and Fiberglass Casts with 3D-Printed PLA and PLA–CaCO3 Composite Splints for Bone-Fracture Management”. In: *Polymers* 14.17 (2022), p. 3571. DOI: 10.3390/polym14173571.

[61] C. Ekanayake et al. “Revolution in orthopedic immobilization materials: A comprehensive review”. In: *Heliyon* 9.3 (2023), e13640. DOI: 10.1016/j.heliyon.2023.e13640.

[62] W. K. M. Brauers and C. Zopounidis. “The use of multi-criteria decision analysis in the selection of materials”. In: *International Journal of Production Research* 42.1 (2004), pp. 123–143.

[63] T. Pamminger and A. Ziegler. “Multi-Criteria Decision Analysis for Sustainable Material Selection”. In: *Materials Science and Engineering: A* 668 (2016), pp. 60–68.

[64] J. Bendig and L. Eberhardt. “Multi-Criteria Decision Making in Materials Selection: A Case Study in the Automotive Industry”. In: *Materials & Design* 151 (2018), pp. 166–178.

[65] Forward AM. *Ultrafuse Pellets rPETg*. Accessed: 2024-10-23. 2023. URL: https://forward-am.com/material-portfolio/ultrafuse-pellets/ultrafuse-pellets-rpetg/.

[66] Mohammad Awal et al. “Mechanical Properties of PLA/Wood Composites”. In: *Bulletin of the Institute of Polymeric Materials* 7.1 (2023). Accessed: 2024-10-23. URL: https://intapi.sciendo.com/pdf/10.2478/bipcm-2023-0006.

[67] John Smith et al. “Mechanical Characterization of PLA/Wood Composites”. In: *Journal of Applied Polymer Science* (2021). Accessed: 2024-10-23. URL: https://www.proquest.com/openview/1c5e33885bb328df79e33f113fe8d885/1?pq-origsite=gscholar&cbl=5038271.

[68] Carl Roth GmbH. *Safety Data Sheet for Poly(L-lactic acid)*. Accessed: 2024-10-23. 2021. URL: https://www.carlroth.com/medias/SDB-8460-GB-EN.pdf?context=bWFzdGVyfHNlY3VyaXR5RGF0YXNoZWV0c3wzMTEyNjB8YXBwbGljYXRpb24vcGRmfHNlY3VyaXR5RGF0YXNoZWV0cy9oOGUvaGY5LzkwNDU1MTA1NTM2MzAucGRmfDZjOWZmZmJiZGMxM2QzZjFlYWIyNDBhMTc2ZGRkNjk2ZDExYWJiNjg3NWY1MzE1MWU3NzkyNTU2OTlhMDllYTQ.

[69] Y. E. Belarbi et al. “Effect of Printing Parameters on Mechanical Behaviour of PLA-Flax Printed Structures by Fused Deposition Modelling”. In: *Materials (Basel, Switzerland)* 14.19 (2021). Accessed: 2024-10-23, p. 5883. DOI: 10.3390/ma14195883. URL: https://doi.org/10.3390/ma14195883.

[70] Alfonso Jimenez, L. Torre, and Jose Kenny. “Processing and properties of recycled polypropylene modified with elastomers”. In: *Plastics Rubber and Composites - PLAST RUBBER COMPOS* 32 (Oct. 2003), pp. 357–367. DOI: 10.1179/146580103225004126.

[71] Oumaima Boughanmi et al. “Repetitive recycling effects on mechanical characteristics of polylactic acid and PLA/spent coffee grounds composite used for 3D printing filament”. In: *Polymer Engineering and Science* 64.11 (Aug. 2024), pp. 5613–5626. DOI: 10.1002/pen.26938. URL: https://doi.org/10.1002/pen.26938.

[72] Tatjana M. Lazović and Milan S. Stojanović. “Preparation of specimens for standard tensile testing of plastic materials for FDM 3D printing”. In: *University of Belgrade, Faculty of Mechanical Engineering, Belgrade, Serbia* (2021). URL: https://stumejournals.com/journals/mtm/2021/5/205.

[73] Jeffrey Hopewell, Robert Dvorak, and Edward Kosior. “Plastics recycling: challenges and opportunities”. In: *Philosophical Transactions of the Royal Society B: Biological Sciences* 364.1526 (2009), pp. 2115–2126. DOI: 10.1098/rstb.2008.0311.

[74] Robert D. Rogers, Andrew S. Holmes, and Scott W. D. Davidson. “Recycling in the Chemical and Mechanical Processing of Polymers”. In: *Journal of Applied Polymer Science* 115 (2010), pp. 2919–2933. DOI: 10.1002/app.31314.

[75] Daniel V. A. Ceretti et al. “Molecular Pathways for Polymer Degradation during Conventional Processing, Additive Manufacturing, and Mechanical Recycling”. In: *Molecules* 28.5 (2023). ISSN: 1420-3049. DOI: 10.3390/molecules28052344. URL: https://www.mdpi.com/1420-3049/28/5/2344.

[76] Swagat Mahapatra and Nandakumar Rengarajan. “Use of recycled external fixators in management of compound injuries”. In: *Expert Review of Medical Devices* 14.1 (Dec. 2016), pp. 83–85. DOI: 10.1080/17434440.2017.1265886.

[77] Visalakshi Nachal et al. “A Review on Recycle of Waste To Make Prosthetics”. In: 10 (May 2023), pp. 5–13. DOI: 10.5281/zenodo.7964869.

[78] SUEZ Recycling and Recovery. *Recycling plastics for healthcare: A UK initiative*. 2021. URL: https://www.suez.co.uk.

[79] Philips. *Sustainability in healthcare: Using recycled materials for medical devices*. 2021. URL: https://www.philips.com.

[80] Reflow Filament. *Collaborations*. Accessed: 2024-09-26. 2024. URL: https://reflowfilament.com/collaborations/.

[81] Fraunhofer Innovation Platform for Advanced Manufacturing. *Using waste polymers to create filament for 3D printing of recyclable end-products*. Accessed: 2023-10-24. 2022. URL: https://fip.utwente.nl/project/waste2print/.

[82] Brightlands Chemelot Campus. *3D Printing: Practice Valuable Partnerships*. Accessed: 2024-10-25. 2023. URL: https://www.brightlands.com/en/chemelot-campus/community-events/blogs-stories/3d-printing-practice-valuable-partnerships-between.

[83] NHL Stenden University. *Circular Plastics Research*. Accessed: 2024-10-25. 2023. URL: https://www.nhlstenden.com/onderzoek/lectoraten/circular-plastics.

[84] Hartplastic. *Mission Vision*. Accessed: 2024-10-25. 2023. URL: https://hartplastic.com/mission-vision-2.

[85] 24ChemicalResearch. *Global PETG for Medical Market Research Report 2024*. Retrieved from https://www.24chemicalresearch.com/reports/260955/global-petg-for-medical-market-2024-409. 24ChemicalResearch, July 2024.

[86] Meryem Boudalal. “Revolutionizing Healthcare Waste Management: A Sustainable Approach through PETG Recycling and 3D Printing”. All rights reserved. Bachelor’s thesis. NHL Stenden University of Applied Sciences, 2024. URL: https://urn.fi/URN:NBN:fi:amk-202403265162.

[87] ColorFabb. *colorFabb PLA Regrind*. https://colorfabb.com/nl/pla-regrind. Accessed: 2024-09-05. 2024.

[88] 3Devo. *PLA Recycling: Everything You Need to Know*. Accessed: 2024-11-17. 2024. URL: https://www.3devo.com/blog/pla-recycling-everything-you-need-to-know#:~:text=PLA%20(Polylactic%20Acid)%20is%20a,breaking%20it%20down%20into%20monomers..

[89] Bambu Lab. *Bambu Lab X1 Carbon Product Page*. Accessed: 2024-09-27. 2023. URL: https://eu.store.bambulab.com/nl-nl/products/x1-carbon?gad_source=1&gclid=Cj0KCQjwmOm3BhC8ARIsAOSbapVXGTKq22C5DrGwcF-y5dn0l_nstScQbLZyPzS2KLQvwJxdfKadCSEaAjMqEALw_wcB.

[90] International Organization for Standardization. *Plastics – Determination of tensile properties – Part 1: General principles*. Geneva, Switzerland. ISO, 2023.

[91] ASTM International. *Standard Test Method for Tensile Properties of Plastics*. West Conshohocken, PA. ASTM International, 2023.

[92] Julien Gardan. “Additive Manufacturing Technologies: State of the Art and Trends”. In: *International Journal of Production Research* 54 (Nov. 2015). DOI: 10.1080/00207543.2015.1115909.

[93] Ultimaker. *Ultimaker PETG Technical Data Sheet*. https://um-support-files.ultimaker.com/materials/2.85mm/tds/PETG/Ultimaker-PETG-TDS-v1.00.pdf. Accessed: 2024-09-09. 2024.

[94] Forward AM. *Ultrafuse® PLA*. https://forward-am.com/material-portfolio/ultrafuse-filaments-for-fused-filaments-fabrication-fff/standard-filaments/ultrafuse-pla/. Accessed: 2024-09-09. 2024.

[95] HartPlastic. *Wat wij doen*. https://hartplastic.com/wat-wij-doen-1. Accessed: 2024-09-09. 2024.

[96] International Organization for Standardization. *Plastics – Determination of Charpy impact strength – Part 1: Non-instrumented impact test*. 2010. URL: https://www.iso.org/standard/44786.html.

[97] Rachel Djonyabe Habiba, Cândida Malça, and Ricardo Branco. "Exploring the Potential of Recycled Polymers for 3D Printing Applications: A Review". In: *Materials (Basel)* 17.12 (June 2024). Accessed: 2024-06-29, p. 2915. DOI: 10.3390/ma17122915. URL: https://doi.org/10.3390/ma17122915.

[98] European Commission. *Reprocessing of Medical Devices - Public Health*. Accessed: 2024-11-18. 2024. URL: https://health-ec-europa-eu.ezproxy2.utwente.nl/medical-devices-topics-interest/reprocessing-medical-devices_en.

[99] Bob Peeters, Nadine Kiratli, and Janjaap Semeijn. "A barrier analysis for distributed recycling of 3D printing waste: Taking the maker movement perspective". In: *Journal of Cleaner Production* 241 (2019), p. 118313. ISSN: 0959-6526. DOI: https://doi.org/10.1016/j.jclepro.2019.118313. URL: https://www.sciencedirect.com/science/article/pii/S095965261933183X.

[100] David Durán Redondo. "Circular economy through plastic recycling process into 3D printed products: A frugal solution for schools". Master's thesis. Institution of Industrial Engineering and Management, 2019. URL: https://upcommons.upc.edu/bitstream/handle/2117/172290/circular-economy-through-plastic-recycling-process-into-3d-printed-products-a-frugal-solution-for-schools-davidduran-194622.pdf?sequence=1&isAllowed=y.

[101] M. Bremer et al. "Influence of plastic recycling—a feasibility study for additive manufacturing using glycol modified polyethylene terephthalate (PETG)". In: *SN Applied Sciences* 4.156 (2022). Received: 07 May 2021; Accepted: 12 April 2022; Published: 28 April 2022, pp. 1–11. DOI: 10.1007/s42452-022-05039-3. URL: https://doi.org/10.1007/s42452-022-05039-3.

A APPENDIX A

Literature study

Below is the data extracted from the Excel sheet, presented in PDF format.

author	year	Article type	Additiv	full material name	material abbr	chemical composition	what is tested	how is it tested	recycle/biodegradable	recycle cyclus	tensile strength (MPa	E-Modulus (MPa	flexural strength (	thermal decomposition	Glass transition temperature
Li.Y.	2023	review --> (Sutton. J.T.et al 2018)	SLA	Lignin-based photosensitive resins	LR15	lignin resin (LR 15 wt.%) pulp-grade wood chips of hybrid poplar	viscosity, chemical characterization, UTS and E modulus	rheometer, FI-IR, tensile test		virgin	15	372			
Morales.M.A.	2023	review --> Meza-de Luna	FDM	Urban waste plastic	Bh20	plastic from water (BH20)bottles(BL)	resistance, deformation and rupture behavior under tensional load	tensile testing	recycle		123.5	478			
Li.Y.	2023	review --> (Sutton. J.T.et al 2018)	SLA	Lignin-based photosensitive resins	LR10	lignin resin (LR 10 wt.%) pulp-grade wood chips of hybrid poplar	viscosity, chemical characterization, UTS and E modulus	rheometer, FI-IR, tensile test		virgin	18	482			
Morales.M.A.	2023	review --> Meza-de Luna	FDM	Urban waste plastic	BA	plastic from dressing (BA) bottles	resistance, deformation and rupture behavior under tensional load	tensile testing	recycle		90	597			
Morales.M.A.	2023	review --> Meza-de Luna	FDM	Urban waste plastic	BL	plastic from milk bottles(BL)	resistance, deformation and rupture behavior under tensional load	tensile testing	recycle		28	603			
Li.Y.	2023	review --> (Sutton. J.T.et al 2018)	SLA	Lignin-based photosensitive resins	LR05	lignin resin (LR 5 wt.%) pulp-grade wood chips of hybrid poplar	viscosity, chemical characterization, UTS and E modulus	rheometer, FI-IR, tensile test		virgin	11	642			
Samoylenko.D.E.	2023	article	FDM	calcium carbide residue-based composite	CCR/SBS	calcium hydroxide (Ca(OH)2) and SBS	Mechanical properties, specifically tensile strength, Young's modulus, and shape retention/shrinkage	tensile test, SEM,EDX	recycle		20.4	1190			
Driscoll.C.O.	2024	article	FDM	recycled Polyethylene Terephthalate by UOWD	rPET	single source recycled PET water bottles	UTS and E modulus	variable nozzle temperature, layer height, infill density, print speed.	recycle	1	43	1330			
Driscoll.C.O.	2024	article	FDM	recycled Polyethylene Terephthalate	rPET	recycled PET water bottles from BASF	UTS and E modulus	variable nozzle temperature, layer height, infill density, print speed.	recycle	1	43	1330			
Van der Ham.E.	2024	Conference paper	SLS	Polyamide 12	PA12	pure PA12	mechanical properties	Tensile test, FEM			19.2	1640			
Samoylenko.D.E.	2023	article	FDM	calcium carbide residue-based composite	CCR/Nylon	calcium hydroxide (Ca(OH)2) and Nylon	Mechanical properties, specifically tensile strength, Young's modulus, and shape retention/shrinkage	tensile test, SEM,EDX	recycle		43.4	1790			
Rashwan.O.	2023	article	FDM	recycled polyethylene terephthalate with additives.	rPET	rPET, SEBS-g-MA, e-EA-GMA, EEA	Thermal and mechanical properties	three-point flexural, DSC, IZOD impact test, TGA, DMA, SEM	recycle		36	1813	28.46		79,5
Rashwan.O.	2023	article	FDM	recycled polyethylene terephthalate with IMA	rPET/IM	rPET, SEBS-g-MA, e-EA-GMA, EEA	Thermal and mechanical properties	three-point flexural, DSC, IZOD impact test, TGA, DMA, SEM	recycle		33.2	1872	34.82		81,3
Morales.M.A.	2023	review --> Matsuzaki et al.	FDM	carbon fiber-reinforced polylactid acid	CFRTP	Commercially available PLA + Polyacrylonitrile (PAN)-based carbon fibers	mechanical properties	three-point bending			185.2 (±24.6)	1950			
Samoylenko.D.E.	2023	article	FDM	calcium carbide residue-based composite	CCR/ABS	calcium hydroxide (Ca(OH)2) and ABS	Mechanical properties, specifically tensile strength, Young's modulus, and shape retention/shrinkage	tensile test, SEM,EDX	recycle		38.6	1950			
Cui.J.	2023	article	DLP	Dynamic thermosetting photopolymers	HEA-CANs	2-hydroxyethyl acrylate (HEA) monomer, bis(2-acryloyloxyethyl) malonate (BAM) crosslinker, diphenyl (2,4,6-trimethylbenzoyl) phosphine oxide (TPO) as photoinitiator	Tg, storage modulus, UTS and ε	tensile test, DMA, SRA, recycling experiments	recycle	1 & 2	0.93-5.66	2000			
Morales.M.A.	2023	review --> Vaucher et al.	FDM	Polyethene terephthalate and high density polyethylene	PET/HDPE	PET from beverage bottles and HDPE from caps and rings (95/5% wt)	microstructure, mechanical performance, and printing quality	TGA, tensile test, DSC, SEM	recycle	1	49.5 ± 1.7	2100			73.6
Morales.M.A.	2023	review --> Kariz et al.	FDM	wood content-filled polylactide acid	Wood/PLA	wood flour (50 wt %) in a PLA matrix	Tensile properties	SEM, TGA, DSC, XRD tensile test			30	2100			
Samoylenko.D.E.	2023	article	FDM	calcium carbide residue-based composite	CCR/HIPS	calcium hydroxide (Ca(OH)2) and HIPS	Mechanical properties, specifically tensile strength, Young's modulus, and shape retention/shrinkage	tensile test, SEM,EDX	recycle		24.2	2320			
Samoylenko.D.E.	2023	article	FDM	calcium carbide residue-based composite	CCR/PETG	calcium hydroxide (Ca(OH)2) and PETG	Mechanical properties, specifically tensile strength, Young's modulus, and shape retention/shrinkage	tensile test, SEM,EDX	recycle		24.6	2320			
Li.Y.	2023	review --> (Rosa.R.P. et al 2023)	SLA	Vegetable oil-based photosensitive resin	AESO-IBOMA	acrylate epoxidized soybean oil (AESO)+ isobornyl methacrylate (IBOMA) +diphenyl(2,4,6-trimethylbenzoyl)phosphine oxide (TPO) 50/50 wt.%	UV-curing progress, rheological measurments, swelling ratio, UTS, elogation E-modulus, fracture energy, thermal analysis	FT-IR, rheometer, tensile test, TGA, CA		virgin	37.2	2400			
Rashwan.O.	2023	article	FDM	recycled polyethylene terephthalate with pyromellitic dianhydride	rPET/PMDA	rPET, PMDA, SEBS-g-MA, e-EA-GMA, EEA	Thermal and mechanical properties	three-point flexural, DSC, IZOD impact test, TGA, DMA, SEM	recycle		42.8	2452	46.10		83,3
Madhu.N.R.	2022	review --> Singh et al.	FDM	harakeke fiber filaments with recycled polypropylene	HFF/rPP	harakeke fibers (30 wt.%) with rPP	tensile strengh, young modulus		recycle		39	2800			
Seok.W.	2023	article	FDM	Recycled carbon fiber reinforced acrylonitrile butadiene styrene composites	rCF/ABS	pure ABS, 10 wt% rCF	Mechanical properties, specifically tensile and flexural properties, as well as dimensional stability	tensiletest, dimensional analysis, SEM	recycle		26.33	2840	61.36		
Morales.M.A.	2023	review --> Kariz et al.	FDM	wood content-filled polylactide acid	Wood/PLA	wood flour (40 wt %) in a PLA matrix	Tensile properties	SEM, TGA, DSC, XRD tensile test			42	3000			
Seok.W.	2023	article	FDM	Recycled carbon fiber reinforced acrylonitrile butadiene styrene composites	rCF/ABS	pure ABS, 20 wt% rCF	Mechanical properties, specifically tensile and flexural properties, as well as dimensional stability	tensiletest, dimensional analysis, SEM	recycle		29.59	3360	39.73		
Morales.M.A.	2023	review --> Kariz et al.	FDM	wood content-filled polylactide acid	Wood/PLA	wood flour (30 wt %) in a PLA matrix	Tensile properties	SEM, TGA, DSC, XRD tensile test			48	3400			

Morales.M.A.	2023	review --> Kariz et al.	FDM	wood content-filled polylactide acid	Wood/PLA	wood flour (20 wt %) in a PLA matrix	Tensile properties	SEM, TGA, DSC, XRD tensile test			49	3500			
Morales.M.A.	2023	review --> Kariz et al.	FDM	wood content-filled polylactide acid	Wood/PLA	wood flour (10 wt %) in a PLA matrix	Tensile properties	SEM, TGA, DSC, XRD tensile test			57	4000			
Morales.M.A.	2023	review --> Matsuzaki et al.	FDM	jute fiber-reinforced polylactid acid	JFRTP	Commercially available PLA + twisted jute natural plant fibers	mechanical properties	three-point bending			57.1 (±5.33)	5110			
Morales.M.A.	2023	review --> Munoz-Blandon et al.	FDM	fique fiber	fique fiber	high holocellulose content and low lignin and pectin content	physical, thermal, mechanical, and textile properties	AFM and SEM images, respectively. Mechanical testing	biodegradable		355.07	11540			
Morales.M.A.	2023	review --> Cruz et al.	FDM	Recycled polylactide acid	rPLA	PLA type 4043D, a product of NatureWorks	variation in mechanical properties after multiple recycle cycli	tensile test	recycle	1,2,3,4,5	54.76 ± 3.85	3449 ± 81			
Andanje, M	2023	review --> DeStefano et al.	FDM	Poly(DL-lactide)	PDLLA	pure	mechanical properties	literature search	biodegradable		27.6-50.0	1000-3450			50-60
Andanje, M	2023	review --> DeStefano et al.	FDM	Poly(DL-lactide) and poly(glycolic acid)	PDLLA/PGA	50/50 wt. %	mechanical properties	literature search	biodegradable		41.4-55.2	1000-4340			50-55
Morales.M.A.	2021	article	FDM	rice husk an agricultural residue, and recycled polypropylene	rPP/RH	rPP post industrial waste & RH (5 wt. %) from Ambala grinder composite angle at 90°	Physical, thermal, mechanical, and morphological properties	TGA, Tensile test, SEM, warping assesment	recycle	1	7.92 ± 0.67	1010 ± 120			
Vidakis.N.	2021	Article	FFF	recycled Polyamide 12	rPA12	rPA12 recycled 6 times	mechanical and thermal properties	tensile test, TGA analysis, raman analysi, SEM, DSC	recycle	1,2,3,4,5,7	19.6-39.1	102.3-176.6	21.7-44.1		
Morales.M.A.	2021	article	FDM	rice husk an agricultural residue, and recycled polypropylene	rPP/RH	rPP post industrial waste & RH (10 wt. %) from Ambala grinder composite angle at 0°	Physical, thermal, mechanical, and morphological properties	TGA, Tensile test, SEM, warping assesment	recycle	1	13.78 ± 0.59	1040 ± 40			
Morales.M.A.	2023	review --> Pabón Rojas et al.	FDM	epoxy and morich biocomposite	Epoxy/Moriche	epoxy resin biocomposites from morisch	compatibility and vacuum level in the material's mechanical properties	SEM, FTIR, TGA, mechanical testing	biodegradable		22.5 ± 2.4.	1049.9 ± 47.4			
Morales.M.A.	2021	article	FDM	rice husk an agricultural residue, and recycled polypropylene	rPP/RH	rPP post industrial waste & RH (5 wt. %) from Ambala grinder composite angle at 0°	Physical, thermal, mechanical, and morphological properties	TGA, Tensile test, SEM, warping assesment	recycle	1	13.62 ± 2.71	1060 ± 130			
Stouten.J.	2023	Article	DLP	Acrylic photopolymer resins	CROSS	BDG (0,5,10 wt.%) + IBOMA (20 wt. %)+Biobased content (73,74 en 75 wt. %)	physical properties, mechanical properties, thermal properties	NMR, HRMS, UV-VIS, DMA, TGA, rheometer, tensile test, FTIR,	recycle	1,2,3	24-35	1100-1450			
Pinho.A.C.	2020	Article	FDM	recycled acrylonitrile butadiene styrene	rABS	recycled from food packages and car dashboards, respectively.	chemical, thermal and mechanical properties	FTIR, TGA tensile test, SEM,	recycle	1	30.9 ± 1.1	1110 ± 100			
Liguori.A.	2023	article	DLP	isosorbide-based photocurable resins	SB_MI50	Methacrylated isosorbide (MI monomer) (50 wt.%)+ vanillin-derived Schiff-base (SB monomer) (50 wt.%)	printability, physical and chemical properties	spectrometer, TGA, stress-strain measurements	recycle		42 ± 4	1163 ± 215		422 ± 1	93 ± 11
Kechagias, J. D.	2022	article	FDM	NEEMA3D™ PLA	Pure PLA	100% PLA polymers	UTS and E modulus	variable Layer thickness, nozzle temp. Raster deposition angle and printing speed			31-39	1246-1538	-	-	
Morales.M.A.	2023	review --> Singh et al.	FDM	banana fibers in recycled polyamide 6	BF-PA6	recycled RA6 filled with banana fiber (5 wt.%).	thermal/mechanical/morphological	photomicrographs, thermographs and mechanical testing.	recycle		increase 37.52%	126.98			
Fico.D.	2022	review --> Osman et al.	FDM	Acrylonitrile Butadiene Styrene rice straw filaments	ABS-RS	rice straw (5,10,15 wt. %) in ABS	mechanical, physical thermal properties	tensile test, SEM	biodegradable		11293	1300-2500			
Morales.M.A.	2021	article	FDM	recycled polypropylene	rPP	rPP post industrial waste. composite angle at 0°	Physical, thermal, mechanical, and morphological properties	TGA, Tensile test, SEM, warping assesment	recycle	1	26.02 ± 0.47	1340 ± 50			
Morales.M.A. 1	2021	article	FDM	recycled polypropylene	rPP	filaments of rPP and CBS composite angle at 0°	Physical, thermal, mechanical, and morphological properties	TGA, Tensile test, SEM, warping assesment	recycle		26.02 ± 0.47	1340 ± 50			
Andanje, M	2023	review --> Le Duigou et al.	FDM	continuous flax fibre with polylactide acid longitudinal printed	cFF/PLA	PLA + PHA + recycled wood fibers	Longitudinal and transverse mechanical behaviour and properties	tensile test, SEM	recycle		253.7 ± 15.0	13600-23300			
Morales.M.A.	2023	review --> Le Duigou et al.	FDM	continuous flax fibre with polylactide acid longitudinal printed	cFF/PLA	PHA + PLA + recycled woodfibers	Longitudinal and transverse mechanical behaviour and properties	tensile test, SEM	recycle		253.7 ± 15.0	13600-23300			
Garwacki.M	2024	Article	FDM	polyethylene terephthalate Glycol-based	PETG	poly(ethylene terephthalate)-glycol copolymer (PETG)+ PET-based foil waste(PET/PE, PET/EVOH, PET/MET) + CE(SAN-g-GMA) +IM(POE-g-GMA)	mechanical performance evaluation, thermal analysis, and rheological measurements	Static tensile and charpy Impact testing. DMT analysis and HDT testing, SAOS and MFR test		virgin	27-53	1400-2700			70-75
Fico.D.	2022	review --> Le Guen et al.	FDM	polylactid acid and pine wood	PLA-wood	wood powder (32 wt. %) blended by twin-screw extrusion with PLA	mechanical, physical thermal properties	SEM, tapped density and particle size analyzer, PH measurements, NMR, Ash content, chemical composition, rheology, GPC, DMTA, flexural test	biodegradable		30–40	1500-2000	35-58		65
Fico.D.	2022	review --> Le Guen et al.	FDM	polylactid acid and rice husk	PLA-rice	rice husk powder (39 wt.%) blended by twin-screw extrusion with PLA	mechanical, physical thermal properties	SEM, tapped density and particle size analyzer, PH measurements, NMR, Ash content, chemical composition, rheology, GPC, DMTA, flexural test	biodegradable		30–40	1500-2000	30-50		65
Pinho.A.C.	2020	Article	FDM	recycled polylactide	rPLA	recycled from food packages and car dashboards, respectively.	chemical, thermal and mechanical properties	FTIR, TGA tensile test, SEM,	recycle	1	39.6 ± 1.2	1540± 300			
Farina.I.	2019	Article	FDM	recycled Nylon-6 with acrylonitrile butadiene styrene and titanium dioxide	rNylon-6/ABS/TiO2	pure Nylon-6 grains/mixtures with ABS and TiO2.	mechanical, physical thermal properties	MFI, DSC, Tensile test	recycle		76.20–86.91	1640-2340			
Fico.D.	2022	review --> Farina et al.	FDM	recycled Nylon-6 with acrylonitrile butadiene styrene and titanium dioxide	rNylon-6/ABS/TiO2	pure Nylon-6 grains/mixtures with ABS and TiO2.	mechanical, physical thermal properties	MFI, DSC, Tensile test	recycle		76.20–86.91	1640-2340			
Laoutid F.	2021	Article	FDM	acrylonitrile butadiene styrene copolymer with recycled tire rubbers	ABS-GTR	abs with recycled GTR (15 wt.% and 30 wt.%)	Physical and thermal properties, mechanical properties	SEM, TGA, tensile test, MFI	recycle	1		1660 - 1930			

Morales.M.A.	2023	review --> Cerpa Ospino	FDM	Manicaria saccifera in Polylactid acid	MS-PLA	Manicaria saccifera fiber with and without a 5% sodium hydroxide and 1% acetic acid treatment , PLA pellets	weight percentage concentraion chemical treatment, laminate orientation on mechanical properties	taguchi method	biodegradable		20.762-35.870	1668 - 2689	34.999-63.664		
Madhu.N.R.	2022	review	FDM	Recycled Polymers with Nanocrystalline Powders	PP and HDPE	Nanocrystalline powders of Fe, Si, Cr, and Al	Yield strength, Young modulus		recycle		1% powder combination increased 37%	17% increase			
Morales.M.A.	2023	review --> taborda-Rios et al.	FDM	bamboo fibers reinforced polylactic acid	Bamboo/PLA	Bamboo fiber content up to 70 % in PLA	mechanical testing to evaluate the influence of process parameters tensile strength, strain, and elastic modulus	tensile test, SEM			17-24	1700 - 2700			
Morales.M.A.	2023	review --> Vaucher et al.	FDM	Polyethene terephthalate	PET/HDPE	PET from beverage bottles (100% wt)	microstructure, mechanical performance, and printing quality	TGA, tensile test, DSC, SEM	recycle	1	44.8 ± 7.7	1700 ± 300			73.4
Vaucher.J.	2022	Article	FDM	Polyethene terephthalate	PET/HDPE	PET from beverage bottles (100% wt)	microstructure, mechanical performance, and printing quality	TGA, tensile test, DSC, SEM	recycle	1	44.8 ± 7.7	1700 ± 300			73.4
Cui.J.	2023	article	DLP	Dynamic thermosetting photopolymers	HEA-CANs	2-hydroxyethyl acrylate (HEA) monomer, bis(2-acryloyloxyethyl) malonate (BAM) crosslinker, diphenyl (2,4,6-trimethylbenzoyl) phosphine oxide (TPO) as photoinitiator	Tg, storage modulus, UTS and ε	tensile test, DMA, SRA, recycling experiments	recycle	virgin	0.93-5.66	1746–2698		-	11.6-24.4
Crapnell.R.D.	2024	Article	FFF	Recycled polyethylene terephthalate glycol embedded with graphene, multiwalled carbon nanotubes and carbon black	rPETg	rPETg & CB/MWCNT/GNP (25/2.5/2.5 wt%)	Physical and thermal properties, mechanical properties	tensile test, TGA analysis, XPS, raman analysi, SEM	recycle			1753 ± 83			
Tolcha.D.A.	2023	Article	FDM	Short glass fiber-reinforced recycled high-density polyethylene and recycled polyethylene terephthalate	SGF/rHDPE/rPET	rHDPE/rPET (75/25 %), rHDPE/rPET reinforced with 15 % SGF, and rHDPE/rPET reinforced with 30 % SGF wt%).	physical properties, mechanical properties, thermal properties	DSC, tensile test, SEm	recycle	1	27-49.896	1768-2363			
Vidakis.N. 1	2021	Article	FFF	recycled Polyethylene Terephthalate Glycol	rPETG	rPETG recycled 6 times	mechanical and thermal properties	tensile test, TGA analysis, raman analysi, SEM, DSC	recycle	1,2,3,4,5,6	33.3-46.1	183.3-247.0	53.1-71.5		
Valente.M.	2023	Article	FDM	recycled Short carbon fiber reinforced PA6,6	Pa6,6/rCF	PA6,6 + rCF (5 wt.%, 10 wt. %)	physical properties, mechanical properties, thermal properties	SEM, pycnometer,tensile test	recycle		56.54-61.74	1850-2240			
Liguori.A.	2023	article	DLP	isosorbide-based photocurable resins	MI75	Methacrylated isosorbide (MI monomer) (75 wt.%)+ methacrylated vanillin (MV monomer) (25 wt.%)	printability, physical and chemical properties	spectrometer, TGA, stress-strain measurements	recycle		58 ± 9	1925 ± 484		423 ± 1	56 ± 1
Fico.D.	2022	review --> John et al.	FDM	recycled cellulose in Polylactid acid	rCellulose/PLA	extracted cellulose nanofibres were chemically modified	mechanical, physical thermal properties	FTIR, TEM, Tensile test, DSC	recycle		32.71–38.74	2000-2800			
Liguori.A.	2023	article	DLP	isosorbide-based photocurable resins	MI50	Methacrylated isosorbide (MI monomer) (50 wt.%)+ methacrylated vanillin (MV monomer) (50 wt.%)	printability, physical and chemical properties	spectrometer, TGA, stress-strain measurements	recycle		47 ± 13	2026 ± 250		423 ± 1	60 ± 3
Morales.M.A.	2023	review --> Vaucher et al.	FDM	Polyethene terephthalate and high density polyethylene	PET/HDPE	PET from beverage bottles and HDPE from caps and rings (98/2% wt)	microstructure, mechanical performance, and printing quality	TGA, tensile test, DSC, SEM	recycle	1	51.7 ± 1.1	2100 ± 100			75.6
Morales.M.A.	2023	review --> Vaucher et al.	FDM	Polyethene terephthalate and high density polyethylene	PET/HDPE	PET from beverage bottles and HDPE from caps and rings (90/10% wt)	microstructure, mechanical performance, and printing quality	TGA, tensile test, DSC, SEM	recycle	1	45.6 ± 1.8	2100 ± 200			74.0
Morales.M.A.	2023	review --> Zhang et al.	FFF	Continuous Flax Fiber-Reinforced Thermoplastic Composites	CFFRP	Flax fibers (10.6, 20.4 36.7 wt/wt) in PLA	Tensile strength and tensile modulus, flexibel strength/modulus	tensile test, three-point bending			52-89	2100-2900	132		
Andanje, M	2023	review --> DeStefano et al.	FDM	Polycaprolactone	PCL	pure	mechanical properties	literature search	biodegradable		20.7-42	210-440			60-56
Morales.M.A.	2023	review --> Badouard et al.	FDM	flax fibers reinforced polylactic acid	PBAT	PBAT-flax fibres at 10%-wt	thermal, hygroscopic stability and characterized	tensile machine, SEM, extensometer	biodegradable		8.7 ± 0.6	217 ± 16			
Morales.M.A.	2023	review --> Badouard et al.	FDM	flax fibers reinforced polylactic acid	PLLA/PBS	PLLA/PBS 50/50-10%-wt flax fibres (PLLA-PBS-10-S)	thermal, hygroscopic stability and characterized	tensile machine, SEM, extensometer	biodegradable		34.1 ± 1.9	2190 ± 114			
Fico.D.	2022	review --> GKartzou et al.	FDM	biobased blends of polylactid acid with low-cost kraft lignin	PLA/low-cost kraft lignin	PLA filaments with 5 to 15 wt. % concentrations of kraft pine lignin (Indulin AT)	morphological, mechanical and thermal properties	tensile testing, DSC, optical and SEM	biodegradable		40.8-51.2	2280-2470			
Morales.M.A.	2023	review --> Singh et al.	FDM	banana fibers in recycled Acrylonitrile Butadiene Styrene	BF-ABS	recycled ABS filled with banana fiber (5 wt.%).	thermal/mechanical/morphological	photomicrographs, thermographs and mechanical testing.	recycle		increase 10.99%	23.1			
Morales.M.A.	2023	review --> Depuydt et al.	FDM	flax fibers reinforced polylactic acid	FF/PLA	PLA pellets with two pasticizers from Proviron Industries NV. with bamboo and flax	differente fiber length vs diameter ratio on mechanical properties	tensile test			28	2328 ± 90			
Morales.M.A.	2023	review --> montoya et al.	FDM	bacterial cellulose microfibrils in thermoplastic starch	BC	BC microfibrils from fermented juice of pinceapple peels, starch from potato (32.8 wt% amylase and 67.1 wt.% amylopectin)	processing method and cellulose microfibrils content in material behavior	ATR-FTIR, mechanical testing,TGA	biodegradable		7.8-9.4	233-412.9			
Morales.M.A.	2023	review --> Depuydt et al.	FDM	bamboo fibers reinforced polylactic acid	Bamboo/PLA	PLA pellets with two pasticizers from Proviron Industries NV. with bamboo and flax	differente fiber length vs diameter ratio on mechanical properties	tensile test			22 - 28	2342 ± 441			
Morales.M.A.	2023	review --> Landes et al.	FDM	bamboo fibers reinforced polylactic acid	Bamboo/PLA	Bamboo filled PLA. Four raster orientation angles (0°, 90°, 0°/90°, and −45°/45°)	raster orientation on tensile, flexural, compression, impact, shear	extensometer, 3 point flexure fixture, LVDT, Izod impact tester, V notched beam,			29.21- 32.50	2360-2630	49.35 - 56.76		
Fico.D.	2022	review --> Daver et al.	FDM	polylactid acid and cork biofilament with tributyl citrate	PLA/cork/TBC	PLA filaments with 5 %-w/w cork and 5%-w/w TBC content	mechanical, physical thermal properties	DSC, TGA, DMA, tensile testing, Izod impact test, SEM	biodegradable		30.53 ± 1.0	2490 ± 150			
Fico.D.	2022	review --> Figueroa-velarde et al.	FDM	recycled Agave leaves in Polylactid acid	rAF/PLA	PLA filled with agave fibers (0,3,5,10 wt%) from tequila waste	weight percentages and raster angles on mechanical, physical thermal properties	DSC, tensile test, Charpy impact,	recycle		28–51	2500–3400			
Fico.D.	2022	review --> Lendvai et al.	FDM	recycled marble dust in Polylactid acid	MD/PLA	PLA filmanents with 5,10,15,20 % MD	mechanical, physical thermal properties	SEM, tensile, static three point bending test, charpy impact, DSC	recycle		49.1–53.08	2690–3830			

Andanje, M	2023	review --> DeStefano et al.	FDM	Poly(L-lactide)	PLLA	pure	mechanical properties	literature search	biodegradable		15.5-150	2700-4140			55-65
Fico.D.	2022	review --> Stoof et al.	FDM	Hemp and Harakeke fibers in polylactide Acid	PLA/hemp-harakeke	Hemp Harakeke (10,20,30 wt. %) in PLA (90/80/70 wt. %)	mechanical, physical thermal properties	tensile test, SEM	biodegradable		24-30	2700-4200			
Morales.M.A.	2023	review --> Badouard et al.	FDM	flax fibers reinforced polylactic acid	PLLA/PBS	PLLA/PBS 50/50-10%-wt flax fibres (PLLA-PBS-10-F)	thermal, hygroscopic stability and characterized	tensile machine, SEM, extensometer	biodegradable		30.3 ± 2.5	2786 ± 251			
Morales.M.A.	2023	review --> montoya et al.	FDM	Vegetable cellulose microfibrils in thermoplastic starch	VC	VC microfibrils from vascular bundles of banana rachis, starch from potato (32.8 wt% amylase and 67.1 wt.% amylopectin)	processing method and cellulose microfibrils content in material behavior	ATR-FTIR, mechanical testing,TGA	biodegradable		4.0-10.2	29.3-145.5			
Morales.M.A.	2023	review --> Tao et al	FDM	wood fluor-filled with polylactide acid	WF/PLA	wood flour (5 wt %) in a PLA matrix	Tensile properties	SEM, TGA, DSC, XRD tensile test				30% increase		330	60
Fico.D.	2022	review --> Kariz et al.	FDM	wood content-filled polylactid acid	PLA/beech wood	dust from beech wood up to 50 wt. % in PLA Matrix	morphological and thermal properties	SEM, TGA, DSC, XRD tensile test	biodegradable		30–57	3000-3940			
Fico.D.	2022	review --> Rahimizadeh et al.	FDM	Wind turbine wast in Polylactid acid	WTW/PLA	PLA filaments reinforced with 3, 5, and 10 wt% recyclate content	mechanical, physical thermal properties	TGA, µCT, tensile test	recycle		41.94–57.57	3170–4030			
Andanje, M	2023	review --> tran et al.	FDM	micronized cocoa shell in Polycaprolactone.	PCL.CSW	cocoa shell (up to 50 wt. %) in PCL	mechanical and thermal properties	SEM, tensile test, FTIR and XRD analysis	biodegradable		decreasewith higher CSW content	319 - 356			260-390
Morales.M.A.	2023	review --> tran et al.	FDM	micronized cocoa shell in Polycaprolactone.	PCL.CSW	cocoa shell (up to 50 wt. %) in PCL	mechanical and thermal properties	SEM, tensile test, FTIR and XRD analysis	biodegradable		decreasewith higher CSW content	319 - 356			260-390
Andanje, M	2023	review --> Tarrés et al.	FDM	Bio-polyethylene reinforced with thermomechanical pulp fibers	TMP/bioPE	TMP (30% w/w) + 2 bioPE + MAPE (6% w/w) injection molded	mechanical and micromechanical characteristics	MFI, tensile test, SEM			38.72 ± 0.61	3260 ± 60			
Morales.M.A.	2023	review --> oussai et al	FDM	recycled polyethylene terephthalate	rPET	From Pet bottles	Mechanical properties	tensile test	recycle	1	29.742 ± 2.8	3346 ± 413			
Andanje, M	2023	review --> Ambone et al.	FDM	cellulose nanofiber in Polylactid acid	PLA/CNF	PLA + CNF (1 wt.%)	different volume fraction on material properties	testile tesing, SEM, TGA			41.15 ± 0.95	3365.66 ± 212.92			
Kechagias, J. D.	2022	article	FDM	polylactide acid with coconut wood	PLA/C	70 % PLA, 30% coconut fibers	Variable print parameters on mechanical properties (UTS and E)	variable Layer thickness, nozzle temp. Raster deposition angle and printing speed			5.48-17.42	347-692	-	-	
Andanje, M	2023	review --> DeStefano et al.	FDM	Polyhydroxybutyrate	PHB	pure	mechanical properties	literature search	biodegradable		40	3500-4000			15
Andanje, M	2023	review --> DeStefano et al.	FDM	polylactic acid	PLA	pure	mechanical properties	literature search	biodegradable		21-60	350-3500			45-60
Morales.M.A.	2023	review --> oussai et al	FDM	recycled polyethylene terephthalate	rPET	From Pet bottles	Mechanical properties	tensile test	recycle	virgin	34.871 ± 1.6	3670 ± 224			
Morales.M.A.	2023	review --> Badouard et al.	FDM	Poly(L-lactide) with Flax fibers	PLLA/FF	PLLA-10%-wt flax fibres (PLLA-10-F)	thermal, hygroscopic stability and characterized	tensile machine, SEM, extensometer	biodegradable		34.2 ± 2.6	3968 ± 245			
Andanje, M	2023	review --> Le Duigou et al.	FDM	continuous flax fibre with polylactide acid transverse printed	cFF/PLA	PLA + PHA + recycled wood fibers	Longitudinal and transverse mechanical behaviour and properties	tensile test, SEM	recycle		27 ± 3.3	4150 ± 350			
Morales.M.A.	2023	review --> Le Duigou et al.	FDM	continuous flax fibre with polylactide acid transverse printed	cFF/PLA	PHA + PLA + recycled woodfibers	Longitudinal and transverse mechanical behaviour and properties	tensile test, SEM	recycle		27 ± 3.3	4150 ± 350			
Andanje, M	2023	review --> DeStefano et al.	FDM	poly(glycolic acid)	PGA	pure	mechanical properties	literature search	biodegradable		60-99.7	6000-7000			35-45
Andanje, M	2023	review --> Morales et al.	FDM	rice husk an agricultural residue, and recycled polypropylene	rPP/RH	rPP post industrial waste & RH (0,5,10 wt. %) from Ambala grinder	different concentration and angle on Physical, thermal, mechanical, and morphological properties	TGA, Tensile test, SEM, warping assesment	recycle	1	5.6-13.6	600-1000			
Fico.D.	2022	review --> Ferrari et al.	FDM	recycled polyethylene terephthalate	rPET	recycled Pet from bottles	mechanical, physical thermal properties	DSC, XRD, rheological, TGA, tensile test	recycle		33.79–47.08	650-1360			
Morales.M.A.	2021	article	FDM	rice husk an agricultural residue, and recycled polypropylene	rPP/RH	rPP post industrial waste & RH (10 wt. %) from Ambala grinder composite angle at 90°	Physical, thermal, mechanical, and morphological properties	TGA, Tensile test, SEM, warping assesment	recycle	1	5.66 ± 0.82	660 ± 130			
Laoutid F.	2021	Article	FDM	thermoplastic polyolefins with recycled tire rubbers	TPO-GTR	TPO with recycled GTR (15 wt.% and 30 wt.%)	Physical and thermal properties, mechanical properties	SEM, TGA, tensile test, MFI	recycle	1	10	68-100			
Omar.N.W.Y.	2021	Article	FDM	recycled-carbon-fiber in polylactide	cF/PLA	carbon fiber loading (10 wt%, 20 wt%, and 30 wt%)	Physical and thermal properties, mechanical properties, water absorptivity	SEM, tensile test	recycle	1	45200	700-1750			
Singh.E.	2019	Article	FDM	acrylonitrile butadiene styrene, polylactic acid and high impact polystyrene	ABS/HPA/PHA	different combination of top, middle and bottom layers (of ABS/PLA/HIPS)	thermal and mechanical testing	tensile test, pull-out test, DSC	recycle	1	133.9 - 206.9	72.92- 325			
Morales.M.A.	2021	article	FDM	recycled polypropylene	rPP	rPP post industrial waste. composite angle at 90°	Physical, thermal, mechanical, and morphological properties	TGA, Tensile test, SEM, warping assesment	recycle	1	4.33 ± 1.73	740 ± 370			
Morales.M.A. 1	2021	article	FDM	recycled polypropylene	rPP	filaments of rPP and CBS composite angle at 90°	Physical, thermal, mechanical, and morphological properties	TGA, Tensile test, SEM, warping assesment	recycle		4.33 ± 1.73	740 ± 370			
Morales.M.A.	2023	review --> Pabón Rojas et al.	FDM	epoxy Fique fibers in cotton	Epoxy/Fique-Cotton	epoxy resin biocomposites from fique-cotton fibers	compatibility and vacuum level in the material's mechanical properties	SEM, FTIR, TGA, mechanical testing	biodegradable		31.5 ± 0.5	774.2 ± 16.1			
Morales.M.A. 1	2021	article	FDM	recycled polypropylene and cocoa bean shells	rPP/CBS	filaments of rPP/CBS with 10 wt.% of CBS on composite angle 90°	Physical, thermal, mechanical, and morphological properties	TGA, Tensile test, SEM, warping assesment	recycle		7.93 ± 1.29	780 ± 140			
Cui.J.	2023	article	DLP	Dynamic thermosetting photopolymers	HEMA-CANs	2-hydroxyethyl methacrylate (HEMA) monomer, bis(2-acryloyloxyethyl) malonate (BAM) crosslinker, diphenyl (2,4,6-trimethylbenzoyl) phosphine oxide (TPO) as photoinitiator	Tg, storage modulus, UTS and ε	tensile test, DMA, SRA, recycling experiments	recycle	virgin	12.8-14.1	784-1043		-	83.4-84.6

Occasi.G.	2022	article	FDM	recycled polypropylene and chemical recycling of whole face mask	rPP	92.3 wt% high-grade polypropylene (PP)	Physical and chemical characterization, mechanical recycling of filter and chemical recycling of whole mask	FTIR-ATR	recycle	1	25-40	800-1300			
Morales.M.A.	2023	review --> Pabón Rojas et al.	FDM	epoxy Fique fibers	Epoxy/Fique	epoxy resin biocomposites from fique	compatibility and vacuum level in the material's mechanical properties	SEM, FTIR, TGA, mechanical testing	biodegradable		50.7 ± 1.3	889 ± 16.6			
Morales.M.A. 1	2021	article	FDM	recycled polypropylene and cocoa bean shells	rPP/CBS	filaments of rPP/CBS with 5 wt.% of CBS composite angle at 0°	Physical, thermal, mechanical, and morphological properties	TGA, Tensile test, SEM, warping assesment	recycle		15.23 ± 0.91	950 ± 40			
Kristiawan.R.B.	2022	Article	FDM	glass powder and recycled polypropylene	rPP/GP	GP fraction of 2.5%, 5%, and 10% fractions	Physical and thermal properties, mechanical properties	FTIR, DSC, TGA and tensile test	recycle	1	20.23-27.64	960-1270			
Morales.M.A.	2023	review --> Daver et al.	FDM	Cork in polyactic acid	Cork-PLA	cork (up to 50 wt. %) from the outer bark of an oak tree in PLA	mechanical and physcical properties	DSC, DMA, tensile test,Izod impact test, SEM, TGA, SEM.	biodegradable		10.4-38.3	985.3-2815.4			68.5
Morales.M.A.	2023	review --> Osman et al.	FDM	Rice straw in Acrylonitrile Butadiene Styrene	ABS-RS	rice straw (5,10,15 wt. %) in ABS	mechanical properties	ASTM standards			decrease as Rice straw content increased	decrease as Rice straw content increased			
Morales.M.A.	2023	review --> Rojas-Vargas et al.	FDM	colombian coffee in polyester	CCSF/polyester	alkali treatment with NaOH (5%, 10%, and 15% of CCSF/polyester biocomposites	thermal/mechanical/morphological	tensile test, flexural test, SEM	biodegradable		increase if NaOH increased	increase if NaOH increased	increase if NaOH increased		
Morales.M.A.	2023	review --> Stoof et al.	FDM	Hemp and Harakeke fibers in polylactide Acid	hemp/PLA Harakeke/PLA	Hemp Harakeke (10,20,30 wt. %) in PLA (90/80/70 wt. %)	mechanical properties	tensile test, SEM			decrease if fiber wt. % increases	Increases if fiber wt. % increases			
Morales.M.A.	2023	review --> Rodriguez-Soto et al.	FDM	Natural fibers from sheet-stalk of the plantain plant in polyactic acid	NF/PLA	PLA semicrystalline and amorphous + thermosplastic strarch (TPS) + NF from plantain plant (surface chemical modification of fibres (SMNF))	surface, mechanical properties, biodegradation properties, thermal and optical properties	SEM, FTIR, TGA, mechanical testing	biodegradable		SMNF increases strength	SMNF increases modulus			
Andanje, M	2023	review --> Wang et al.	FDM	micro/nanocellulose-polylactic acid composite	MNC/PLA	30 wt. % MNC + 5 wt. % PEG6000 +65 wt. % PLA	method preparation on properties	testile tesing, SEM, TGA	biodegradable		59.7		50.7		
Andanje, M	2023	review --> Kearns et al.	FDM	cotton based fibers (0-20%)	LDPE/pCOT	virgin low density polyethylene (LDPE) + 25 wt.% pCot from recycled t-shirts	materials challenges of cotton-loaded	SEM, TEM, mechanical testing	recycle						
CHi. H.	2022	Article	DLP	recycled epoxy resin and graphene nanoplatelet	GN/EP	EP/GN ink with 10% GN	Physical and thermal properties, variable printing parameters, mechanical properties	LS-pop, rheometer, SEM, tensile test, resistance tester, thermal conductivity.	recycle	1,2,3,4	28 - 31				
Cui.J.	2023	article	DLP	Dynamic thermosetting photopolymers	HEMA-CANs	2-hydroxyethyl methacrylate (HEMA) monomer, bis(2-acryloyloxyethyl) malonate (BAM) crosslinker, diphenyl (2,4,6-trimethylbenzoyl) phosphine oxide (TPO) as photoinitiator	Tg, storage modulus, UTS and ε	tensile test, DMA, SRA, recycling experiments	recycle	1 & 2	12.8-14.1				
Fico.D.	2022	review --> Wei et al.	FDM	recycled aluminum-plastic packaging waste and expandable graphite	rAPWW/EG	APPW/EG (80/20)	mechanical, physical thermal properties	Tensile testing, S3M technology, rheological	recycle		13.58				
Fico.D.	2022	review --> esposito Corcione et al.	FDM	Lecce stone waste in Polylactid acid	LSW/PLA	PLA filaments with 50% wt and 60% wt. of LS waste powder.	mechanical, physical thermal properties	TGA, DSC, rheometer	recycle						
Fico.D.	2022	review --> Zhao et al.	FDM	Bamboo plastic composite	PLA/bamboo powder/PEG	Bamboo powder and PLA	mechanical, physical thermal properties		biodegradable						
Fico.D.	2022	review --> Bi et al.	FDM	Flexible wood flour in thermoplastic polyurethane	WF-TPU	TPU/WF (up to 40 wt. %) composite with EPDM-g-MAH/POE-g-MAH, PEG6000, Chitosan, MDI	The mechanical properties, microtopography and chemical structures after modification.	tensile test, SEM, FTIR, XPS, rheology	biodegradable		43770				
Fico.D.	2022	Article	FFF	recycled polylactic acid and artisanal ceramic waste	rPLA/CF	PLA (90 wt.%) & CF (10 wt.%)	morphological, thermal, rheological, and mechanical properties	SEM, XRD, DSC, rheometer, flexural test.	recycle				80		55.11
Häußler.M.	2021	Article	FFF	recycled polyester-18,18	PE-18,18	mix of PP, HDPE and PC-18	mechanical properties	tensile test	recycle	1	23				
Kim.S.	2022	article	FFF	Acrylonitrile Butadiene Styrene	ABS-vitrimers	Acrylonitrile Butadiene Styrene(ABS) polymer + cross-linker glutaradeheyde/Acetylacetone(AcAc)	mechanical performance evaluation, thermal analysis, and rheological measurements	Tensile test, DMA, TGA, rheometer,chemical-solvent resistance test.	recycled (up)	virgin,1,2,3	~28-45				
Kim.S.	2022	article	FFF	untreaded Acrylonitrile Butadiene Styrene	Neat-ABS	Acrylonitrile Butadiene Styrene(ABS) polymer + cross-linker glutaradeheyde/Acetylacetone(AcAc)	mechanical performance evaluation, thermal analysis, and rheological measurements	Tensile test, DMA, TGA, rheometer,chemical-solvent resistance test.	recycled (up)	virgin,1,2,3	~25				
Kolitha.B.S.	2023	article	FDM	poly(ethylene terephthalate)	PET	PET hydrolyzing enzymes +bacterial metabolic pathways	new chemo-bio approach to upcycle PET	combining enzymatic hydrolysis, microbial conversion, metabolic engineering, economic analysis, and sustainability assessments	recycled (up)	1					
Li.Y.	2023	review --> (Long.H et al, 2018)	FFF	Bamboo plastic composite	BF/PP/PLA	Bamboo fiber, poly lactic acid (PLA), polypropylene (PP) (5% MAPP)	mechanical and thermal properties	tensile test, TGA, DSC		Virgin	33.73				
Li.Y.	2023	review --> (liu.L et al, 2019)	FFF	Wood plastic composite	lignin/PLA	plant fiber, polylactic acid (PLA), silane coupling agent (KH550) (lignin 15%)	physical properties	tensile test, MFR test, DSC		virgin	20.7				
Liguori.A.	2023	article	DLP	isosorbide-based photocurable resins	MI100	Methacrylated isosorbide (MI monomer) (100wt.%)	printability, physical and chemical properties	spectrometer, TGA, stress-strain measurements						424 ± 1	64 ± 3

Lopez de pariza.X.	2023	article	DLP	recyclabe photoresins	PSU	Isophorone diisocyanate (IPDI), polypropylene glycol (PPG), thiol monomers, isopropylthioxanthone (ITX), and additives like trimethylpropane tris(3-mercaptopropionate) (triSH) and 1,1,3,3-tetramethylguanidine (TMG)	chemcial structure, thermal properties, viscosity, rehological measurements, relaxation behavior, mechanical properties after recycling	FT-IR, rheometer, tensile test, TGA, CA, DSC,DMTA	recycle	virgin,1,2					
Madhu.N.R.	2022	review	FDM	Recycled High Density Polyethylene with SiC/Al2O3 and Paraffin Wax	HDPE	SiC/Al2O3 and paraffin wax	Mechanical strength		recycle						
Madhu.N.R.	2022	review	FDM	Recycled High Density Polyethylene with Zirconia	HDPE	ZrO2	Coefficient of friction		recycle						
Madhu.N.R.	2022	review	FDM	Polyethene Terephthalate and Post-Pyrolysis Packaging Waste	PET	Post-pyrolysis packaging waste	Strength, thermal stability		recycle		Significant increase			Significant increase	Significant increase
Madhu.N.R.	2022	review	FDM	Polyethylene terephthalate, polypropylene, and Polyethylene with styrene-ethylene-butylene-styrene	PET/SEBS, PP/SEBS, PE/SEBS	polymers with Stabilisation promoter SEBS	Tensile strength		recycle		< pure rPET				
Madhu.N.R.	2022	review	FDM	Lignocellulose-Based Mats with Recycled PET	rPET	Lignocellulose-based mats	Mechanical properties		recycle		Enhanced				
Madhu.N.R.	2022	review	FDM	Recycled Gypsum and Hemp or Harakeke Fiber Filaments	rG, rHFF	recycled gypsum, hemp or harakeke fiber filaments	Mechanical properties		recycle		Improved value				
Mishra.V.	2023	review	FDM	Recycled High-Density Polyethylene	R-HDPE	Thermoplastic polymer composed of repeating ethylene units	Physical characterization, mechanical properties		recycle		High strength, toughness, and chemical resistance				
Mishra.V.	2023	review	FDM	Recycled Polylactic Acid	rPLA	Biodegradable thermoplastic polyester derived from renewable resources	Mechanical properties, tensile strength, elastic properties		Biodegradable and compostale		Good tensile strength, stiffness, and biocompatibility				
Mishra.V.	2023	review	FDM	Recycled Acrylonitrile Butadiene Styrene	R-ABS	Similar to virgin ABS, consisting of acrylonitrile, butadiene, and styrene monomers	MFI,Tg, mechanical properties		recycle	up to 5 cycli	decrease				decrease
Mishra.V.	2023	review	FDM	Recycled Polyethylene Terephthalate	rPET	Thermoplastic polymer made from terephthalic acid and ethylene glycol	3D print suitability		recycle		Good strength, stiffness, and chemical resistance				
Morales.M.A.	2023	review --> Zander et al.	FFF	recycled polyethylene terephthalate	rPET	From Pet bottles	Thermal and mechanical properties	FTIR, tensile test, tree-point bending test, rheology	recycle	1	35.1 ± 8				
Morales.M.A.	2023	review --> Zander et al.	FFF	recycled polyethylene terephthalate	rPET	From Pet bottles injection molded	Thermal and mechanical properties	FTIR, tensile test, tree-point bending test, rheology	recycle	1	68 ± 1				
Morales.M.A.	2023	review --> Pepi et al	FDM	recycled polyethylene terephthalate	rPET	from plastic soda bottles	Thermal and mechanical properties	tensile test, DSC, FTIR-ATR,SEM	recycle		36.4 ± 3.1				
Morales.M.A.	2023	review --> Pepi et al	FDM	recycled polystyrene	rPS	Petri dishes and utensils (opaque)	Thermal and mechanical properties	tensile test, DSC, FTIR-ATR,SEM	recycle		19.9 ± 3.9				
Morales.M.A.	2023	review --> Pepi et al	FDM	recycled polypropylene	rPP	from yogurt containers	Thermal and mechanical properties	tensile test, DSC, FTIR-ATR,SEM	recycle		20.1 ± 2.3				
Morales.M.A.	2023	review --> Zander et al.	FDM	recycled polypropylene and polyethene terephthalate	rPP/PET	rPP from paque yogurt containers, rPET from clear plastic salad containers (50/50 %wt)	Thermal and mechanical properties	tensile test, DSC, FTIR-ATR, DMA, rheometer	recycle	1	17.2 ± 4				
Morales.M.A.	2023	review --> Zander et al.	FDM	recycled polypropylene and polystyrene	rPP/PS	rPP from paque yogurt containers, rPS from petri dishes (50/50 %wt)	Thermal and mechanical properties	tensile test, DSC, FTIR-ATR, DMA, rheometer	recycle	1	23.0 ± 1				
Morales.M.A.	2023	review --> Zander et al.	FDM	recycled polypropylene and polyethene terephthalate	rPP/PET/SEBS	rPP from paque yogurt containers, rPET from clear plastic salad containers (50/50 %wt) + 5 wt. % unfunctionalized (SEBS)	Thermal and mechanical properties	tensile test, DSC, FTIR-ATR, DMA, rheometer	recycle	1	23.1 ± 1				
Morales.M.A.	2023	review --> Zander et al.	FDM	recycled polypropylene and polyethene terephthalate	rPP/PET/SEBS-MA	rPP from paque yogurt containers, rPET from clear plastic salad containers (50/50 %wt) + 5 wt. % maleic anhydride functionalized SEBS (SEBS-MA)	Thermal and mechanical properties	tensile test, DSC, FTIR-ATR, DMA, rheometer	recycle	1	24.2 ± 1				
Morales.M.A.	2023	review --> Zander et al.	FDM	recycled polypropylene and polystyrene	rPP/PS/SEBS	rPP from paque yogurt containers, rPS from petri dishes (50/50 %wt) + 5 wt. % unfunctionalized (SEBS)	Thermal and mechanical properties	tensile test, DSC, FTIR-ATR, DMA, rheometer	recycle	1	19.0 ± 3				
Morales.M.A.	2023	review --> Zander et al.	FDM	recycled polypropylene and polystyrene	rPP/PS/SEBS-MA	rPP from paque yogurt containers, rPS from petri dishes (50/50 %wt) + 5 wt. % maleic anhydride functionalized SEBS (SEBS-MA).	Thermal and mechanical properties	tensile test, DSC, FTIR-ATR, DMA, rheometer	recycle	1	22.9 ± 1				
Morales.M.A.	2023	review --> Kain et al.	FDM	Wood fluor with polylactide acid	wood/PLA	wood fibers (15 wt. %) in PLA (85 wt.%)	infill pattern on tensile strength, compressive strength, structure, charpy impact strength, HDT	SEM, tensile test, charpy impact test, HDT test			15 - 30				
Morales.M.A.	2023	review --> Kain et al.	FDM	Wood fluor with polylactide acid	wood/PLA	wood fibers (25 wt. %) in PLA (75 wt.%)	infill pattern on tensile strength, compressive strength, structure, charpy impact strength, HDT	SEM, tensile test, charpy impact test, HDT test			25- 33				
Morales.M.A.	2023	review --> Zhang et al.	FFF	Continuous carbon Fiber-Reinforced Thermoplastic Composites	CCFRP	carbon fibers (10.6, 20.4 36.7 wt/wt) in PLA	Tensile strength and tensile modulus, flexibel strength/modulus	tensile test, three-point bending					372		
Morales.M.A.	2023	review --> Le Guen et al.	FDM	Wood biomass in polylactic acid	PLA-wood	wood flour powder (10% wt) in PLA	different printing angle on mechanical properties. next to chemical en physical properties	tensile test, SEM, NMR, Ash, rheometer, GPC, DMTA					40-58		65
Morales.M.A.	2023	review --> Le Guen et al.	FDM	Rice Husk in polyactic acid	PLA-rice	Carmargue rice (Oryza) husks (10 % wt) in PLA	different printing angle on mechanical properties. next to chemical en physical properties	tensile test, SEM, NMR, Ash, rheometer, GPC, DMTA					30 - 52		65
Morales.M.A.	2023	review --> Girdis et al.	FDM	macadamia nutschell in Acrylonitrile Butadiene Styrene	ABS-MNs	macadamia nutschell (19,29 wt.%) in ABS	mechanical properties	tensile test			decrease if level of MN increases				

Morales.M.A.	2023	review --> Páez et al.	FDM	chambira fiber in Polylactic acid	CF-PLA	colombia chambira fiber in PLA matrix	pullout behaviour of fibers, IFSS,	extensometer	biodegradable						
Morales.M.A.	2023	review --> Hidalgo-Salazar et al.	FDM	cane bagasse in polypropylene	PP bag	bargass fibers in PP matrix	mechanical, viscoelastic, and thermal behaviors	DSC, TGA, DMA, and SEM	biodegradable				48.0 ± 1.1	423	5.3
Morales.M.A.	2023	review --> Hidalgo-Salazar et al.	FDM	cane bagasse in polypropylene	PP bag NaOH	NaOH treatment of bagasse fiber on PP matrix	mechanical, viscoelastic, and thermal behaviors	DSC, TGA, DMA, and SEM	biodegradable				43.3 ± 0.5	422	3.4
Morales.M.A.	2023	review --> Hidalgo-Salazar et al.	FDM	cane bagasse in polypropylene	PP bag NaOH Silane	NaOH treatment of bagasse fiber on PP matrix with silanizationn with hexadecyl triethoxysilane	mechanical, viscoelastic, and thermal behaviors	DSC, TGA, DMA, and SEM	biodegradable				38.6 ± 1.9	311	5.7
Patti.A.	2022	article	FDM	Polylactide acid	neat PLA	virgin PLA-matrix	Physical and thermal properties, variable printing parameters, mechanical properties	ATR, DSC, TGA, DMA,	recycle	1					60
Patti.A.	2022	article	FDM	Recycled polylactide acid	rPLA	waste from the production of biobags	Physical and thermal properties, variable printing parameters, mechanical properties	ATR, DSC, TGA, DMA							
Patti.A.	2022	article	FDM	Wood-based biocomposite	Wood/PLA	PLA and Fir wood fibres	Physical and thermal properties, variable printing parameters, mechanical properties	ATR, DSC, TGA, DMA,		virgin					60
Reich.M.J.	2019	Article	FPF/FGF	recycled polycarbonate	rPC	Recycled PC regrind	mechanical properties	ASTM type 4 tensile test, ASTM copression test	recycle	1	64.9				
Samoylenko.D.E.	2023	article	FDM	calcium carbide residue-based composite	CCR/PLA	calcium hydroxide (Ca(OH)2) and PLA	Mechanical properties, specifically tensile strength, Young's modulus, and shape retention/shrinkage	tensile test, SEM,EDX	recycle						
shou.T.	2021	Article	FDM	Biobased and Recydable Polyurethane	PLA/TPU	modified polylactic acid polyols, 4,4'-diphenylmethane diisocyanate, and 1,4-butanediol. PLA-based TPU	Physical and thermal properties, mechanical properties	DSC, TMA, FTIR, thermal analysis tensile test, TA, MTT	recycle	1,2,3	19- 23				
Spoerk.M.	2019	Article	FFF	Recyclability of Polypropylene with coated mineral filler	PP/MF	PP(83.7 wt.%)/MF (15.0 wt.%)/compatibilizer (1.3 wt.%)	physical properties, mechanical properties, thermal properties	SEM, charpy test, rheometer, TGA, tensile test	recycle		23-35				
Zgodavova.K.	2021	Article	FDM	Polyalactid	PLA	pure	optimization parameters 3d printing	tensile test, weigthed sum method for multi-objective optim.			31.3				
Zgodavova.K.	2021	Article	FDM	polyhydroxyalkanoate biowoodRosa	PHA/wood	from 100% natural and renewable biopolymer	optimization parameters 3d printing	tensile test, weigthed sum method for multi-objective optim.			14				
Zgodavova.K.	2021	Article	FDM	Polyethylene Terephthalate Glycol	PETg	Prusament PETG Orange PPE	optimization parameters 3d printing	tensile test, weigthed sum method for multi-objective optim.			31.2				
Morales.M.A.	2023	review --> Stoof et al.	FDM	Polypropylene	PP	plain PP	mechanical properties, shrinkage	SEM, tensile test,	recycle		22	892			

Table A.1: Key terms and synonymous terms in Boolean search style.

Recycl*	**”3D print*”**	**Sustain***	**Material***	**”Trauma care”**
Reus*	”Additive manufactur*”	Biodegrad*	Filament*	Splint*
”Waste management”	”Three-dimensional print*”	”Circular economy”	Plastic*	Plaster
Reproces*	”Fused deposition model*”	”Bio based”	Polymer*	Cast*
Upcycl*	”Digital fabrication”	”Environmentally friendly”	Compound*	Brace
Regenerat*	”Layered manufactur*”	Green	Component*	”Fracture management”
Refurbish*	”Rapid prototyp*”	Eco-friendly		Stabiliz*
Repurpos*	”Stereolithography”	Compos*		”Orthopedic treatment”
Redeem*	”Digital light processing”	Nature-Based		Immobiliz*
	Renewable	Biocompatib*		

Table A.2: Inclusion/exclusion criteria for studies

Criteria	**Inclusion**	**Exclusion**
Keywords	3D Printing, Additive manufacturing, Three-dimensional printing, Recycling, sustainable, biodegradable, stereolithography, circular economy, rapid prototyping, digital light processing, fused deposition modeling	Metal, tissue engineering, bone tissue, bone regeneration, food packaging, scaffolds, drug, sensors.

Rubric for material selection

This rubric is used to score the requirements according to the objective of the 3DxSplint from 1 to 5. Every 3DxSplint objective has a scoring of the requirements of the splint. They are presented in this section.

Criteria	1	2	3	4	5
Low Environmental Impact	High environmental footprint, significant resource use and pollution during production and disposal.	Moderate negative impacts, some recyclable components but still contributes to waste.	Balanced impact, with both positive and negative aspects; limited recyclability.	Low environmental impact, utilizes renewable resources or lower energy processes, effective recycling pathways.	Minimal impact, made from sustainable sources, high recyclability, and no significant pollution.
Recyclable and/or Biodegradable	Neither recyclable nor biodegradable, leading to substantial waste.	Partially recyclable or biodegradable but takes a long time to degrade.	Limited in recyclability or biodegradability; conditions exist for either.	Either fully recyclable or fully biodegradable, but has some limitations.	Both biodegradable & recyclable, readily accepted in recycling systems.
Thermal Decomposition Temp > 80°C	< 50°C not suitable far below the required temperature	50-60°C, Significantly far from required temperature	60-70°C	70-80°C	>80°C, suitable
Ultimate Tensile Strength (42-84 MPa)	< 25 MPa, or >105 MPa, not suitable for below or above the required range	25-30 MPa, or 100-105 Significantly outside the optimal range	30-35 MPa, or 95-100 Mpa Close to the lower or upper limit, not ideal	35-42 MPa, or 84-95 MPa, Slightly above or below the ideal range, still functional	42 MPa - 84 MPa (Meets the requirement, ideal tensile strength)
Flexural Modulus (1590-2000 MPa)	< 1000 MPa, or > 2600 MPa. Far below or above the required range	1000-1199 MPa, or 2401-2600 MPa. Too flexible or too rigid, far from the optimal range	1200-1399 MPa, or 2201-2400 MPa. Close to the lower/upper limit, flexibility or rigidity is starting to be suboptimal	1400-1589 MPa, or 2001-2200 MPa. Slightly above or below, still within an acceptable range	1590-2000 MPa, Meets the requirement, ideal rigidity and flexibility

Criteria	1	2	3	4	5
Hardness (80D-96D)	< 50D, far below the required range	50-60D, too soft.	60D-70D, close to the lower limit.	70D-80D, or 96D-100D. Slightly above or below the ideal range, still functional.	80D-96D Meets the requirement, ideal hardness.
E-modulus ≥ 2460 MPa	<1000 MPa	1000-1400 MPa, not suitable for structural applications.	1400-2000 MPa, slightly below the required range	2000-2460 MPa, good stiffness.	> 2460 MPa, excellent stiffness for demanding applications.
Not soluble in water	Highly soluble, leading to degradation in aqueous environments or not available.	Moderately soluble, significant water absorption that can affect performance.	Slightly soluble, some degradation but generally maintains structural integrity.	Mostly hydrophobic, minimal water absorption issues.	Fully hydrophobic, no water solubility concerns.
Not prone to self-ignition	Highly reactive, significant risk of spontaneous ignition under normal conditions or not available.	Prone to self-ignition under certain conditions; requires careful handling.	Fairly stable, but some materials show increased risk of ignition.	Generally stable, not prone to self-ignition.	Extremely stable, designed for high-temperature applications, not prone to ignition.
Not explosive	Highly reactive and explosive under various conditions or not available.	Some risk of explosive reactions; requires careful management.	Moderate risk; generally stable but can react under specific conditions.	Non-explosive, stable under standard conditions.	Inert and completely non-explosive, safe for a wide range of applications.
Does not propagate fire	Highly flammable and readily propagates fire or not available.	Moderate flammability, can support fire propagation under certain conditions.	Somewhat flammable, may propagate fire but less readily.	Generally resistant to fire propagation; good flame resistance.	Excellent fire resistance; specifically designed to prevent fire propagation.

Criteria	1	2	3	4	5
Produced within EU	Not available	produced outside the EU	Produced within the broader EU	produced in neighboring countries	Produced in NL
Compatibility with Print Methods	Cannot be reliably printed	Printing with frequent issues	Can be printed with limitations	Reliably print with minimal adjustments	Material can be optimized with a method and has outstanding print quality

Table A.4: Sustainability and environmental impact of various materials. The ratings are from 1 (low) to 5 (high) across the categories: Low Environmental Impact, Recyclability/Biodegradability, and Overall Sustainability.

Material	Low Environmental Impact (1-5)	Recyclable and/or Biodegradable (1-5)	Sustainability (1-5)
rPLA	5	5	5
rPETg	5	4	4.5
CFF-PLA	5	4	4.5
PLLA	5	4	4.5
PLA/Wood	5	4	4.5
rPP	4	4	4
rPET	4	4	4
Biofusion	4	3	3.5
GreenTEC	5	4	4.5
GreenTEC Pro	5	4	4.5
Polyamide 12	1	3	2
Elastic resin with 85% Bio content	4	4	4

Continued on next page

Material	Low Environmental Impact (1-5)	Recyclable and/or Biodegradable (1-5)	Sustainability (1-5)
Flexible resin with 85% Bio content	4	4	4
Hard resin with 85% Bio content	4	4	4
PolyHydroxy Alkanoates	5	4	4.5
niceBIO filaments	4	4	4
Recycled PEEK	4	3	3.5
Plant-based UV resin	3	1	2
Multicomp Pro LCD PLA resin	3	1	2
rApolloX	5	4	4.5

Table A.5: Mechanical properties of various materials. The ratings are from 1 (low) to 5 (high) across the categories: Thermal Decomposition, Ultimate Tensile Strength, Flexural Modulus, Hardness, E-modulus, and Immobilize DRF.

Material	Thermal De-composition Temp > 80°C (1-5)	Ultimate Tensile Strength (42-84 MPa) (1-5)	Flexural Modulus (1590-2000 MPa) (1-5)	Hardness (80D-96D) (1-5)	E-modulus ≥ 2460 MPa (1-5)	Immobilize DRF (1-5)
rPLA	5	5	1	3	5	3.8
rPETg	5	5	5	3	3	4.2
CFF-PLA	5	4	4	4	5	4.4
PLLA	5	5	1	5	5	4.2
PLA/Wood	5	4	1	4	5	3.8
rPP	5	1	2	3	2	2.6

Continued on next page

Material	Thermal De-composition Temp > 80°C (1-5)	Ultimate Tensile Strength (42-84 MPa) (1-5)	Flexural Modulus (1590-2000 MPa) (1-5)	Hardness (80D-96D) (1-5)	E-modulus ≥ 2460 MPa (1-5)	Immobilize DRF (1-5)
rPET	5	4	5	3	3	4
Biofusion	5	5	4	1	5	4
GreenTEC	5	5	1	1	5	3.4
GreenTEC Pro	5	5	1	1	5	3.4
Polyamide 12	5	5	4	1	3	3.6
Elastic resin with 85% Bio	1	1	1	1	1	1
Flexible resin with 85% Bio	1	1	1	1	1	1
Hard resin with 85% Bio	1	1	1	4	2	1.8
PolyHydroxy Alkanoates	1	2	5	2	5	3
niceBIO filaments	1	5	1	1	5	2.6
Recycled PEEK	5	4	1	1	5	3.2
Plant-based UV resin	2	3	1	1	5	2.4
Multicomp Pro MP004398	1	5	1	4	1	2.4
rApolloX	1	5	5	1	3	3

Table A.6: User safety ratings of various materials. The ratings are from 1 (low) to 5 (high) across the categories: Not Soluble in Water, Not Prone to Self-Ignition, Not Explosive, Does Not Propagate Fire, and Overall User Safety.

Material	Not Soluble in Water (1-5)	Not Prone to Self-Ignition (1-5)	Not Explosive (1-5)	Does Not Propagate Fire (1-5)	User Safety (1-5)
rPLA	5	4	5	5	4.75
rPETg	5	4	5	5	4.75
CFF-PLA	4	5	5	3	4.25
PLLA	5	5	3	5	4.5
PLA/Wood	5	5	5	4	4.75
rPP	5	2	5	1	4.25
rPET	5	5	5	3	4.5
Biofusion	5	5	5	5	5
GreenTEC	5	5	5	5	5
GreenTEC Pro	5	5	5	5	5
Polyamide 12	5	5	5	1	4
Elastic resin with 85% Bio content	5	5	5	3	4.5
Flexible resin with 85% Bio content	5	5	5	3	4.5
Hard resin with 85% Bio content	5	5	5	3	4.5
PolyHydroxy Alkanoates	1	5	5	5	4
niceBIO filaments	1	1	1	1	1
Recycled PEEK	1	2	5	5	3.25
Plant-based UV resin	1	1	1	1	1

Continued on next page

Material	Not Soluble in Water (1-5)	Not Prone to Self-Ignition (1-5)	Not Explosive (1-5)	Does Not Propagate Fire (1-5)	User Safety (1-5)
Multicomp Pro MP004398	5	1	1	3	2.5
rApolloX	5	5	5	5	5

Table A.7: Material ratings for production location within the EU and compatibility with printing methods. The ratings are from 1 (low) to 5 (high) across the categories: Produced within EU, Compatibility with Print Methods, and Logistics.

Material	Produced within EU (1-5)	Compatibility with Print Methods (1-5)	Logistics (1-5)
rPLA	5	5	5
rPETg	5	5	5
CFF-PLA	3	4	3.5
PLLA	5	5	5
PLA/Wood	4	3	3.5
rPP	3	3	3
rPET	5	5	5
Biofusion	3	5	4
GreenTEC	3	5	4
GreenTEC Pro	3	5	4
Polyamide 12	4	3	3.5
Elastic resin with 85% Bio content	3	3	3
Flexible resin with 85% Bio content	3	3	3
Hard resin with 85% Bio content	3	3	3

Continued on next page

Material	Produced within EU (1-5)	Compatibility with Print Methods (1-5)	Logistics (1-5)
PolyHydroxy Alkanoates	5	4	4.5
niceBIO filaments	3	4	3.5
Recycled PEEK	5	3	4
Plant-based UV resin	2	3	2.5
Multicomp Pro MP004398	3	3	3
rApolloX	5	5	5

B APPENDIX B

First recycle protocol performed at CHILL

Materials

- Filament Type: Virgin PLA from BASF
- Filament Diameter: 2.85 mm
- Total Mass of Printed Parts: 1940 g
- Printer Model: Ultimaker S5
- Granulator Model: ZERMA GSL-180/180 (Machine No./Year: #8942/2013)
- Filament Extruder: 3Devo Filament Maker 450 – Precision (Machine No.: FMV1P-141547)

The test parts were printed using an Ultimaker S5 3D printer with the following settings: a 0.4 mm nozzle, a nozzle temperature of 200 ° C, a bed temperature of 60 ° C and a print speed set to 70 mm/s. The layer thickness was 1.0 mm, with 100% infill using a zigzag pattern. The support structures were applied everywhere with a horizontal expansion of 0.8 mm. Retraction was enabled with Z-hop when retracted and the cooling fan operated at 100%. The printed parts consisted of tensile test strips and 3x3x3 cm cubes. After printing, the support material was manually removed and the parts were stored in bags prior to further processing.

The printed parts were granulated using a ZERMA GSL-180/180 granulator. The material was initially processed through a 5 mm screen, resulting in 70 g loss of material due to static build-up and retention within the granulator. To reduce particle size and improve flowability, the granulated material was then passed through a second screen with smaller holes 4 mm in diameter. This process resulted in an additional 85 g of material loss. Compressed air was used to remove stuck particles from the machine and it was recommended to process larger batches to minimize the relative percentage of material loss.

For filament production, a 3Devo Precision Filament Maker was used. The machine was first purged with standard PLA pellets to ensure a clean extruder. In the first attempt, the PLA granulated from the 5 mm screen caused a motor overload error due to the size of the granules B.2. Following regranulation with the 4 mm screen, the extrusion process proceeded but still experienced material losses and irregular flow.

To optimize filament production, adjustments were made to both the extrusion temperature (increased by 5°C) and the screw speed. Despite these changes, fluctuations in the diameter of the filament persisted. These fluctuations were attributed to the irregular shape of the granules, which caused inconsistent pressure and volume within the extruder. As the 3Devo Filament Maker does not dynamically adjust screw speed or temperature based on real-time diameter feedback, achieving a stable diameter remained a challenge.

Figure B.1: Granulation of second-time process material with reduction of particle size, screen with 4 mm diameter holes

The extrusion process was carried out under laboratory conditions at 23° C and 50% relative humidity. The target filament diameter was 1.75 mm, suitable for a Bambulabs X1 Carbon 3D printer.

Second recycle protocol at CHILL

Materials

- Filament Type: Recycled PLA granules (processed in first recycle process)
- Filament Diameter Goal: 2.85 mm
- Extruder Model: COLLIN Teach-Line E20T
- Extrusion Process Using COLLIN Teach-Line E20T

The extrusion process was carried out using a COLLIN Teach-Line E20T extruder equipped with a screw-based feed system (the setup is shown in Figure B.3). PLA granules were loaded into the machine, where they were heated in four controlled heating zones. Each zone was designed to ensure even melting and mixing of the material as it moved through the screw mechanism. The temperature was precisely regulated to promote uniform melting and to prevent degradation of the recycled PLA. Once the PLA was fully melted, it was pushed through the extruder's nozzle, producing a continuous molten filament. Immediately after extrusion, the hot filament passed through a water bath for rapid cooling. The water bath allowed the filament to solidify quickly, preserving its shape and preventing sagging. The extrusion process focused on maintaining consistency in the filament's shape. After being cooled, the filament was pulled from the water bath using a drawing machine. The drawing speed was carefully controlled to ensure a uniform diameter throughout the length of the filament. Consistent tension was applied to prevent any stretching or inconsistencies. The cooled filament was then wound onto a spool. The spooling mechanism was operated at a regulated speed to ensure uniform winding, preventing tangling or loose spots that could affect subsequent printing operations. The COLLIN Teach-Line features built-in controls to monitor and maintain the filament's diameter during extrusion. Adjustments were made to optimize the diameter, but the target of 2.85 mm

(a) Granulate feed into the 3devo filament maker with 4 mm diameter

(b) Granulate with a diameter of 5 mm and to big for the feeder of the 3Devo

Figure B.2: Granulate from the shredder used to determine which diameter is needed for the 3Devo filament extrusion step.

was not achieved. The resulting filaments were slightly smaller in diameter than intended ($\approx 2.6mm$); $the diameter of the filament was manually measured to inspect the diameter of the filament. The filamen$

Third Recycle Protocol at CHILL

The material used in this study was PLA regrind purchased from ColorFabb (Figure B.8f). It was stored in a dry environment at room temperature before processing. A total of 2.6 kg of material was printed in blocks with dimensions of 30x30x100 mm (Figure B.8b) and an infill density of 80%, using standard PLA settings. The printing was carried out using a Bambulab X1 Carbon 3D printer over a period of three days.

Following printing, the material was weighted and systematically fed, block by block, into a ZERMA GSL-180/180 granulator equipped with a 5 mm diameter screen B.8c. The shredded PLA flakes were then weighed and transferred to a Coperion K-SFS-24 Smart Flow Meter, which automatically and uniformly transported the granulated flakes into the Coperion ZSK 18 MEGAlab twin screw extruder. Within the extruder, the material was heated, mixed to achieve homogeneity, and extruded through a 4 mm nozzle. The extruded material was passed through a Coperion CT 120-100-2000 water bath, filled with water at room temperature, to cool the extrudate. Upon exiting the water bath, the material was dried using an air blower. The dried material was subsequently pelletized using a Coperion SP30 EN pelletizer, producing PLA pellets. The setup is shown in figure B.6.

These pellets were weighed and dried in an oven at 80°C for 1.5 hours. During the day, the 3Devo Precision 450 filament maker was preheated. After drying, the pellets were fed into the

Figure B.3: COLLIN Tech-Line extruder with a water bath

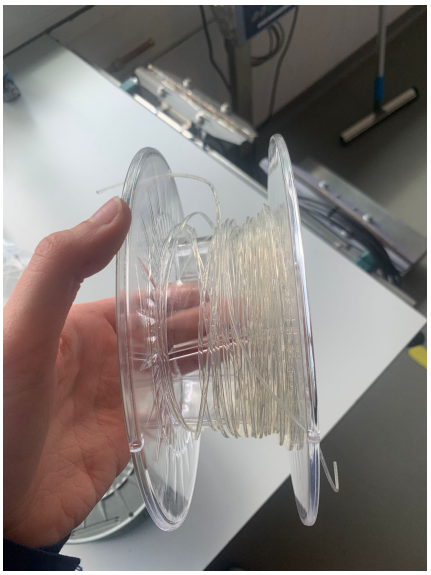

Figure B.4: Results from second recycle protocol at CHILL with the COLLIN. A short filament spooled with air bubbles and inconsistent diameter

Figure B.5: Granulation of the shredded print PLAregrind material

Figure B.6: Filament extrusion on the Corperion extruder left, in the middle the water bath and right the Corperion pelletizer is placed.

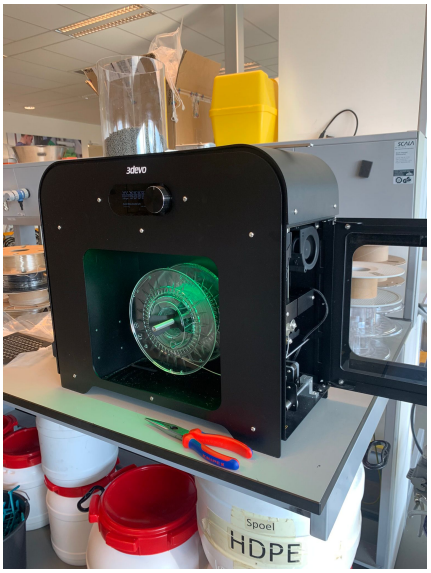

Figure B.7: 3Devo filament maker during filament spooling with PLAregrind material

filament maker, using the default PLA 1.75mm settings: Heater 1 at 180°C, Heater 2 at 190°C, Heater 3 at 185°C, and Heater 4 at 160°C. The extrusion speed was set to 3.7 RPM and the fan speed was maintained at 60% the spooling of the regrindPLA material is shown in Figure B.7.

Initial attempts to stabilize filament output involved manual adjustments to achieve a consistent filament diameter. Once the diameter fluctuations stabilized around 1.75 mm, the filament was spooled. After enough filament was in the spool, the spool was tested on the Bambulab 3D printer.

Recycle protocol at NHL Stenden Hogeschool

The PETg recycling protocol at NHL Stenden begins with the preparation of virgin materials, specifically the PETg packaging that is typically used for surgical instruments B.9a. The material is manually cut to remove any adhesive borders, ensuring that only clean material is utilized for recycling. Following preparation, PETg sheets are processed using the 3Devo GP20 Plastic Shredder Hybrid, where they are reduced to smaller flakes with an approximate diameter of 3

(a) PLA regrind on spool

(b) Printed blocks

(c) Granulate

(d) Pellets

(e) Filament extrusion

(f) recycled PLA regrind filament on Spool

Figure B.8: Comparison of recycled PLA in various stages: (a) PLA regrind filament on spool (1.75mm), (b) Printed blocks of regrind PLA, (c) Granulate, (d) Pellets, (e) Filament extrusion of rPLA, (f) Recycled PLA regrind filament on spool.

mm B.10a. This shredding process takes about 15 minutes, resulting in a total of 930 grams of shredded flakes after a material loss of approximately 68 grams.

The shredded PETg flakes are then dried in the 3Devo AIRID- Polymer Dryer for 4 hours at 65 ° C to remove the moisture content B.10b. After drying, a further loss of about 6 grams occurs, yielding a final weight of 924 grams. The dried flakes are then fed into the 3Devo Filament Maker Precision 350 for filament production, where they are processed for about 1.5 hours B.6. The extruder is set with specific temperature zones H4: 210 °C, H3: 220 °C, H2: 230 °C, H1: 220 °C and RPM: Set to 6.5, with the cooling fan operating at 100%, allowing the material to melt and be extruded through a nozzle. During this process, the diameter consistency of the filament is monitored, ultimately achieving an average diameter of 2.83 mm. Filament production results in a loss of approximately 74 grams, which yields a total of 376 grams of filament, which is equivalent to 48 meters in length B.9d. The whole recycling process is presented in figure B.9.

3DxSplint design

The splint design was created with a 3D scan of the wrist using Spentys software based on a hand scan. The design was sliced using Ultimaker Cura software to optimize the print settings (Figure B.11). The print configuration included a 50% infill density and a cubic infill pattern, with only support structures at the bottom (10mm) for strong adhesion to the bed. The final splint design required 42 grams of material and 5.24 meters of filament to produce.

(a) Virgin PETg

(b) shredded rPETg

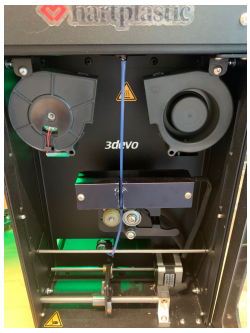

(c) Filament extrusion

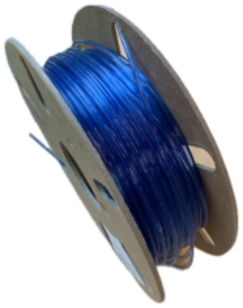

(d) Recycled PETg filament on spool

Figure B.9: Comparison of recycled PETg in various stages: (a) Virgin PETg packaging material, (b) shredded rPETg, (c) filament extrusion, (d) Recycled PLA regrind filament on spool.

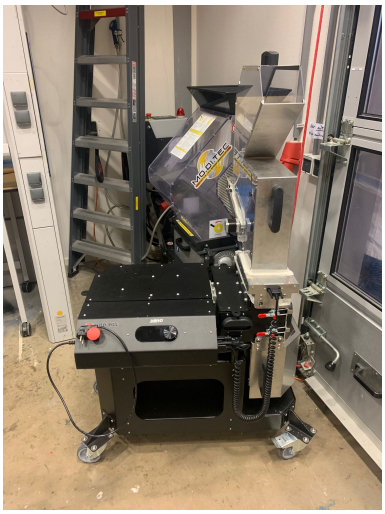

(a) 3Devo shredding machine for making flakes of 3 mm

(b) 3Devo drying machine for drying the flakes before filament extrusion.

Figure B.10: Overview of the shredding and drying processes in the PETg recycling protocol.

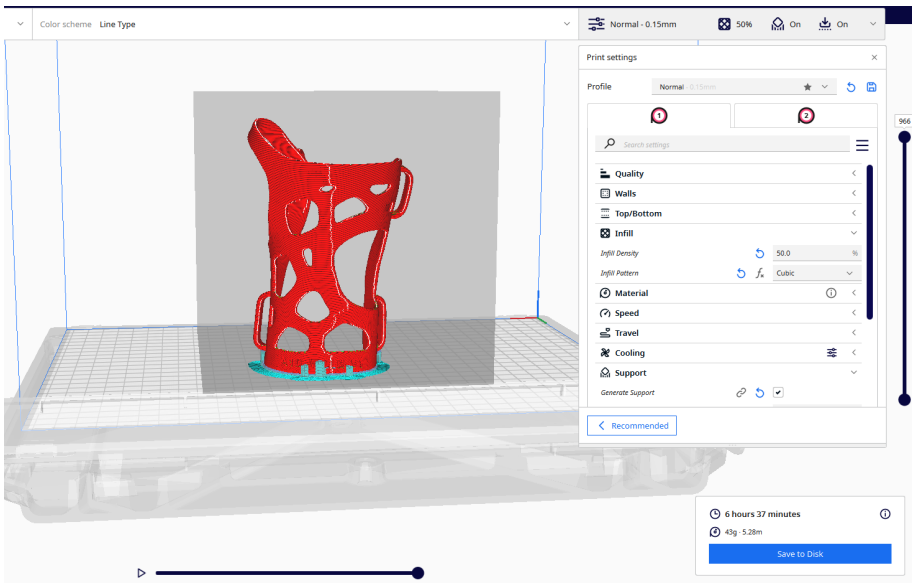

Figure B.11: 3DxSplint sliced in Ultimaker Cura software with the PETg default settings and the change settings. In blue the support is visible in 10 mm from the bottom.

C APPENDIX C

Technical Data Sheets for the tested materials

Technical Data Sheet for Ultrafuse PLA — Version No. 4.4

Mechanical Properties

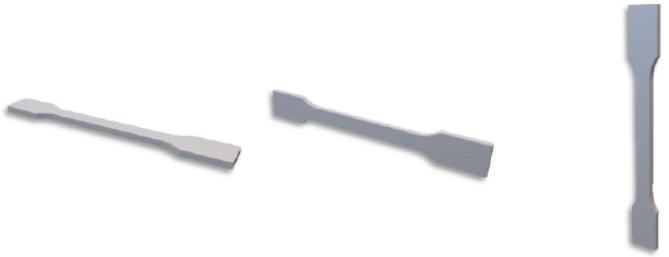

Print direction	Standard	XY	XZ	ZX
		Flat	On its edge	Upright
Tensile strength	ISO 527	34.7 MPa / 5.0 ksi	-	21.2 MPa / 3.1 ksi
Elongation at Break	ISO 527	4.2 %	-	1.2 %
Young's Modulus	ISO 527	2308 MPa / 335 ksi	-	2131 MPa / 309 ksi
Flexural Strength	ISO 178	98.0 MPa / 14.2 ksi	105 MPa / 15.2 ksi	54.9 MPa / 8.0 ksi
Flexural Modulus	ISO 178	1860 MPa / 270 ksi	1708 MPa / 247 ksi	1715 MPa / 249 ksi
Flexural Strain at Break	ISO 178	4.8 %	4.2 %	1.9 %
Impact Strength Charpy (notched)	ISO 179-2	2.5 kJ/m²	1.9 kJ/m²	1.7 kJ/m²
Impact Strength Charpy (unnotched)	ISO 179-2	13.2 kJ/m²	14.3 kJ/m²	4.3 kJ/m²
Impact Strength Izod (notched)	ISO 180	3.3 kJ/m²	2.1 kJ/m²	1.6 kJ/m²
Impact Strength Izod (unnotched)	ISO 180	11.0 kJ/m²	9.6 kJ/m²	4.7 kJ/m²

Figure C.1: Technical Data Sheet of PLA from manufacturer BAS-F, adapted from [94].

Technical datasheet
PLA Regrind

colorFabb

Date of issue: December 12th, 2023
Version: v2.0

Description

colorFabb PLA Regrind is produced from 100% post-filament extrusion waste from colorFabb premium printing filament. The production team meticulously separates out-of-spec PLA filament waste, which is then recycled inhouse to create colorFabb PLA Regrind.

Please note: each production run will entail slight deviation in color due to the deviation in the filament that is used for recycling. Each batch of PLA Regrind therefor has a unique color.

Typical Properties

Mechanical Properties – 3D Printed

	Method	*Value*	*Unit*
Youngs Modulus	Tensile, ISO 527-1A	3150	MPa
Tensile Strength	Tensile, ISO 527-1A	53	MPa
Elongation at break	Tensile, ISO 527-1A	4,2	%
Flexural Modulus	Flexural, ISO 178	2900	MPa
Flexural Strength	Flexural, ISO 178	91	MPa
Impact Strength	Charpy Notch, ISO 179	2,9	kJ/m^2

Mechanical Properties – 3D Printed PLA Premium Printing Filament*

	Method	*Value*	*Unit*
Youngs Modulus	Tensile, ISO 527-1A	3300	MPa
Tensile Strength	Tensile, ISO 527-1A	70	MPa
Elongation at break	Tensile, ISO 527-1A	3,5	%
Flexural Modulus	Flexural, ISO 178	2400	MPa
Flexural Strength	Flexural, ISO 178	97	MPa
Impact Strength	Charpy Notch, ISO 179	4,0	kJ/m^2

Mechanical Properties – Injection Molded**

	Method	*Value*	*Unit*
Youngs Modulus	Tensile, ISO 527-1A	3500	MPa
Tensile Strength	Tensile, ISO 527-1A	45	MPa
Elongation at break	Tensile, ISO 527-1A	≤5.0	%
Flexural Strength	Flexural, ISO 178	N/A	MPa
Charpy Impact Strength	Charpy Notch, ISO 179	≤5.0	kJ/m^2
Density	ISO 1183	1,2	g/cm^3

Thermal Properties**

	Method	*Value*	*Unit*
Glass Transition Temp.	DSC, ISO 11357	55-60	°C
Melting Temp.	DSC, ISO 11357	150-160	°C
Decomposition Temp.	TGA, ISO 11358	N/A	°C
Heat Deflection Temp.	HDT-B, ISO 75	60	°C
Melt Flow Index	MFI, (210°C/2.16 kg), ISO 1133-A	6	g/10min
Melt Flow Index	MFI, (190°C/1,16 kg), ISO 1133-A	3	g/10 min

*This data is obtained from the PLA Premium Printing filament recycled by colorFabb
**These results are obtained from the information provided by the supplier of the raw material

colorFabb B.V.
Bremweg 7
5951 DK Belfeld
The Netherlands

T +31 (0)77 – 4664015
F +31 (0)77 – 3971414
E sales@colorfabb.com
I colorfabb.com

KvK nr: 53498607
VAT nr: NL850902770B01
IBAN:
NL54RABO0151849188
BIC: RABONL2U

Technical datasheet
PLA Regrind

colorFabb

Date of issue: December 12th, 2023
Version: v2.0

Filament Specifications

	Unit		
Diameter	mm	1.75	2.85
Max. roundness deviation	mm	± 0.05	± 0.1
Net. Filament weight	g	2200	2200

Guideline for print settings

	Unit	
Nozzle Temp.	°C	195-220
Bed Temp.	°C	50-60
Bed / surface modification	-	Tape, Glue Stick
Active cooling fan	%	100
Print Speed	mm/s	40-100

Notes

The reported properties are an average of a batch of 3D specimens.
The specimens have been printed in XY plane, using 0,15 mm layer height, 100% infill, 0,4 mm nozzle, 210°C nozzle temperature and 55°C bed temperature.

colorFabb B.V.
Bremweg 7
5951 DK Belfeld
The Netherlands

T +31 (0)77 – 4664015
F +31 (0)77 – 3971414
E sales@colorfabb.com
I colorfabb.com

KvK nr: 53498607
VAT nr: NL850902770B01
IBAN:
NL54RABO0151849188
BIC: RABONL2U

Figure C.2: Technical Data Sheet of PLA Regrind from manufacturer ColorFabb, adapted from [87].

Mechanical properties

All samples were 3D printed. See 'Notes' section for details.

	Test method	Typical value		
		XY (Flat)	YZ (Side)	Z (Up)
Tensile (Young's) modulus	ASTM D3039 (1 mm / min)	1939 ± 28 MPa	1874 ± 31 MPa	1711 ± 45 MPa
Tensile stress at yield	ASTM D3039 (5 mm / min)	46.2 ± 0.8 MPa	50.3 ± 1.0 MPa	–
Tensile stress at break	ASTM D3039 (5 mm / min)	38.5 ± 1.4 MPa	44.0 ± 3.7 MPa	19.0 ± 6.4 MPa
Elongation at yield	ASTM D3039 (5 mm / min)	5.9 ± 0.1%	6.0 ± 0.2%	–
Elongation at break	ASTM D3039 (5 mm / min)	7.6 ± 0.2%	6.4 ± 0.6%	1.8 ± 0.8%
Flexural modulus	ISO 178 (1 mm / min)	1882 ± 30 MPa	1681 ± 61 MPa	1489 ± 25 MPa
Flexural strength	ISO 178 (5 mm / min)	78.9 ± 1.0 MPa at 5.5% strain	75.8 ± 2.0 MPa at 5.5% strain	50 ± 3.5 MPa at 3.6% strain
Flexural strain at break	ISO 178 (5 mm / min)	No break (>10%)	No break (>10%)	3.6 ± 0.4%
Charpy impact strength (at 23 °C)	ISO 179-1 / 1eB (notched)	7.9 ± 0.6 kJ/m²		
Hardness	ISO 7619-1 (Durometer, Shore D)	76 Shore D		

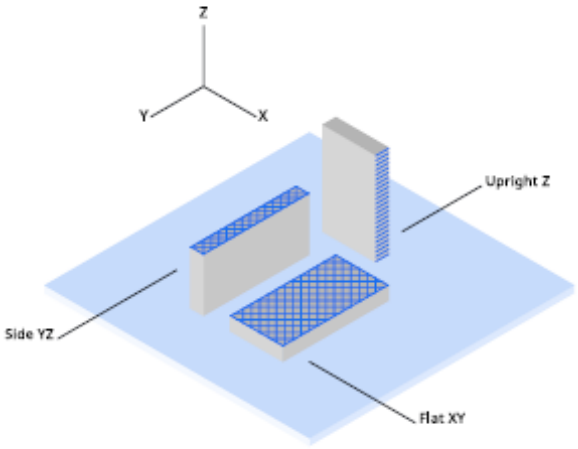

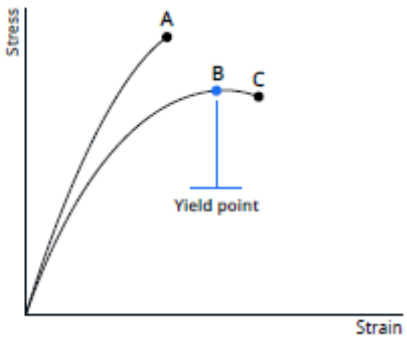

A. Tensile stress at break, elongation at break (no yield point)
B. Tensile stress at yield, elongation at yield
C. Tensile stress at break, elongation at break

Print orientation

As the FFF process produces part in a layered structure, mechanical properties of the part vary depending on orientation of the part. In-plane there are differences between walls (following the contours of the part) and infill (layer of 45° lines). These differences can be seen in the the data for XY (printed flat on the build plate - mostly infill) and YZ (printed on its side - mostly walls). Additionally, the upright samples (Z direction) give information on the strength of the interlayer adhesion of the material. Typically the interlayer strength (Z) has the lowest strength in FFF.

Note: All samples are printed with 100% infill - blue lines in the ilustration indicate typical directionality of infill and walls in a printed part.

Tensile properties

Printed parts can yield before they break, where the material is deforming (necking) before it breaks completely. When this is the case, both the yield and break points will be reported. Typical materials that yield before breaking are materials with high toughness like Tough PLA, Nylon and CPE+.

If the material simply breaks without yielding, only the break point will be reported. This is the case for brittle materials like PLA and PC Transparant, as well as elastomers (like TPU).

Figure C.3: Technical Data Sheet of PETg from manufacturer Ultimaker adapted from [93].

Technical Data Sheet

Multi-purpose resin with optimum toughness and processing speed.

General Properties	Norm	Typical Values
Appearance	-	Black
Viscosity, 25°C	Cone/Plate Rheometer[1]	320 mPas
Viscosity, 30°C	Cone/Plate Rheometer[1]	230 mPas
Density (Printed Part)	ASTM D792	1.2 g/cm³
Density (Liquid Resin)	ASTM D4052-18a	1.12 g/cm³

Tensile Properties[2]	Norm	Typical Values
E Modulus	ASTM D638	2000 MPa
Ultimate Tensile Strength	ASTM D638	53 MPa
Elongation at Break	ASTM D638	21%

Flexural Properties	Norm	Typical Values
Flexural Modulus	ASTM D790	2100 MPa
Flexural Strength	ASTM D790	95 MPa

Impact Properties	Norm	Typical Values
Notched Izod (Machined), -30°C	ASTM D256	20 J/m
Notched Izod (Machined), 23°C	ASTM D256	30 J/m
Unnotched Izod, 23°C	ASTM D256	515 J/m
Notched Charpy (Machined), 23°C	ISO 179-1	2.6 kJ/m²

Thermal Properties	Norm	Typical Values
HDT at 0.45 MPa	ASTM D648	63°C
HDT at 1.82 MPa	ASTM D648	54°C
Glass transition temperature (DMA, tan(d))	ASTM D4065	100°C

Ultracur3D® ST 45 B

Thermal Properties	Norm	Typical Values
Flammability	UL 94 (1.5 mm)	HB
Glow-wire Test	IEC 60695-2-12/-13 (2 mm)	GWIT: 625°C GWFI: 600°C

Dielectric/Electric Properties	Norm	Typical Values
Dielectric Strength	DIN EN 60243-1	29 kV / mm

Biocompatibility	Norm	Typical Values
Cytotoxicity – Neutral Red	ISO 10993-5 (2009)	PASS[3]

Abrasion	Norm	Typical Values
Scratch resistance (in print direction)	DIN EN ISO 1518-1[4]	Up to 35N (no visible abrasion)
Scratch resistance (against print direction)	DIN EN ISO 1518-1[4]	Up to 25N (no visible abrasion)

Other	Norm	Typical Values
Hardness Shore D	ASTM D2240	80
Water Absorption, Short-Term (24 hours)	ASTM D570	>5%

Mechanical properties overview

1) Determined with TA-Instrument DHR rheometer, cone/plate, diameter 60 mm, shear rate 100 s^{-1}
2) Tensile type ASTM D638 type IV, Pulling speed 5 mm/min
3) For the statement on Biocompatibility data see Chapter: Biocompatibility.
4) Constant-loading method
5) If not noted otherwise, all specimens are 3D printed. Samples were tested at room temperature, 23°C. ASTM sample size (L x W x H): ASTM D790 80 x 4 x10 mm, ASTM D256 63 x 3.2 x 12 mm, ASTM D648 127 x 3.2 x 13 mm, ISO 179-1 80 x 4 x 10 mm, UL 94 125 x 1.5 x 13 mm, IEC 60695-2-12/-13 60 x 2 x 60 mm.

Printing Performance

The combination of 3D printer and material has a huge impact on the quality of the parts produced. The measured design characteristics as well as the printing speed can be found in the Printing Evaluation Guideline of Ultracur3D® Resins.

The data contained in this publication is based on our current knowledge and experience. In view of the many factors that may affect processing and application of our product, this data does not relieve processors from carrying out their own investigations and tests; neither does this data imply any guarantee of certain properties, nor the suitability of the product for a specific purpose.

Any descriptions, drawings, photographs, data, proportions, weights etc. given herein may change without prior information and do not constitute the agreed contractual quality of the product. It is the responsibility of the recipient of our products to ensure that any proprietary rights and existing laws and legislation are observed.

The safety data given in this publication is for informational purposes only and does not constitute a legally binding MSDS. The relevant MSDS can be obtained upon request from your supplier or you may contact BASF 3D Printing Solutions GmbH directly at sales@basf-3dps.com.

Figure C.4: Technical Data Sheet of ST45 from manufacturer BASF, adapted from [8].

Set up Mechanical testing tensile and Charpy test

Figure C.5: Tensile test set up with the Zwick/Roell Z020 tensile testing machine.

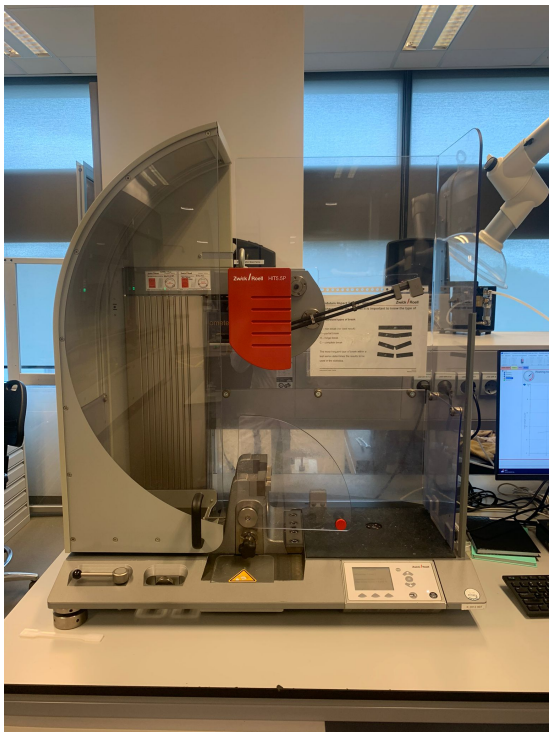

Figure C.6: Charpy Impact test setup with the Zwick/Roell HIT 5.5P testing machine with a 1J pendulum.

Figure C.7: Alignment of the specimen in the testing machine.

Raw Data from Tensile and Impact Tests

In this section, the raw data collected from both tensile and impact tests for a range of materials, including st45, PLA, rPLA, PETG, and several variations of rPETG. Each dataset is displayed with tables, statistics, and visualizations to highlight the material properties derived from these tests.

For each material, the impact energy values in a table from the report, along with key statistical metrics. are presented in the figures below. Additionally, a plot that visually compares the impact energy values across all tested specimens to compare of energy absorption capacity between materials.

Results:

No.	b mm	b_N mm	h mm	W J	ak kJ/m²	Type of failure	ak - series
1	9,85	7,83	4,1	0,09662	3,01	C	3.06C*
2	9,9	8,1	4,01	0,10379	3,20	C	
3	10,03	7,98	4,06	0,09901	3,06	C	
4	9,95	7,99	4,04	0,09662	2,99	C	
5	9,93	7,95	4,11	0,09543	2,92	C	
6	10,02	7,99	4,1	0,09662	2,95	C	
7	9,96	7,92	4,07	0,10483	3,25	C	
8	9,83	7,83	4,02	0,09528	3,03	C	
9	9,99	7,96	4,11	0,10363	3,17	C	
10	10,02	7,89	4,24	0,10244	3,06	C	

Statistics:

Total/Hinge break n = 10	b mm	b_N mm	h mm	W J	ak kJ/m²
x	9,948	7,944	4,086	0,09943	3,06
s	0,07084	0,0814	0,06535	0,00383	0,11
ν [%]	0,71	1,02	1,60	3,85	3,55

Series graph:

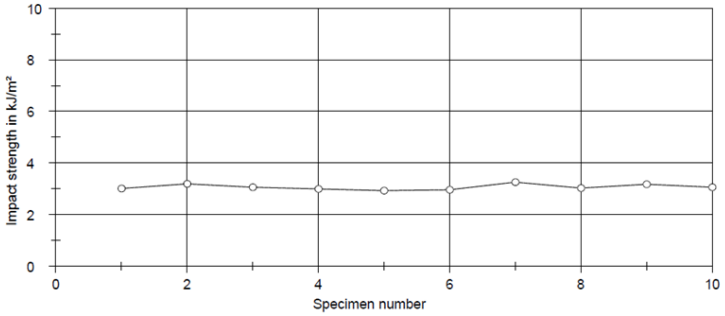

Figure C.8: Impact Energy Data for ST45

Results:

No.	b mm	b_N mm	h mm	W J	ak kJ/m²	Type of failure	ak - series
1	10,18	8,17	4,02	0,08588	2,61	C	2.82C*
2	10,22	8,18	3,96	0,08588	2,65	C	
3	10,52	8,39	3,96	0,13379	4,03	C	
4	10,2	8,04	3,98	0,08588	2,68	C	
5	10,34	8,28	4	0,08469	2,56	C	
6	10,34	8,38	4	0,09543	2,85	C	
7	10,29	7,98	3,95	0,08469	2,69	C	
8	10,2	7,96	4,01	0,08469	2,65	C	
9	10,15	7,8	4,01	0,08588	2,75	C	
10	10,16	7,95	3,99	0,08827	2,78	C	

Statistics:

Total/Hinge break n = 10	b mm	b_N mm	h mm	W J	ak kJ/m²
x	10,26	8,113	3,988	0,09151	2,82
s	0,1148	0,1985	0,0244	0,01520	0,43
ν [%]	1,12	2,45	0,61	16,61	15,24

Series graph:

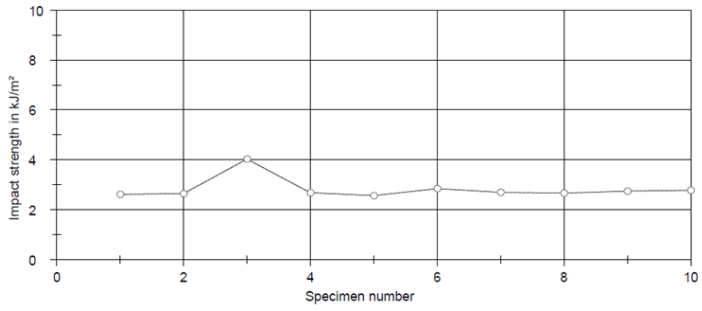

Figure C.9: Impact Energy Data for PLA

Results:

No.	b mm	b_N mm	h mm	W J	ak kJ/m²	Type of failure	ak - series
1	9,95	8,13	4,06	0,09423	2,85	C	3.05C*
2	9,97	8,11	4,08	0,09543	2,88	C	
3	9,95	8,15	4,05	0,09781	2,96	C	
4	9,99	8,15	4,07	0,09901	2,98	C	
5	9,99	8,11	4,06	0,09304	2,83	C	
6	10,02	8,19	4,04	0,10379	3,14	C	
7	10	8,13	4,05	0,10140	3,08	C	
8	9,93	8,12	4,05	0,09781	2,97	C	
9	9,96	8,13	4,06	0,12297	3,73	C	
10	9,98	8,12	4,06	0,10260	3,11	C	

Statistics:

Total/Hinge break n = 10	b mm	b_N mm	h mm	W J	ak kJ/m²
x̄	9,974	8,134	4,058	0,10081	3,05
s	0,02716	0,02413	0,01135	0,00855	0,26
ν [%]	0,27	0,30	0,28	8,48	8,47

Series graph:

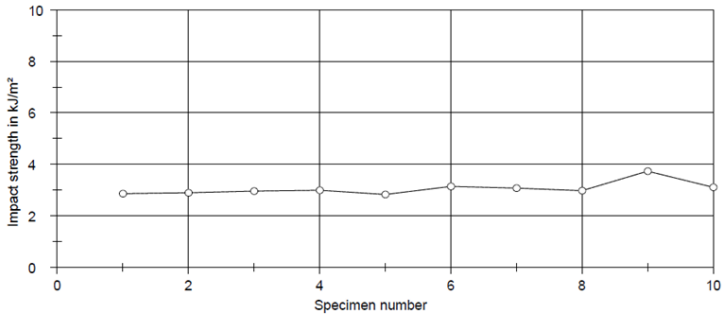

Figure C.10: Impact Energy Data for Regrind PLA

Results:

No.	b mm	b_N mm	h mm	W J	ak kJ/m²	Type of failure	ak - series
1	10,11	8,16	3,93	0,09065	2,83	C	2.17C*
2	10,06	8,15	3,91	0,08231	2,58	C	
3	10,11	8,21	3,91	0,08112	2,53	C	
4	10,05	8,17	3,93	0,03853	1,20	C	
5	10,06	8,16	3,91	0,05030	1,58	C	
6	10,1	8,2	3,92	0,08469	2,63	C	
7	10,03	8,14	3,92	0,07161	2,24	C	
8	10,02	8,12	3,9	0,05857	1,85	C	
9	10,06	8,16	3,92	0,03970	1,24	C	
10	10,11	8,18	3,92	0,08588	2,68	C	
11	10,02	8,08	3,9	0,07993	2,54	C	

Statistics:

Total/Hinge break n = 11	b mm	b_N mm	h mm	W J	ak kJ/m²
x̄	10,07	8,157	3,915	0,06939	2,17
s	0,03585	0,03608	0,01036	0,01922	0,60
ν [%]	0,36	0,44	0,26	27,70	27,63

Series graph:

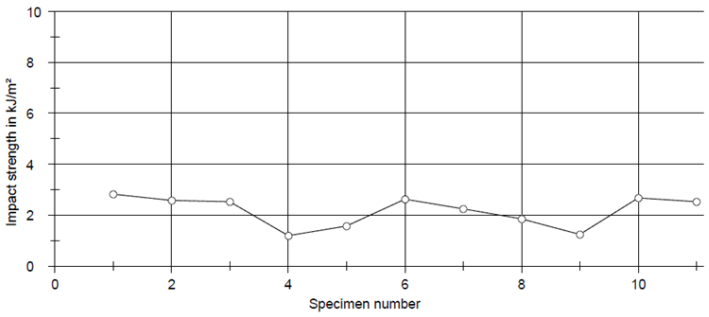

Figure C.11: Impact Energy Data for PETg

Results:

No.	b mm	b_N mm	h mm	W J	ak kJ/m²	Type of failure	ak - series
1	10,1	8,23	4,01	0,13258	4,02	C	4.47C*
2	10,14	8,25	3,94	0,09304	2,86	C	
4	10,13	8,27	4,03	0,15547	4,66	C	
5	10,11	8,27	3,96	0,12177	3,72	C	
7	10,11	8,27	3,96	0,10858	3,32	C	
8	10,07	8,22	3,98	0,08469	2,59	C	
9	10,08	8,17	3,99	0,08827	2,71	C	
10	10,15	8,28	3,94	0,09423	2,89	C	
11	10,11	8,25	3,95	0,06212	1,91	C	
12	10,15	8,26	3,94	0,09184	2,82	C	
13	10,1	8,24	3,99	0,04912	1,49	C	

Statistics:

Total/Hinge break n = 11	b mm	b_N mm	h mm	W J	ak kJ/m²
$\bar{x}$	10,11	8,246	3,972	0,09834	3,00
s	0,02656	0,03139	0,0306	0,03033	0,91
ν [%]	0,26	0,38	0,77	30,84	30,20

Series graph:

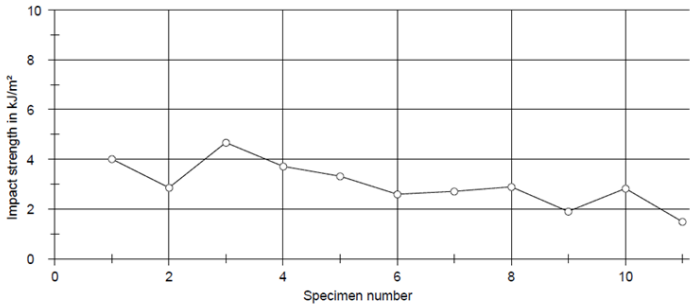

Figure C.12: Impact Energy Data for rPETg

Results:

No.	b mm	b_N mm	h mm	W J	ak kJ/m²	Type of failure	ak - series
1	9,98	8,02	3,95	0,08946	2,82	C	2.68C*
2	9,83	8,07	3,92	0,07636	2,41	C	
3	10	8,05	3,94	0,04559	1,44	C	
4	9,76	8	3,91	0,11937	3,82	C	
5	9,98	8,04	3,93	0,12657	4,01	H	
6	10	8,06	3,92	0,04795	1,52	C	
7	10,01	8,11	3,93	0,12898	4,05	C	
8	9,86	8	3,92	0,08112	2,59	H	
9	10,04	8,09	3,92	0,07874	2,48	C	
10	9,86	8,02	3,94	0,05739	1,82	C	
11	9,98	8,03	3,93	0,07874	2,50	C	

Statistics:

Total/Hinge break n = 11	b mm	b_N mm	h mm	W J	ak kJ/m²
$\bar{x}$	9,936	8,045	3,928	0,08457	2,68
s	0,09168	0,0356	0,01168	0,02953	0,93
ν [%]	0,92	0,44	0,30	34,91	34,91

Series graph:

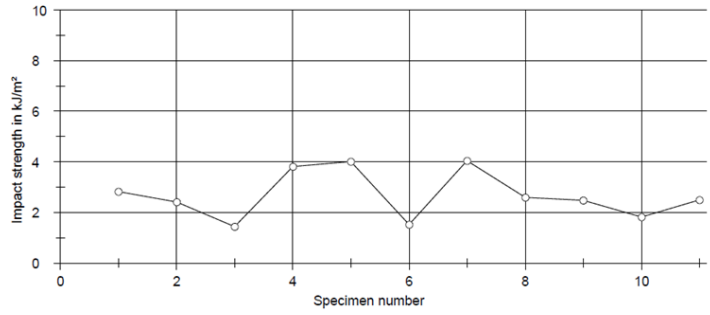

Figure C.13: Impact Energy Data for rPETg Batch 2 (B2)

Results:

No.	b mm	b_N mm	h mm	W J	ak kJ/m²	Type of failure	ak - series
1	9,75	7,86	3,95	0,03970	1,28	C	1.75C*
2	10,02	8,08	3,94	0,08350	2,62	C	
3	9,81	7,99	3,92	0,04088	1,31	C	
4	9,79	8,03	3,92	0,04912	1,56	C	
5	9,78	8,06	3,94	0,04559	1,44	C	
6	9,77	7,95	3,95	0,07755	2,47	C	
7	9,7	7,97	3,92	0,05148	1,65	C	
8	9,74	7,87	3,89	0,04088	1,34	C	
9	9,78	7,9	3,91	0,04795	1,55	C	
10	9,78	7,93	3,9	0,04441	1,44	C	
11	9,75	7,91	3,92	0,08112	2,62	C	

Statistics:

Total/Hinge break n = 11	b mm	b_N mm	h mm	W J	ak kJ/m²
x	9,788	7,959	3,924	0,05474	1,75
s	0,08232	0,07449	0,01963	0,01712	0,54
V [%]	0,84	0,94	0,50	31,28	30,78

Series graph:

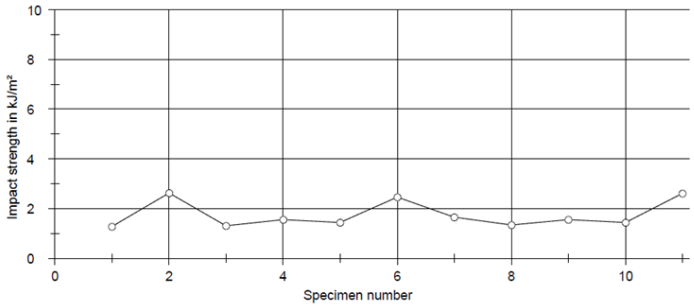

Figure C.14: Impact Energy Data for rPETg Second Cycle (2e)

From the tensile test, the stress-strain curves for all tested specimens per material are displayed in the figures below. Each plot represents the individual performance of the materials, with a distinct curve for each specimen.

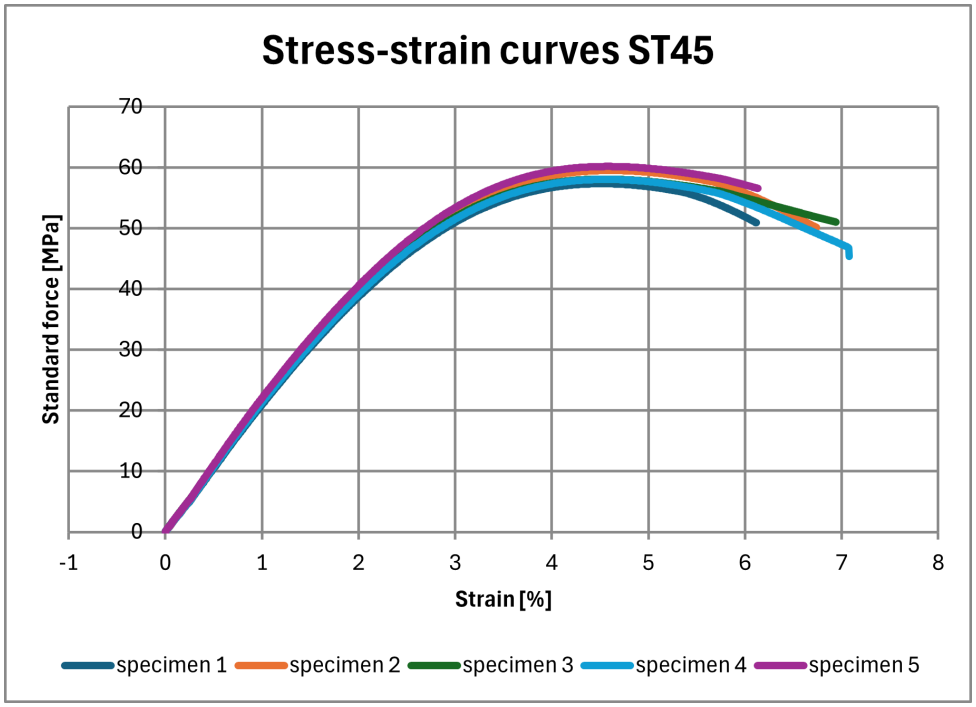

Figure C.15: Stress-strain curves for ST45

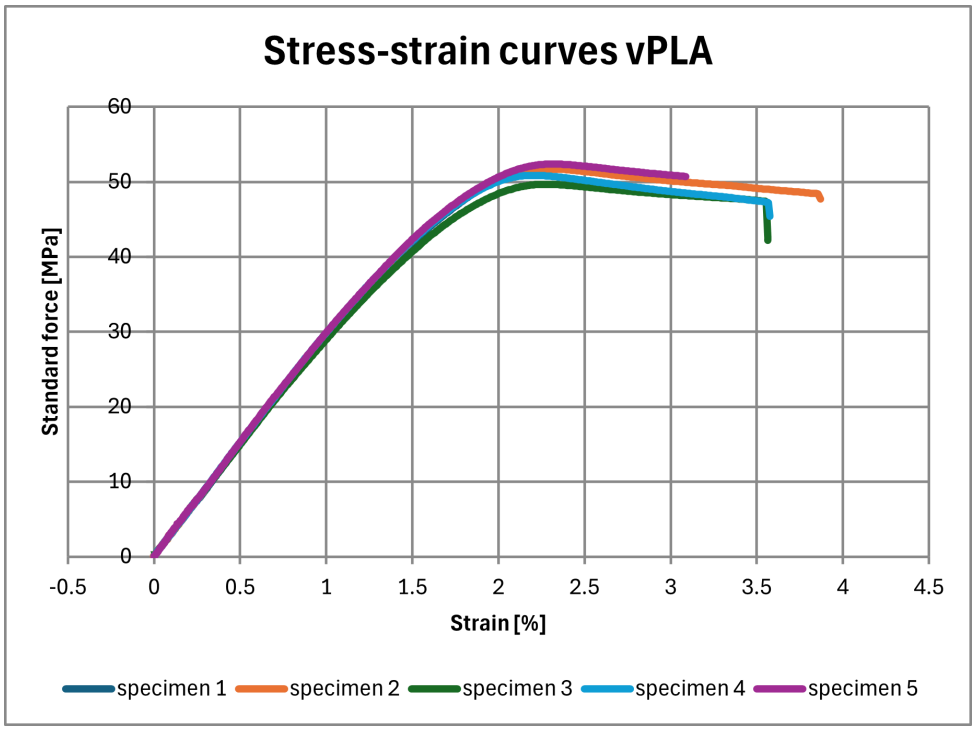

Figure C.16: Stress-strain curves for PLA

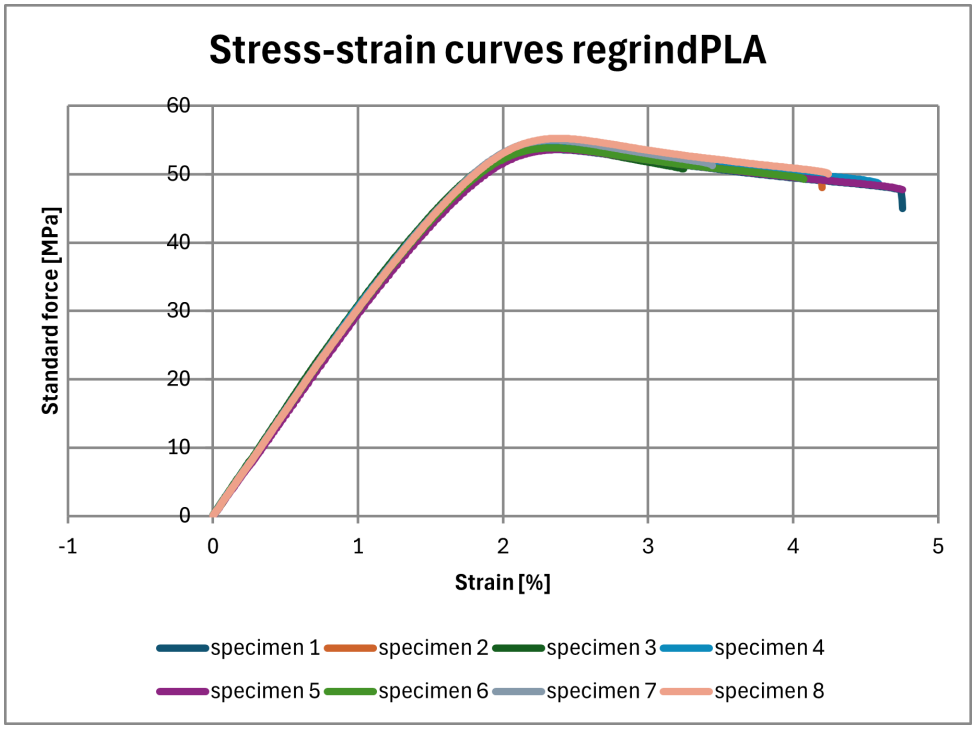

Figure C.17: Stress-strain curves for Regrind PLA

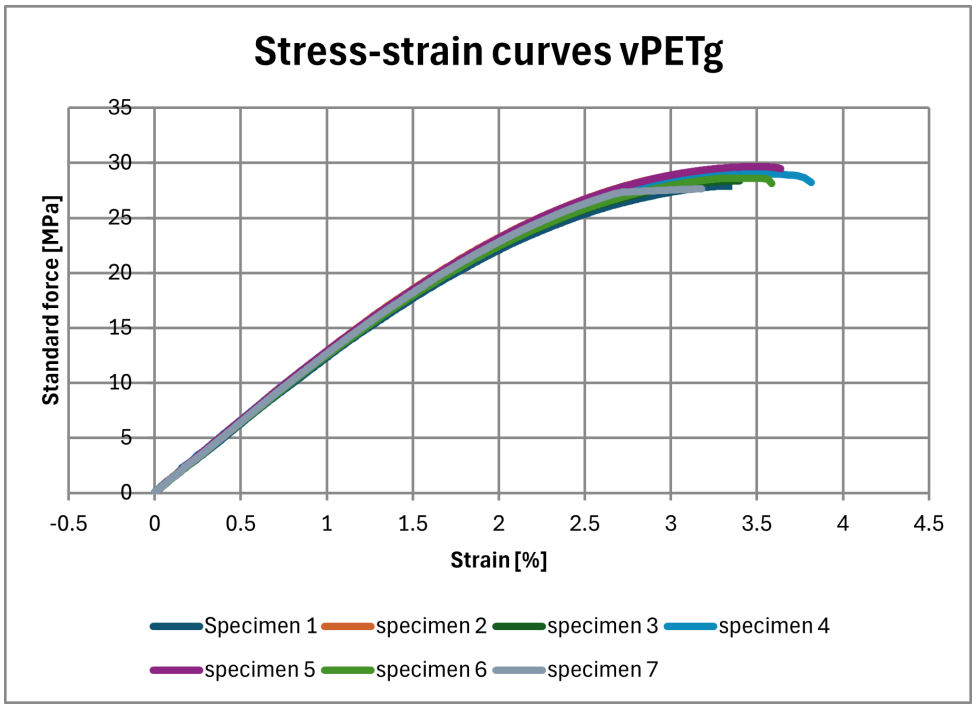

Figure C.18: Stress-strain curves for PETg

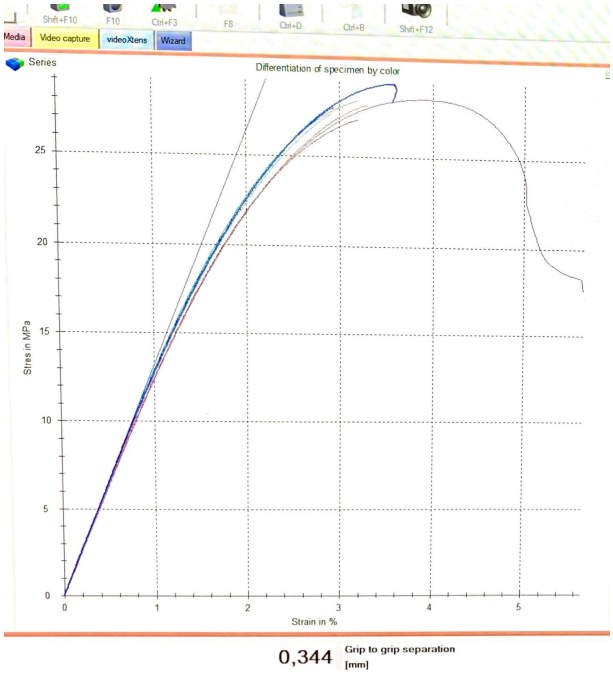

Figure C.19: Stress-strain curves for rPETg

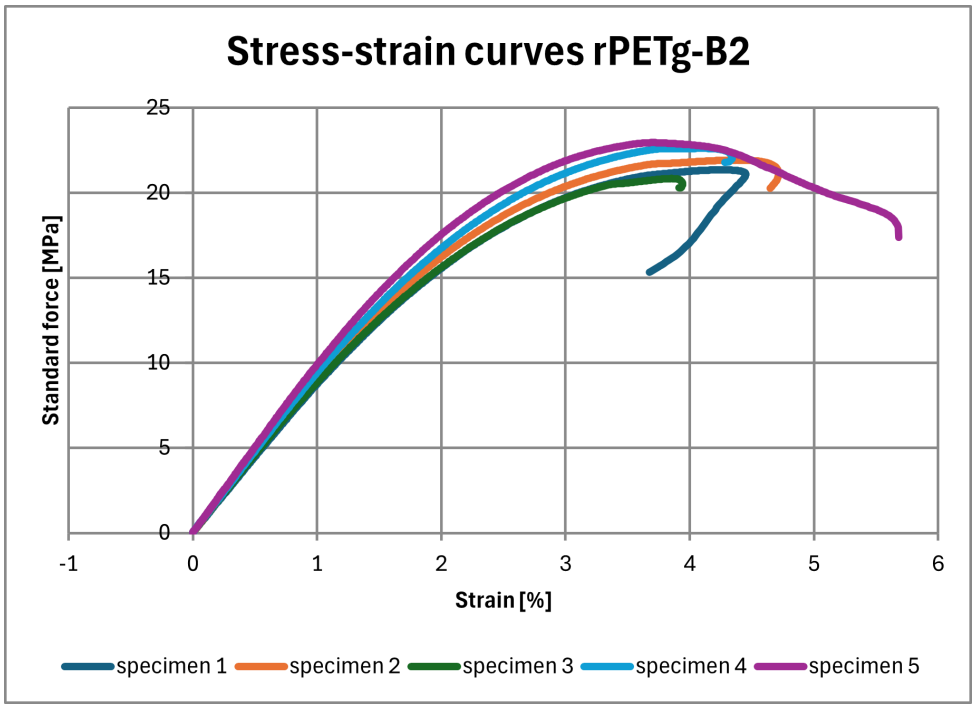

Figure C.20: Stress-strain curves for rPETg Batch 2 (B2)

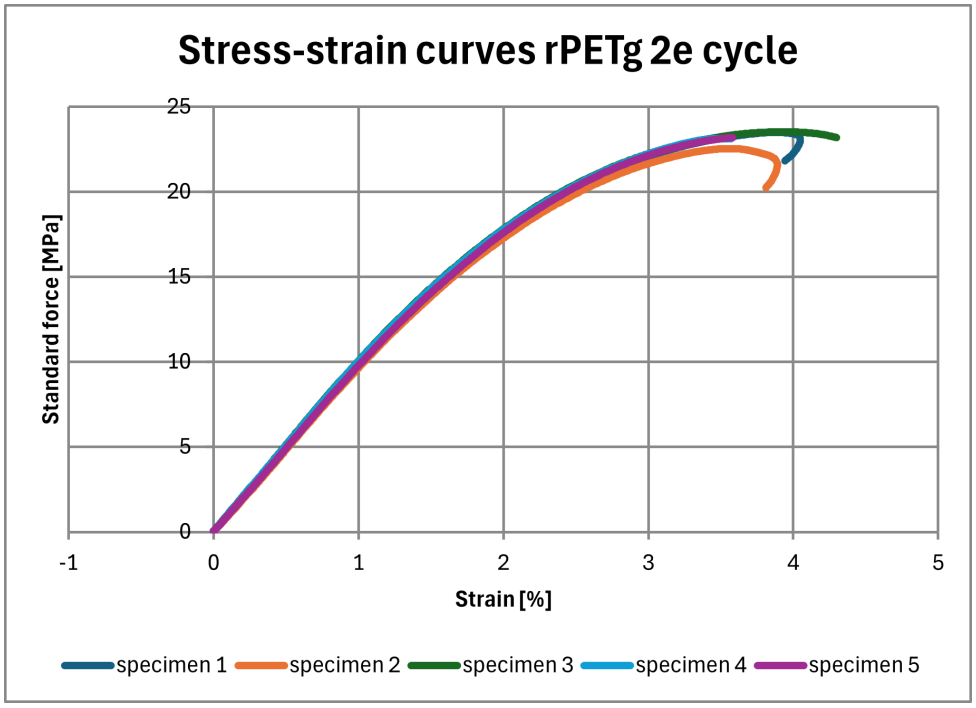

Figure C.21: Stress-strain curves for rPETg Second Cycle (2e)

Print settings per material

Ultrafuse PLA white and ColorFabb PLA regrind were printed with the settings in C.1 and printed on a Bambu Lab X1 Carbon printer. Their filament diameter was 1.75 mmm.

Table C.1: Bambu Lab PLA general printing settings with 100% infill

Setting	Value
Filament type	PLA
Layer height	0.15 mm
Infill	100%
Nozzle temperature	210°C
Bed temperature	60°C
Print speed	250 mm/s
Cooling fan speed	100%
Initial layer height	0.3 mm
Initial layer speed	30 mm/s
Retraction distance	1 mm
Retraction speed	40 mm/s
Flow rate	100%

Ultimaker PETg was printed with the settings in C.2 on the Ultimaker S5 printer.

Table C.2: Ultimaker S5 generic PETg settings with 100% infill

Setting	Value
Filament type	PETG
Layer height	0.15 mm
Nozzle temperature	240°C
Bed temperature	75°C
Print speed	60 mm/s
Infill	100%
Retraction distance	6.5 mm
Retraction speed	25 mm/s
Fan speed	50-100%
Flow rate	100%
Initial layer height	0.27 mm
Initial layer speed	30 mm/s

Hartplastic rPETg was printed with the settings indicated C.3.

Table C.3: Ultimaker S5 generic PETg settings with 100% infill

Setting	Value
Filament type	PETG
Layer height	0.15 mm
Nozzle temperature	230°C
Bed temperature	75°C
Print speed	60 mm/s
Infill	100%
Retraction distance	6.5 mm
Retraction speed	25 mm/s
Fan speed	50-100%
Flow rate	100%
Initial layer height	0.27 mm
Initial layer speed	30 mm/s

ST45 was printed with the following settings. The same settings are used for printing the 3DxS-plint, currently.

Table C.4: ST45 Resin Print Settings on Atum3D DLP Printer

Parameter	**Setting**
Wavelength	405 nm
Curing Time per Layer	2 seconds (CT1), 2.4 seconds (CT2)
Layer Thickness	0.1 mm (LT1), 0.3 mm (LT2)
Print Bed Temperature	room temperature